



HAL
open science

Collections of solids in interaction: suspensions, granular media and micro-swimmers.

Aline Lefebvre-Lepot

► **To cite this version:**

Aline Lefebvre-Lepot. Collections of solids in interaction: suspensions, granular media and micro-swimmers.. Numerical Analysis [math.NA]. Institut polytechnique de Paris, 2021. tel-04525973

HAL Id: tel-04525973

<https://hal.science/tel-04525973>

Submitted on 29 Mar 2024

HAL is a multi-disciplinary open access archive for the deposit and dissemination of scientific research documents, whether they are published or not. The documents may come from teaching and research institutions in France or abroad, or from public or private research centers.

L'archive ouverte pluridisciplinaire **HAL**, est destinée au dépôt et à la diffusion de documents scientifiques de niveau recherche, publiés ou non, émanant des établissements d'enseignement et de recherche français ou étrangers, des laboratoires publics ou privés.



Institut Polytechnique de Paris

Laboratoire CMAP, Ecole Polytechnique (UMR 7641 CNRS)



Mémoire présenté pour l'obtention du

Diplôme d'habilitation à diriger des recherches

Discipline : Mathématiques

par

Aline Lefebvre-Lepot

**Collections of solids in interaction: suspensions,
granular media and micro-swimmers.**

Rapporteurs : Grégoire Allaire
Alexandre Ern
Shravan Veerapaneni

Date de soutenance : 14 décembre 2021

Composition du jury : Grégoire Allaire (Rapporteur)
Didier Bresch (Examinateur)
Eric Climent (Examinateur)
Alexandre Ern (Rapporteur)
Céline Grandmont (Examinatrice)
Stéphanie Salmon (Examinatrice)
Shravan Veerapaneni (Rapporteur)

Aline Lefebvre-Lepot

Collections of solids in interaction: suspensions, granular media and micro-swimmers.

Date de soutenance HDR : 14 décembre 2021

Rapporteurs : Grégoire Allaire, Alexandre Ern and Shravan Veerapaneni

Institut Polytechnique de Paris

Laboratoire CMAP, Ecole Polytechnique (UMR 7641 CNRS)

Route de Saclay

91128 Palaiseau Cedex

Remerciements

Je tiens tout d'abord à remercier chaleureusement Grégoire Allaire, Alexandre Ern et Shravan Veerapaneni pour le temps qu'ils ont accepté de prendre pour relire ce manuscrit ainsi que pour l'intérêt qu'ils ont porté à mon travail. Je suis également très reconnaissante à Didier Bresch, Eric Climent, Céline Grandmont et Stéphanie Salmon d'avoir accepté de se joindre à eux pour faire partie du jury, malgré l'organisation pour le moins incertaine ! A l'heure où j'écris ces remerciements, j'espère encore que nous pourrions nous voir "en présentiel" comme il est maintenant coutume de dire...

Merci également à Yvan Martel, responsable HDR, pour sa disponibilité et son aide qui m'ont été très précieuses pour le bon déroulement de toutes les étapes de ce projet, du premier contact à la soutenance.

Je voudrais remercier ici chaleureusement François Alouges. Ton enthousiasme, ton soutien, tes encouragements et ta confiance me sont précieux, ce manuscrit te doit beaucoup ! Ce fut également un plaisir de travailler avec toi toutes ces années, d'abord sur les micro-nageurs puis les méthodes d'éléments finis de frontière. Ces travaux ouvrent des perspectives enthousiasmantes ! Un immense merci également à Bertrand Maury. Tu m'as fait plonger dans l'univers des mathématiques et mes thématiques de recherche reflètent ce goût, que tu m'as transmis, de travailler au plus près des applications. Ton soutien et tes conseils m'ont souvent été d'un grand secours et j'apprends toujours énormément de nos discussions ! Je suis très heureuse que les circonstances nous aient donné l'occasion de travailler à nouveau ensemble autour des problèmes de friction. Je tiens également à exprimer ma gratitude à Grégoire Allaire : nous n'avons pas eu l'occasion de collaborer mais ton soutien, ton intérêt pour mon travail et tes conseils m'ont beaucoup aidée. Un merci tout particulier à tous les trois pour votre patience et votre gentillesse ces derniers mois : je suis consciente de vous avoir beaucoup sollicités ! Je profite enfin de ces lignes pour remercier Céline Grandmont à qui je dois beaucoup : tes encouragements, à chacune de nos rencontres, m'ont été d'une aide précieuse !

Ce manuscrit n'aurait évidemment pu voir le jour sans le travail de mes collaboratrices et collaborateurs. Merci à tous pour ces échanges et partages scientifiques (ou non-scientifiques d'ailleurs) sources d'idées et de solutions ! Merci à François Alouges,

Matthieu Aussal, Franck Pigeonneau et Antoine Sellier de m'avoir initiée aux méthodes BEM. Merci à Benoît Merlet et Flore Nabet avec qui nous avons combattu la lubrification et à Fabien Vergnet qui nous a rejoint dans la bataille. Merci à Yvon Maday, Anne Mangeney, Hugo Martin et Bertrand Maury pour nos longues séances de travail sur la friction. Merci à Sylvain Faure et Loïc Gouarin sans qui les codes de calcul n'auraient jamais vu le jour et à Georges Gauthier, Philippe Gondret et Antoine Seguin grâce à qui ces même codes sont aujourd'hui utilisés.

Travailler au CMAP est particulièrement agréable et je tiens ici à remercier les directions et les équipes administratives du laboratoire et du département pour leur efficacité sans faille. Merci à mes partenaires de la pause café de 10h, nos discussions à bâtons rompus sur tout (et surtout sur rien) font partie des petits plaisirs de la journée ! Un merci particulier à Lucas, ex-partenaire de tableau excel : partager ton bureau est un plaisir ! Je profite également de ces quelques lignes pour adresser mes remerciements à Flore : nos discussions interminables me sont très précieuses !

Enfin, merci à ma famille qui s'est drôlement agrandie ces dernières années ! Les retrouver régulièrement m'est toujours aussi indispensable ! Merci à ma petite famille : à Eric, pour son soutien, sa patience et sa compréhension et à Robin et Lise pour leurs rires et leurs câlins qui me font tant de bien !

Résumé

Dans ce manuscrit, on s'intéresse à l'étude et à la simulation numérique de systèmes mécaniques formés solides en interaction: suspensions passives ou actives ou encore milieux granulaires. On décrit dans le premier chapitre certains problèmes posés par l'étude de ces systèmes.

On se concentre ensuite sur la simulation numérique de suspensions. Celle-ci nécessite la résolution d'un problème couplé entre le fluide de Stokes et les structures rigides. Dans le second chapitre, on cherche à résoudre précisément le problème quand les particules sont proches. La méthode proposée est basée sur un développement asymptotique explicite de la solution quand la distance inter-particulaire tend vers zéro. Dans le troisième chapitre on s'intéresse à l'utilisation de méthodes d'éléments finis de frontière pour la résolution du problème fluide-structure. On traite, dans le cas des équations de Stokes, les deux difficultés classiques pour ce type de méthodes : d'une part, le développement d'algorithmes rapides pour la résolution de systèmes pleins et d'autre part, le calcul des intégrales singulières intervenant dans le problème.

Dans le quatrième chapitre, nous nous intéressons à la conception d'algorithmes permettant de traiter les contacts (avec ou sans frottement) dans les systèmes que nous considérons. Les algorithmes décrits sont de type Dynamique des Contacts. A chaque pas de temps, les forces de contact sont calculées de manière implicite, comme solution d'un problème convexe sous contrainte. On présente des études rhéologiques de matériaux granulaires basées sur ces algorithmes.

Enfin, dans le cinquième chapitre, on s'intéresse à l'étude de micro-nageurs évoluant dans un fluide de Stokes. On cherche à savoir si ces nageurs peuvent "nager", c'est-à-dire, effectuer des déformations cycliques (des brassées) générant un déplacement donné. On propose un cadre général pour répondre à cette question en réécrivant le problème comme un problème de contrôle.

Abstract

In this manuscript, we are interested in the study and numerical simulation of mechanical systems composed of interacting solids: passive or active suspensions, or granular media. The first chapter describes some of the problems raised by the study of these systems.

We then focus on the numerical simulation of suspensions. This requires the resolution of a coupled problem between the Stokes fluid and the rigid structures. In the second chapter, we aim to solve precisely the problem when the particles are close. The method we propose is based on an explicit asymptotic expansion of the solution when the inter-particle distance goes to zero. In the third chapter, we focus on the use of boundary element methods to solve the fluid-structure problem. We deal, in the case of Stokes equations, with the two classical difficulties for these methods: on the one hand, the development of fast algorithms to solve full systems and on the other hand, the computation of singular integrals involved in the problem.

In the fourth chapter, we are interested in designing algorithms to deal with contacts (with or without friction) in the systems we consider. The algorithms described are Contact Dynamics algorithms. At each time step, the contact forces are computed in an implicit way, as solution to a convex optimization problem. Rheological studies of granular materials based on these algorithms are presented.

Finally, in the fifth chapter, we study micro-swimmers evolving in a Stokes fluid. We investigate whether these swimmers can swim, that is, perform cyclic deformations (a stroke) generating a given displacement. We propose a general framework to answer this question by rewriting the problem as a control problem.

Publications

The star symbol \star indicates publications resulting from my PhD.

The dagger symbol \dagger indicates proceedings (with peer-review process).

▷ Suspensions

Penalty method and contacts

[1] ^{\dagger,\star} A penalty method for the simulation of fluid - rigid body interaction. With J. Janela and B. Maury. In: *ESAIM: Proceedings* 14 (2005). Ed. by E. Cancès and J.-F. Gerbeau, pp. 115–123

[2] ^{\dagger,\star} Fluid-Particle simulations with FreeFem++ . In: *ESAIM: Proceedings* 18 (2007). Ed. by J.-F. Gerbeau and S. Labbé, pp. 120–132

[3] Contact problems for particles in a shear flow. With N. Verdon, L. Lobry and P. Laure. In: *European Journal of Computational Mechanics* 19.5-7 (2010), pp. 513–531

[4] A necklace model for vesicles simulations in 2D. With M. Ismail. In: *International Journal for Numerical Methods in Fluids* 76.11 (2014), pp. 835–854

[5] Apparent Viscosity of a Mixture of a Newtonian Fluid and Interacting Particles. With B. Maury, In: *Comptes Rendus Mécanique*, 333.12 (2005), pp. 923-933

Lubrication

[6] ^{\star} Numerical simulation of gluey particles. In: *ESAIM: Mathematical Modelling and Numerical Analysis* 43.1 (2009), pp. 53–80

[7] Micro-macro modelling of an array of spheres interacting through lubrication forces. With B. Maury. In: *Adv. Math. Sci. Appl.* 21.2 (2011), pp. 535– 557

[8] Modified Lees–Edwards Boundary conditions and viscous contact for numerical simulations of particles in a shear flow. With N. Verdon, L. Lobry and P. Laure. In: *European Journal of Computational Mechanics* 21.3-6 (2012), pp. 397–406

[9] An accurate method to include lubrication forces in numerical simulations of dense Stokesian suspensions. With B. Merlet, and T. N. Nguyen. In: *Journal of Fluid Mechanics* 769 (2015), pp. 369–386

[10][†] Numerical simulation of suspensions: lubrication correction, including fluid correction. In: *Actes du colloque EDP-Normandie*. (2017)

[11] Numerical simulation of rigid particles in Stokes flow: lubrication correction for general shape of particles. With F. Nabet. *Math. Model. Nat. Phenom.*, 16 (2021), p. 45

Boundary Element Method for Stokes

[12] Application of the Sparse Cardinal Sine Decomposition to 3D Stokes Flows. With F. Alouges, M. Aussal, F. Pigeonneau, and A. Sellier. In: *International Journal of Computational Methods and Experimental Measurements*. 5.3 (2017), pp. 387–394

[13] Motion of a solid particle in a bounded viscous flow using the Sparse Cardinal Sine Decomposition. With F. Alouges and A. Sellier. In: *Meccanica* 55 (2020), pp. 403–419

▷ **Granular flows**

[14][†] Dynamic Numerical Investigation of Random Packing for Spherical and Nonconvex Particles. With S. Faure and B. Semin. In: *ESAIM: Proceedings* 28 (2009). Ed. by M. Ismail, B. Maury, and J.-F. Gerbeau, pp. 13–32.

[15] Existence results for non-smooth second order differential inclusions, convergence result for a numerical scheme and application to the modelling of inelastic collisions. With F. Bernicot. In: *Confluentes Mathematici* 2.4 (2010), pp. 445–471.

[16] Clustering and flow around a sphere moving into a grain cloud. With A. Seguin, S. Faure, and P. Gondret. In: *The European Physical Journal E* 39.6 (2016), p. 63.

An article in preparation with H. Martin, A. Mangeney, Y. Maday, B. Maury. An optimization-based model for dry granular flows: application to granular collapse on erodible beds.

▷ **Micro-Swimmers**

[17]^{*} Optimal Strokes for Low Reynolds Number Swimmers: An Example. With F. Alouges and A. DeSimone. In: *Journal of Nonlinear Science* 18.3 (2008), pp. 277–302

[18]* Biological Fluid Dynamics: Swimming at low Reynolds numbers. With F. Alouges and A. DeSimone. In: *Encyclopedia of complexity and systems science* (2009) Ed. by Robert A Meyers. Springer

[19] Optimal strokes for axisymmetric microswimmers. With F. Alouges and A. DeSimone. In: *The European Physical Journal E* 28.3 (2009), pp. 279–284

[20]† A stokesian submarine. With Benoît Merlet. In: *ESAIM: Proceedings* 28 (2009). Ed. by M. Ismail, B. Maury, and J.-F. Gerbeau, pp. 150–161

[21] Optimally swimming Stokesian robots. With François Alouges, Antonio DeSimone, Luca Heltai, and Benoît Merlet. In: *Discrete & Continuous Dynamical Systems - B* 18.5 (2013), pp. 1189–1215

An article submitted with F. Alouges, P. Weder, Optimal strokes for the 4-sphere swimmer at low Reynolds number in the regime of small deformations.

▷ **Book chapters**

[22] Numerical Modeling of Fluid–Grain Interactions. With B. Maury. In: *Discrete-element modeling of granular material* (2011) Ed. by Radjaï F. and Dubois F. Wiley

[23] Close Interaction of Immersed Grains. With B. Maury. In: *Discrete-element modeling of granular material* (2011) Ed. by Radjaï F. and Dubois F. Wiley

Contents

1	Introduction	1
1.1	Context and open questions	2
1.2	Contributions	15
2	Numerical simulation of suspensions: lubrication correction, including fluid correction.	28
2.1	Traditional method: correction of the forces	31
2.2	A new method: singular/regular splitting of the velocity and pressure fields.	36
3	New tools for Boundary Element Methods for Stokes.	49
3.1	Introduction to Boundary Element Methods (BEM)	53
3.2	First challenge: fast resolution of dense systems. The Sparse Cardinal Sine Decomposition method (SCSD) adapted to Stokes.	60
3.3	Second challenge: Singular and near-singular integrals for the Stokes kernel. A semi-analytic method.	68
4	Contacts: numerical schemes based on convex optimization problems	92
4.1	Non Smooth Contact Dynamics for frictionless contacts	95
4.2	A convex scheme for frictionless contacts	97
4.3	A convex scheme for frictional contacts.	104
5	Stokesian swimmers.	121
5.1	Stokesian robots.	122
6	Conclusion	139

Introduction

1

” *A large scale numerical experiment is as difficult to succeed as a proper experiment or an analytical calculation leading to good results.*

— **Kenneth Wilson (1983)**
La Recherche, 14:1004 –1007

This manuscript is dedicated to the presentation of my research work since my recruitment in 2008. My PhD thesis was entitled “Numerical modelling of fluid/particle flows”. In that work, I developed close interaction models between particles for numerical simulations of suspensions. From then, my research focused on numerical simulations of both suspensions and granular media.

This field of research has been particularly rich and stimulating for me these last years:

- First, it required the development of tools for the simulation of Stokes flows in interaction with particles, leading to the study of fluid/structure problems. After working with finite element discretizations of the flow, I had the opportunity to discover and study boundary element methods.
- In addition, the consideration of close interactions between particles led me to study contact problems, written in the framework of non-smooth convex analysis. This opened the way to new applications such as the study of dry granular materials.
- Finally, we used the fluid/particle solver I had developed to study micro-swimmers. This very first study opened the door to a great amount of research in the field of control and optimal control, in which I was involved in the years following my PhD. These works, together with those related to the study of suspensions, now opens the way to new applications in the field of active suspensions (study of suspensions of active particles, of swimmers).

A great part of my research program is driven by recent advances in the study of suspension and granular media rheology.

“rheology: the branch of physics concerned with the flow and change of shape of matter” [Collins English Dictionary]

I regularly have the opportunity to meet researchers working in this domain, from FAST laboratory in Orsay, Navier laboratory (ENPC) in Marne la Vallée, LPMC in Nice, or LiPhy in Grenoble. I was a member of ANR STABINGRAM (coordinated by P. Gondret, FAST) and participated to GDR Mephy and GDR EGRIN. These collaborations/discussions are fundamental to developing mathematical models and numerical tools that address current challenges. In this spirit, I coordinate the ANR JCJC RheoSUNN (2019-2022), bringing together researchers in the domains of mathematics, numerical analysis, HPC and mechanics and interested in numerical simulations of dense suspensions.

In what follows, I present a state of the art on the rheology of suspensions or granular media. It does not claim to be exhaustive. The objective is to clarify some of the questions that arise and that have partly guided my research work. I then detail my contributions, making the link with the highlighted issues.

1.1 Context and open questions

▷ Rheology of suspensions

Suspensions composed of macroscopic particles immersed in a fluid are found in many fields, including in everyday life. These include industry (food and cosmetics, concrete, reinforced plastics, paper pulp, etc.), nature (silting of rivers, transport of sediments, sandy coasts, lava, etc.), biology (blood tests, etc.) and even ecological concerns (wastewater treatment, etc.). This wide range of applications has led to a large amount of research. However, the flow properties of these systems remain partly poorly understood and raise many questions.

We consider **non-Brownian suspensions, i.e. grains (rigid macroscopic particles) immersed in a viscous fluid**. The forces acting on the particles reduce to hydrodynamic forces exerted by the fluid, contact forces between particles and external forces such as gravity. We are interested in studying the **rheology** of these suspensions: understanding

how they flow or deform due to the application of a force on the system. The first studies of suspension rheology date back to the 1900s and reference is made to [GDR04; GM11; GP18; NSM21] for an overview of the research and issues in this field.

The seminal work dates back to Einstein's thesis in 1905 [Ein05]. In this work he studies the apparent viscosity of a dilute suspension as a function of its concentration. This means that he evaluates the increase in viscosity of a Newtonian fluid when particles are immersed in it. **The link between local viscosity and density is an example of local rheological law.** Although the viscosity of a suspension is only one facet of its rheology, its study reflects the complexity and history of the overall problem. In what follows, I present the evolution of knowledge about the viscosity of suspensions since Einstein's work (for more details, see again [GP18], from which figure 1.1 is taken). The first results date back to the 1900s, in the case of dilute suspensions. It was not until the 1970s and 1980s that results were obtained for semi-dilute suspensions. And it is only recently that the case of dense suspensions has begun to provide answers, leaving many questions still open. As we will see, **experimental studies, theoretical developments and numerical simulations are deeply intertwined and each has its place in the understanding of the problem.**

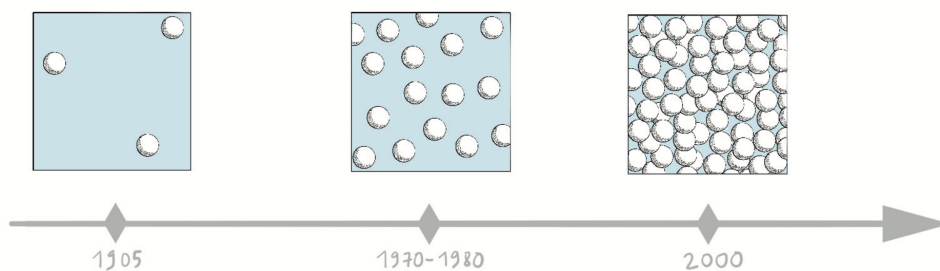


Fig. 1.1: The different regimes of a suspension of rigid spheres: dilute, semi-dilute (or moderately concentrated), and concentrated regimes. Figure from [GP18].

- **Dilute suspensions. Einstein (1905).** The story begins with Einstein's work in 1905, in which he calculates the first order increase in viscosity as a function of the particle density. To do so, he neglects the interactions between the particles. Experimental and numerical works will later show that this approximation is valid for densities below 0.05.
- **Semi-dilute suspensions. (70' -).** In the case of semi-dilute suspensions (density about 0.1), the average distance between particles is of the order of their diameter and their interactions can no longer be neglected. By taking into account the interactions between pairs of particles, Batchelor and Green [BG72] obtained in 1970 the second order expansion of the viscosity as a function of the density. The expansion they obtained is in agreement with experimental and numerical results for solid fractions of the order of 0.1-0.15. More recently, these results have attracted the attention of mathematicians seeking to specify the limits within which they are valid. Techniques such as reflection methods, PDEs, elements of variational or probability methods are used to take into account the interactions between particles (see e.g. [HM12; DG20; GH20; HW20; NS20; Gér21; GH21]).
- **Numerical simulations. (80' -).** Computing the viscosity for denser suspensions is much more difficult. Indeed, it requires not only to compute all the multi-particle interactions but also to determine the micro-structure of the medium: the viscosity now depends on the arrangement of the particles. The previous expansions are no longer valid for densities higher than 0.2. A blow up of the viscosity for a critical value of the density around 0.5-0.6, depending on the physical conditions, is observed in experiments (as a reminder, the maximum compactness of a random packing of spheres is about 0.64). Understanding the behaviour of suspensions with densities greater than 0.2 led to the development of numerical tools since the 1980s, with the widely used Stokesian Dynamics [DBB87; BB88]. This method falls within the framework of the "Discrete Element Method" (DEM). It is a non-direct numerical method: the velocity and pressure fields are not computed and the movements of the particles are deduced from adapted models for the hydrodynamic forces. Direct methods, solving the Stokes equations coupled to the solid motion, were then developed in the 1990s (multipole expansions, finite elements, finite volumes, boundary elements methods...). **Unlike DEM methods, direct methods provide approximations of the velocity and pressure fields in the fluid domain.** One can cite for example the Force Coupling Method [LM03] or fictitious domain methods based on Lagrange multipliers [WT06; Wac09; Wac11; Gal+14b]. These

numerical methods lead to efficient codes that can be used to study the rheology of suspensions (see e.g. [CM03; Gal+14b; Est+17; RHW18; Li+20]).

- **Dense suspensions. (2000 -).** The study of dense suspensions is particularly delicate and few results are available. From a numerical point of view, the stiffness of close interactions between particles makes the problem difficult to solve (see next section on lubrication). Recently, the viscosity blow-up for a critical value of the density has been observed for the first time in numerical simulations. This behaviour could be found numerically by introducing a **friction model** between the particles [Gal+14b; Mar+14]. It suggests that the consideration of solid contact is essential in the study of dense suspensions. From a theoretical point of view, variational methods led to a few homogenisation-like results (see [KB04; BGN09]). One of the goals is to derive **macroscopic laws**, leading to **continuous modelling** of these systems (such as effective fluid models or two-phase models. See e.g. [NGP11; Bou+16]).

100 years after Einstein's original work many questions remain open and the study of suspensions' rheology is still a very dynamic domain of research.

- **Rheology of monodisperse suspensions.** *Despite the large number of works carried out in this field, the study of suspensions composed of spheres with the same radius (mono-disperse suspensions) has not yet revealed all its secrets. While theoretical results for dilute suspensions have been available since the 1900s, the description of semi-dilute or dense suspensions is more difficult. Their behaviour depends finely on the microscopic configuration and writing laws for local macroscopic quantities and deriving continuous models are still opened problems. Progress in the understanding of their behaviour will require the development of numerical simulations. To carry out such studies, it is essential to develop codes based on a **direct resolution method** that takes into account **close hydrodynamic interactions** as well as **solid contacts**.*
- **Polydisperse suspensions and particles with more general shapes.** *The behaviour of suspensions composed of spherical particles with various radii (polydisperse or even bidisperse suspensions) is still poorly documented. Similarly, the case of non-spherical particles has not been much addressed. Let us for example consider the case of fibers, which are very useful from an industrial point of view. Explicit approximations can be made at large distances in the dilute case. However, the results are much more complex than for spherical particles. Indeed, the microstructure now affects the rheology from the lowest concentrations: the relative positions of the fibers influence the overall*

behaviour of the system. The rheology of dense fiber suspensions is still a very open domain of research and numerical simulation should play an important role in its understanding.

▷ **Lubrication and numerical simulations.**

Numerical simulation of suspensions is an indispensable tool for a better understanding of their rheology. This obviously requires a code solving the Stokes problem in the fluid and coupled to the rigid motion of the particles. As already mentioned, a number of solutions are available, ranging from non-direct to direct solvers. However, in general, this is not sufficient. One of the difficulties with numerical simulation of such systems is to take account of the interactions between the particles when they get close to each other.

When two particles move towards each other, the fluid in the gap between the two particles drains away. Being viscous and incompressible, it tries to oppose the deformation induced by the movement and generates in return a force on the particles. This is the so-called **lubrication phenomena**. This force opposes the relative movement of the particles. The study of lubrication forces goes back to the 1960s with the works of Brenner and Maude [Bre61; Mau61]. In 1974, Cox carried out the asymptotic expansion of the force exerted between two smooth solids of any shape, evolving in a Stokes fluid [Cox74]. When the distance tends to zero, the force is proportional to the relative velocity and is singular as the inverse of the distance. Consider for a moment a particle of radius r , mass m , located at a distance d above a plane, immersed in a fluid of viscosity μ and subjected to an external force f (such as gravity). We can then write a simplified model for the evolution of d : we write the fundamental principle of dynamics and approximate the force exerted by the fluid on the particle by the asymptotic expansion given by Cox. We then obtain the following differential equation:

$$m\ddot{d}(t) = -6\pi\mu r^2 \frac{\dot{d}(t)}{d(t)} + mf. \quad (1.1)$$

Lipschitz theorem shows that the solution of this differential equation is global: the distance d remains strictly positive. The lubrication force is sufficiently large that there is never contact between the plane and the particle in finite time. One can also prove the "non-contact in finite time" property for the full model of a rigid smooth particle immersed in a Stokes fluid (see e.g. [HT09]).

The consideration of the lubrication force, which is **singular when the distances are small**, is essential to obtain physical behaviour in the case of semi-dilute or dense suspensions. Indeed, in this case, the pairs of close particles are numerous and their effect becomes dominant. Unfortunately, **the singularity of the phenomenon makes it difficult to capture numerically**.

- **Space singularity.** At each time step, the configuration being given, it is necessary to solve the fluid/particle problem, while capturing the flow in the interstice between the particles. An example of velocity and pressure fields obtained for two close particles approaching each other is plot in figure 1.2 (a precise description of the test is given in chapter 2, section 2.2). In order to capture the effects of

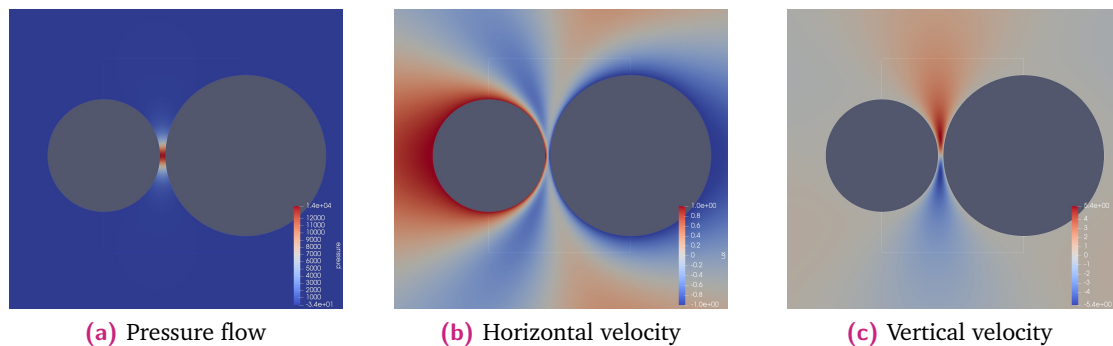


Fig. 1.2: Reference flow for two particles with opposite velocities along the horizontal direction.

the pressure peak and the variation of the velocity field, it is essential to develop methods that capture the singularity, while maintaining reasonable computation times (avoiding, for example, too fine meshes between close particles in the case of direct solvers). For example, the Stokesian Dynamics method proposes to correct the forces computed by the solver [DBB87; BB88]. This correction was extended more recently in [Gal+14a] in the framework of a direct method. Unfortunately, while the **effects of lubrication** are taken into account when calculating the forces on the particles, they **are not transmitted to the pressure and velocity fields**. Moreover, the total force being dependent on the shape and orientation of the particles, the contribution of lubrication **cannot easily be computed for non-monodisperse suspensions**.

- **Time singularity and contact model.** Let us now assume that the lubrication effects can be computed accurately using an adapted solver. The remaining numerical difficulty is similar to that associated with the time discretization of the

stiff differential equation (1.1). We already know that particles cannot touch each other in finite time. Unfortunately, overlaps due to approximation errors cannot be avoided at a fixed spatial and temporal accuracy. It is therefore necessary to develop numerical strategies to avoid these numerical overlaps. Recall now that it has been shown it was necessary to take into account solid friction in simulations of suspension: real particles are not smooth and may touch each other. Then we see that using a **solid contact model** to avoid overlaps is fully justified, both from a physical and numerical point of view. In order to take into account the lubrication effect due to the residual interstitial fluid layer during numerical contact, one can also use the so-called "gluey contact" model [6] that I developed during my PhD thesis, under the supervision of B. Maury.

Although efforts to take into account the lubrication phenomenon in numerical simulations date back to the 1980s, the methods developed do not answer current questions about suspensions' rheology. Indeed, the phenomena studied are becoming more and more refined and lead to new needs, which in turn are sources of new numerical challenges.

- **Lubrication for non-spherical particles.** *As highlighted in the previous section, the study of non-spherical particle suspensions is a very active domain of research. However, techniques to take into account lubrication are currently limited to monodisperse suspensions. There is a great need for methods that can be extended to the polydisperse or even non-spherical case in the semi-dilute and dense regimes.*
- **Precise resolution of the flow.** *The physical phenomena studied are now more and more sophisticated: it becomes necessary to have precise data on the behaviour of particles (position, velocities) but also on the fluid. The development of direct methods, solving the coupled fluid/particle problem provides numerical approximations of the pressure and velocity fields. However, existing methods to account for lubrication do not convey its effects on these fields and algorithms must now be designed to solve this problem.*

▷ **From suspensions to granular media.**

As already seen, for both physical and numerical reasons, simulation of suspensions requires the development of algorithms to manage solid contact between particles. These contact algorithms can of course be used to study **dry granular materials rheology**, which is also a very active research domain.

These materials are composed of **solid particles of macroscopic size** in the sense that they are large enough not to be subject to Brownian forces. They can interact through a wide variety of **inter-particle forces** and are subject to **dissipative contacts that may involve friction**. They are omnipresent in our daily lives (sugar, rice, pasta in the kitchen, piles of pebbles, legos for the youngest...), in nature (piles of sand, dunes, sandy coasts, rock avalanches...), in industry or the agri-food industry (grain silos, storage of medicines...).

Understanding the properties of their flows would provide answers to many industrial and environmental questions. Being able to both "flow" like a fluid or remain motionless like a solid, their behaviour is still poorly understood. **Their behaviour is often divided into three states**. A first "dense/quasi-static" state, in which the grains undergo frictional contact, which lasts over time, the medium then reacts like a **deformable solid**. In contrast, a "diluted" state is defined by a rapid flow, leading to instantaneous collisions between particles, the medium reacts like a **gas**. A final "dense intermediate" state is described, in which there are both frictional contacts that persist and collisions, the medium reacts like a **liquid**.

As for suspensions, understanding the complex rheology of these systems plays a key role for applications. Furthermore, the transition from one state to another (fluid or solid) also plays a major role. In this very active field of research, questions similar to those described for suspensions arise. Indeed, one seeks to obtain rheological laws, linking different macroscopic quantities having a mechanical meaning. The goal is to deduce continuous models for this type of material. Again, the establishment of such models requires the implementation of numerical simulations at microscopic level, in order for example to determine and study the local macroscopic quantities of interest. We refer to [FP08; GDR04; AFP13; RRD17] for the state-of-the-art of the physics of granular media and recent advances in the field. In what follows, I give an idea of some problems that arise and for which numerical simulations can be useful.

Local rheological laws. In the early 2000s, research focused on obtaining local rheological laws for dense cases. In the case of suspensions, it was sought to relate the local density to the local apparent viscosity. In the case of granular media, a dimensional analysis showed that a dimensionless number I , called the inertia number, should control the local flow [Cru+05; LLC05]. This number links the time scale of the macroscopic flow (global flow velocity) to the time scale of the microscopic rearrangements (rate of change of local configurations). When this number is small, one tends towards the dense/quasi-static regime and when it increases, one approaches the dilute regime. In

the same articles, numerical simulations confirm, for example, a link between the local effective friction coefficient and this dimensionless number. Local rheological laws in agreement with the numerical results were then proposed [JFP06; Pou+06]. Attempts have been made to develop macroscopic models, from these local laws (Navier-Stokes models with viscosity depending on I). However, it was shown in [Bar+15] that the resulting problem was well-posed for intermediate values of I but was unstable for large and small values. It becomes well-posed if the fluid is considered compressible [Hey+17] but such models involve new variables for which little information is available.

Towards non-local models. Local laws can correctly describe linear flows (e.g. shear flows) or sufficiently fast 3D flows. Unfortunately, these local laws fail when the density of the medium approaches the maximum compactness and quasi-static flows. Indeed, in this case, **long-range correlations** are observed [RR02; LLC05]. The macroscopic properties in these dense media are then intimately linked to the anisotropy and distribution of contacts [Cru+05], to the formation of clusters [HE05] or arches [MLT99]. Since local rheological laws do not allow for this type of phenomenon, non-local rheological models have been developed. A review of these models is proposed in [Kam19]. All of them involve a notion of **intrinsic length scale of the medium**, allowing non-local effects to be taken into account. They have some success in the case of inhomogeneous systems, where local models fail. Moreover, it has been shown that some of them are well-posed, see [Kam19] for references on this subject.

Granular materials as a first step towards suspension modelling. From a numerical point of view, it has been shown that the consideration of solid contacts in simulations of suspensions is essential to obtain results in agreement with experiments. Any improvement of numerical methods for dry granular materials is therefore immediately translated, via a coupling with a fluid code, by similar progress for suspensions (see e.g. [Mar+14] or [Gal+14b]). Beyond this numerical aspect, the study of granular media also brings new ideas for a better modelling of dense suspensions. For example, the effect of the presence of an interstitial fluid between the grains has been studied. This has led to consider a new dimensionless number J similar to the inertia number I and for which the time scale of microscopic rearrangements is replaced by a viscous time scale [CNP05; SP05]. One then obtains local rheological laws expressing the apparent viscosity and the solid volume fraction in terms of this new dimensionless number [GP18]. In order to model the effects of contacts, the development of non-local rheological laws could also be considered for dense suspensions.

The study of dry granular materials is a rapidly expanding field with multiple applications. Understanding the flowing properties of these materials is all the more interesting as it would also allow progress in the study of dense suspensions.

- **Need for stable, long-time simulations.** *Despite numerous experimental, numerical and theoretical studies, many questions concerning the continuous modelling of granular materials remain open. Macroscopic models are based on variables whose physical origin at the grain scale is not always clear. The difficulty is to identify the relevant local geometrical parameters, leading to new rheological laws and well-posed continuous problems. In order to reproduce the complexity of the medium, these parameters must be closely related to its microscopic structure: anisotropy, orientation of non-spherical particles, geometry of the contact network... Another challenge is the study of length scales in the flow which are fundamental to write non-local models for example. Numerical simulation is of great help in addressing these problems. It requires the use of **stable numerical methods**, allowing long time simulations of a **large number of non-spherical particles**. Note again that such algorithms would also help to answer the questions that still arise for dense suspensions.*

▷ From suspensions to micro-swimmers

The study of suspensions rheology leads to the question of extending (or not) the observed behaviour to more general systems. A natural extension is the study of the so-called "active" suspensions. These are composed of self-propelled particles and micro-organisms that are able to swim by converting chemical energy into mechanical work. One can think for example of bacteria, unicellular eukaryotes or special cells of multicellular organisms such as sperm cells. Both the study of individual swimmers and the study of collections of swimmers are of great interest.

Can a swimmer swim? Understanding the swimming strategy of micro-organisms has several applications in biophysics or medicine. For example, this could help design tools to limit the movement of harmful bacteria or improve the movement of cells such as spermatozoa. Another striking application is the design of micro-robots capable of performing in-vivo sensing and delivering drug to a given localized target. To achieve this goals, it is essential to answer the following two questions: can the swimmer swim and how can it do it? Although seemingly simple, this problem is difficult and has attracted considerable attention in the recent literature, starting from the pioneering works of Taylor [Tay51], Lighthill [Lig52] and later Berg and Anderson [BA73], Purcell [Pur77]

and Shapere and Wilczek [SW89a; SW89b]. We refer to the paper [LP09; Gom+20] for a description of known biological swimming mechanisms and an overview of the subject.

The problem faced by micro-organisms is to **swim at low Reynolds numbers**. Indeed, the Reynolds number (Re) measures the ratio between inertial and viscous forces. Due to the length and time scales involved, the motion of micro-swimmers is dominated by viscosity, while inertia is negligible (see figure 1.3, from [Pur77]).

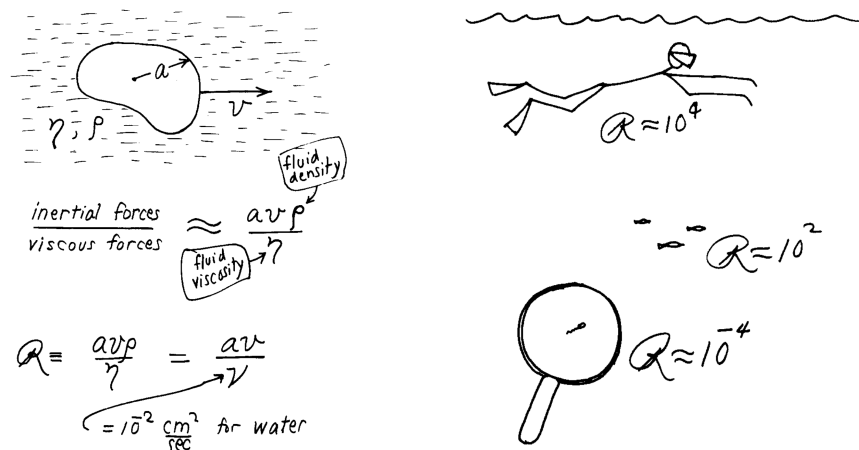


Fig. 1.3: Reynolds number (left) and Swimming at different Reynolds numbers (right). Figures from [Pur77].

Swimming at low Reynolds numbers requires micro-organisms to adopt completely different swimming strategies from those employed by larger organisms., such as fish, or humans (see again figure 1.3). To better understand life at low Reynolds number, one can follow Purcell:

“Now imagine yourself in that condition: you’re under the swimming pool in molasses, and now you can only move like the hands of a clock. If under those ground rules you are able to move a few meters in a couple of weeks, you may qualify as a low Reynolds number swimmer.” [Pur77]

Another striking observation of Purcell (see figure 1.4) is that, at low Re , any organism trying to swim adopting the reciprocal stroke of a scallop, which moves by opening and closing its valves, is condemned to the frustrating experience of not having advanced at all at the end of one cycle. Thus, whatever forward motion is achieved by the scallop by closing its valves, it will be exactly compensated by a backward motion upon reopening them. Since the low Re world is unaware of inertia, it will not help to close

If $Re \ll 1$:

Time doesn't matter. The pattern of motion is the same, whether slow or fast, whether forward or backward in time.

The Scallop Theorem



Fig. 1.4: The scallop theorem. Figure from [Pur77].

the valves quickly and reopen them slowly. This observation, which became known as the *scallop theorem*, started a stream of research aiming at **finding the simplest mechanism by which cyclic shape changes may lead to effective self propulsion at small length scales**. Several proposals have been put forward and analyzed, see e.g. [Tay51; Pur77; NG04; AKO05; BKS03]. A particularly simple example, due to Najafi and Golestanian [NG04], is the three-sphere swimmer. In its simplest form, it consists of three equal spheres of same radius moving along a straight line.

What about collections of swimmers? The interest in active suspensions, composed of collections of swimmers is motivated by several applications. For example, studying the complex collective dynamics of biologically active suspensions would provide a better understanding of biophysical processes such as bacterial transport and diffusion. On the other hand, designing artificial active suspensions would have a wide variety of applications, such as the mixing or transport of substances at the microscopic scale. Active suspensions have surprising characteristics. Indeed, the coupling between the fluid and the deformation of the particles leads to **unusual rheologies**, very different from those observed for passive suspensions. For example, it has been shown that the effective viscosity of an active suspension can decrease with the increase of volume fraction. A second order asymptotic expansion of the viscosity as a function of the density was derived for a specific 2d active suspension in [Hai+08]. The authors obtain the classical result for passive suspensions with an additional term, due to self-propulsion. This term explains the decrease in viscosity for this active suspension. Studying the rheology of active suspensions is therefore quite fascinating. It is a particularly active and challenging domain of research. We refer to [Sai18] for a review of existing results and open questions on this subject.

Swimming at low Reynolds number is an active domain of research. Understanding the individual and collective behaviour of micro-organisms leads to both theoretical and numerical challenges.

- **Swimming mechanisms at low Reynolds numbers.** A great amount of research has been conducted to provide a **theoretical framework** for studying the choices of swimming strategies available to micro-swimmers. The problem writes as a fluid-structure problem in which the fluid domain varies with time (following the swimmer's shape). The objective is to understand whether there exists a succession of cyclic deformations of the shape (a stroke) that allows swimming (moving forward, turning). If the answer is positive, one can then look for the stroke that spends the least amount of energy. The dependence of the solution on the shape of the swimmer is highly non-linear which leads to challenging problems. In addition to theoretical studies, numerical simulation of these swimmers is also important for a better understanding of the mechanisms they use. It requires the solution of a fluid/structure problem for a large number of different shapes. An **efficient fluid/structure solver** is therefore essential.
- **Rheology of active suspensions.** As with passive suspensions, the aim is to write continuous **macroscopic models** to describe active suspensions. Again, **numerical simulation** is of great help in understanding the link between the microscopic configurations and the global behaviour. The simulation of swimmers introduces new numerical needs. For example, it becomes necessary to discretise coupled problems between the Stokesian fluid and **deformable structures**. In addition, the internal forces applied by the swimmer to deform can generate significant hydrodynamic forces. It may then be necessary to use specific strategies to deal with **lubrication forces**, even for intermediate densities.

1.2 Contributions

I describe in this section my different contributions, making the link with the issues highlighted in the previous section. Some of these contributions, further away from my current research concerns, are not discussed in the manuscript. I specify the corresponding articles and chapters where appropriate.

▷ Macroscopic modelling of suspensions

Lubrication: micro-macro modelling. [7]

Collaborator: Resulting from my PhD thesis - supervisor B. Maury (LMO, Orsay).

Issue: Macroscopic modelling of suspensions.

- This work is a first step towards a **macroscopic description of collections of particles interacting through the lubrication force**. We consider a discrete system of aligned spheres interacting through the lubrication force. The force is modelled by the asymptotic expansion given in [Cox74]. It is dissipative, and singular near contact: it behaves like the reciprocal of the interparticle distance. We propose a macroscopic constitutive equation which is built as the natural continuous counterpart of this microscopic lubrication model.

We establish the convergence in a weak sense of solutions to the discrete problem towards the solution to the partial differential equation which we identified as the macroscopic constitutive equation. It is an homogenization-like result. The microscopic solution converges to the macroscopic one when the size of the particles ϵ vanishes. The number of particles increases as $1/\epsilon$. Some previous homogenized models for suspensions had been obtained for sets of particles in dimension 2 or 3. The authors supposed that the configuration was periodic or that distances between neighbouring particles were subject to behave like ϵ . The approach we propose is based on a simpler model from the geometric standpoint, as the spheres are supposed to be aligned. On the other hand it generalizes these works in the sense that no assumption is made on the distances: the macroscopic behaviour depends on the local solid fraction only. Contacts between neighbouring particles are even allowed, and a special attention is paid to the way we express the continuous model so that macroscopic clusters can be taken into account (the local viscosity within a cluster is infinite).

This model, which is of the newtonian type, relies on an extensional viscosity, which is proportional to the reciprocal of the local fluid fraction. If u is the velocity, ρ the density and f the force, the limit model writes:

$$\begin{aligned}\partial_t \rho + \partial_x(\rho u) &= 0, \\ -\partial_x \left(\frac{1}{1-\rho} \partial_x u \right) &= \rho f.\end{aligned}$$

▷ Numerical simulation of suspensions

Direct fluid solver and gluey contact model. [1,2,6]

Collaborator: Resulting from my PhD thesis - supervisor B. Maury (LMO, Orsay).

Issues: Direct numerical simulation of suspensions. Contacts and lubrication.

- During my PhD thesis, I developed a direct method to simulate suspensions. In [1,2], a **penalty method** is proposed to deal with the rigid constraint: the rigid motion is enforced by penalizing the strain tensor on the rigid domain. From a physical point of view, this amounts to considering the rigid particles as a fluid subdomain with infinite viscosity. This method, associated to the method of characteristics for the time discretization leads to a generalized Stokes variational formulation on the whole domain. It can be easily implemented from any finite element Stokes/Navier-Stokes solver. It has been used in [1] to simulate a single body attached at one of its points. In [2] we focus on the simulation of suspensions. In order to ensure robustness, we describe a strategy to take collisions into account. It is based on a time-stepping scheme for inelastic collision proposed by Bertrand Maury in [Mau06]. At each time step, the forces are computed in an implicit way, as solution to a convex optimization problem. This leads to a **stable contact algorithm** which solves the difficulty due to the stiffness of the contact forces.
- One of the main result of my PhD work, described in [6], is the development of a model and a numerical scheme to compute the motion of rigid particles interacting through the lubrication force. In the case of a particle approaching a plane, I propose an algorithm and prove its convergence towards the solution to the gluey particle model described in [Mau07]. Then, I describe a multi-particle version of this **gluey contact model** which is based on the projection of the velocities onto a set of admissible velocities. The corresponding algorithm is an extension of the one proposed for inelastic contacts, leading to a **stable numerical method to model**

lubrication. I implemented the inelastic and gluey contacts in C++ (code SCoPI - Simulation of Collection of Particles in Interaction).

Lubrication: coupling (stable) contact models to fluid solvers. [3,4,8]

Collaborators: M. Ismail (LiPhy, Grenoble), P. Laure (Labo. JA Dieudonné, Nice), L. Lobry (LPMC, Nice), N. Verdon (Labo. JA Dieudonné, Nice).

Issues: Direct numerical simulation of suspensions. Contacts and lubrication.

- The inelastic and gluey models proposed in [Mau06] and [6] have been coupled to fluid solvers to simulate vesicles and suspensions.
- With P. Laure, L. Lobry and N. Verdon, we compared in [3,8] the two contact models for the simulation of solid particles in a Stokesian fluid. The fluid solver is a fictitious domain method and the rigid constraint is imposed using an augmented Lagrangian method. We show that **contact modelling influences the properties of the suspension**. For example, the reversibility of the Stokes equations is usually lost in the simulations, due to numerical discretizations. Using the viscous contact model makes it possible to recover this reversibility, thanks to the good approximation of the lubrication force. We also show that by **using the gluey contact model, larger time steps can be used, while maintaining good accuracy for close interactions**.
- With M. Ismail, we used the penalty method to simulate **2D vesicles interacting with a newtonian fluid**. The inextensible membrane is modelled by a chain of circular rigid particles which are maintained in cohesion by using two different type of forces. First, a spring force is imposed between neighboring particles in the chain. Second, in order to model the bending of the membrane, each triplet of successive particles is submitted to an angular force. The inelastic contact model prevents interpenetration of the particles. Exploring different ratios of inner and outer viscosities, we recover the well known “Tank-Treading” and “Tumbling” motions predicted by theory and experiments. Moreover, for the first time, two dimensional simulations of the “Vacillating-Breathing” regime, predicted by theory and observed experimentally, are achieved without any special ingredient (such as thermal fluctuations).

Lubrication before contact: a precise fluid solver. [9,10,11, Chap.2]

Collaborators: B. Merlet (Labo. Paul Painlevé, Lille), F. Nabet (CMAP, Palaiseau), T.N. Nguyen (PhD CMAP, Palaiseau), F. Vergnet (Post-doc CMAP, Palaiseau / LJLL, Paris).

Issues: Effects of lubrication on the whole flow. Lubrication for non-spherical particles.

- The gluey contact model proposed in [6] provides a stable algorithm to take into account lubrication in numerical simulations. However, it is coupled with fluid solvers through a splitting method. As a result, the effects of lubrication are transmitted to the particles but the fluid velocity and pressure fields are not corrected. Recent rheological studies require accurate information on the whole flow. The objective of these works is to develop a method which transmits the effects of lubrication not only to the particles but also to the velocity and pressure fields in the fluid domain.
- As a first step towards suspensions, we focus on the Dirichlet to Neumann problem (particle velocities are given, we want to calculate the corresponding velocity and pressure fields in the fluid domain). With Benoit Merlet, in the framework of T.N. Nguyen's PhD thesis (supervised by B. Merlet), we proposed in [9] to **decompose the whole flow into a singular part and a regular part**: if (\mathbf{u}, p) is the solution, we write

$$(\mathbf{u}, p) = (\mathbf{u}^{\text{sing}}, p^{\text{sing}}) + (\mathbf{u}^{\text{reg}}, p^{\text{reg}}),$$

where $(\mathbf{u}^{\text{sing}}, p^{\text{sing}})$ is the singular part of the solution arising from lubrication. It is supposed to be known explicitly and is computed off-line. It has to be defined such that the remaining field $(\mathbf{u}^{\text{reg}}, p^{\text{reg}})$ is regular, in the sense that it is bounded independently of the distance between the particles. This regular field is computed online. Since it is regular, an accurate solution can be computed using any fluid/structure solver and there is no need to use a very fine mesh between the particles. At the end of the procedure, an accurate solution (\mathbf{u}, p) , taking into account the lubrication, can be reconstructed.

- To apply the method, it remains to say how the singular field is estimated. In [9], we propose to decompose the singular flow on a vectorial spherical harmonic basis and we interpolate the coordinates of the singular pressure and velocity fields in this basis. For interpolation to be possible, the singular field must depend on a single parameter (here, the distance between the particles). This is only the case if we consider monodisperse suspensions (spherical particles of the same radius). Indeed, in the opposite case, the singularity depends on the ratio between the

radii of the spheres or on the orientation of the particles in case they are not spherical. The proposed method therefore **allows the effects of lubrication to be accurately transmitted throughout the fluid domain** but is restricted to the case of monodisperse suspensions.

- To overcome this limitation, I proposed in [10] to use an **explicit asymptotic expansion of the solution** to estimate the singular field. In [11], we propose with Flore Nabet such an expansion and prove that the remaining field is regular. Our singular field is an adaptation of the asymptotic expansion proposed by Hillairet and Kelai in [HK15], which is modified to make it more tractable from a numerical point of view. The method is tested on 2D academic cases, using a fluid solver based on a fitted mesh. The asymptotic expansion being available for **various shapes of particles** (strictly convex near the contact point), this new method is more general than the interpolation proposed in [9] and meets the needs of recent rheological studies. With Fabien Vergnet and Flore Nabet, we are currently working on extending this method to fictitious domain solvers.

Fluid solvers: development of new BEM tools for Stokes [12,13, Chap. 3]

Collaborators: F. Alouges (CMAP, Palaiseau), M. Aussal (CMAP, Palaiseau), F. Pigeonneau (Saint Gobain Recherche), A. Sellier (LadHyX, Palaiseau).

Issues: Direct numerical simulation of suspensions or micro-swimmers.

- In these works, we are interested in the use of a **Boundary Element Method** (BEM) for the simulation of suspensions. The BEM method falls into the class of direct resolution methods. Compared to volumic methods such as finite elements or finite volumes, one of its advantages is that it is based on a surface mesh of the particles, which limits the number of unknowns. In view of the applications we have in mind, another advantage of these methods is that the geometry of the particles is accurately taken into account. This makes the method **particularly suitable for the fine study of lubrication or for the simulation of swimmer's strokes**. However, there are two classic difficulties in implementing BEM methods: the **design of fast solvers** to compute the solution of the problem (the matrix of the discrete problem is full) and the **computation of singular integrals** appearing in the coefficients of the matrices.
- In [12,13] we show how the methods developed by François Alouges and Matthieu Aussal in the context of Helmholtz and Maxwell equations can be extended to Stokes equations. The main difficulty being that Stokes problem is a three dimensional

problem (three dimensional variables and unknowns). Concerning the fast solver, we extend the so-called Sine Cardinal Sparse Decomposition (SCSD) to Stokes kernel. This method is based on a (sparse) decomposition of radial kernels on a basis of cardinal sines. Since Stokes kernel is not radial, the method does not apply directly. To overcome this difficulty, we rewrite the kernel as a sum of derivatives of radial kernels. Concerning the singular integrals, we again extend a semi-analytic method implemented by François Alouges and Matthieu Aussal for Helmholtz and Maxwell kernels. To do so, we express Stokes' singular integrals as sum of boundary terms and of singular integrals already computed for Laplace kernel. We studied on academic cases in [12] the order of convergence and the CPU time of the method. In [13], it is shown that **the method accurately captures the close interactions between a spheroid and a wall**. This is a very encouraging result in view of its application to simulation of suspensions.

▷ **Numerical simulation of granular flows**

A result of convergence [15, Chap. 4 Sec. 4.2]

Collaborator: F. Bernicot (Labo. Jean Leray, Nantes).

Issue: Stable contact algorithms.

- The inelastic contact algorithm proposed by Bertrand Maury [Mau07] and its extension to viscous contacts [6] are implemented in the code SCoPI and used for the simulation of granular media or suspensions. These methods have excellent stability properties and good behaviour for large time steps. Bertrand Maury has proved, in the case of a single contact, the convergence of the discrete solution to a continuous contact model. The limit model is a Non Smooth Contact Dynamics like model. It enters the framework of **non-smooth convex analysis** developed by JJ Moreau in the 1970s. The model consists in a system of differential inclusions of order two in time, with non-overlapping constraints between the particles. With Frédéric Bernicot, we proved the **convergence of the inelastic contact algorithm in the multi-particle case**. We follow the scheme of B. Maury's proof for a single contact. New arguments allow to handle multiple contacts. These arguments had been used by Juliette Venel in [Ven11] where the author models crowd movements by first order systems with non-overlapping constraints similar to ours.

Some first macroscopic studies [14,16, Chap. 4 Sec. 4.2]

Collaborators: S. Faure (LMO, Orsay), P. Gondret (FAST, Orsay), A. Seguin (FAST, Orsay), B. Semin (PMMH, ESPCI, Paris).

Issue: Rheology of granular media using numerical simulations.

- With Sylvain Faure, we **optimized the code SCoPI and implemented post-processing functions so that it can be used for rheological studies**. Sylvain Faure implemented a shared memory parallelism and revised the format of the output files. The code can return local quantities of physical interests such as pressure, stresses, density, distribution and mean number of contacts...
- In [14], with Benoît Semin, we studied the **random packing of non-convex particles**. The particles are composed of two interpenetrating spheres. After validating the code for spherical particles, we studied the random compaction and the distribution of contacts as a function of the interpenetration length.
- In [16], with Antoine Seguin and Philippe Gondret, we studied the flow in front of a sphere moving into a grain cloud. We launched a simulation campaign, the granular medium being composed of up to 900 000 grains. We studied the cluster size in front of the moving sphere and conducted a **detailed study of the rheology inside the cluster**. The results proved that a local rheology based on the inertial number I can be observed in the case of non-parallel flows, which had never been reported before.

Towards friction [Chap. 4, Sec. 4.3]

Collaborators: H. Martin (PhD IPGP, Paris), B. Maury (LMO, Orsay).

Issues: Stable contact algorithm for friction. Friction in simulations of suspensions.

- This recent work has been initiated in the framework of Hugo Martin's PhD thesis, supervised by Anne Mangeney (IPGP) and Yvon Maday (LJLL). With Bertrand Maury, we participated in the development of a stable algorithm for dry frictional contacts. This is a work in progress, for which an article is being prepared.
- The methods falls in the framework of **Non-Smooth Contact Dynamics** and can be seen as an extension of the inelastic algorithm proposed by Bertrand Maury in [Mau07]. The natural schemes for friction lead to linear complementarity problems which prove to be expensive to solve. Following [Mau07] and in the spirit of [Ani06], we propose a **scheme based on a single convex optimization problem to be solved at each time step**. This is done to the price of a "convexification"

of the constraint, which can generate over estimations of the non-overlapping constraint and dilatancy of the granular media. We prove that the corresponding optimality conditions are a discretization of the continuous problem. The corresponding algorithm was implemented for spherical particules by Hugo Martin during its PhD thesis. It is verified that the convexification of the constraint is not an obstacle to the simulation of granular collapse. To do so, we compare the results with those obtained by a code based on the natural, non-convex scheme. Once validated, the code was used by Hugo Martin to study three dimensional collapses on erodible beds.

▷ **Micro-swimmers**

Some controlability results [17,18,19,20,21, Chap. 5]

Collaborators: *F. Alouges (CMAP, Palaiseau), A. DeSimone (SISSA, Trieste), L. Heltai (SISSA, Trieste), B. Merlet (Labo. Paul Painlevé, Lille).*

Issue: *Swimming and optimal swimming of micro-swimmers.*

- In the series of articles [17,18,20,21], we study 3 self-propelled stokesian robots composed of balls, connected by arms whose length can be controlled by the swimmer. They can move respectively in dimension 1, 2 and 3. In these works we provide a unified theoretical framework, based on geometric control theory. The swimming problem is rephrased as a **controllability problem**: the displacement being given, can the swimmer execute a stroke, i.e. a cyclic shape change (the control) leading to this displacement? Once controllability is known, optimal swimming is written as an **optimal control problem**: what is the stroke leading to the minimal energetic cost? In [21], we end up proposing a general framework, covering the 3 swimmers, and we show that each of them can swim, i.e. control its position, as well as its orientation in 2d and 3d. Numerical computations of optimal strokes are also reported. A similar control framework is proposed in [19] to study general axisymmetric swimmers.

References

- [AFP13] B. Andreotti, Y. Forterre, and O. Pouliquen. *Granular media: between fluid and solid*. Cambridge University Press, 2013 (cit. on p. 9).
- [Ani06] M. Anitescu. “Optimization-based simulation of nonsmooth rigid multibody dynamics”. In: *Mathematical Programming* 105.1 (2006), pp. 113–143 (cit. on p. 21).
- [AKO05] J. E. Avron, O. Kenneth, and D. H. Oaknin. “Pushmepullyou: an efficient micro-swimmer”. In: *New Journal of Physics* 7 (2005), pp. 234–234 (cit. on p. 13).
- [Bar+15] T. Barker, D. G. Schaeffer, P. Bohorquez, and J. M. N. T. Gray. “Well-posed and ill-posed behaviour of the μ -rheology for granular flow”. In: *Journal of Fluid Mechanics* 779 (2015), pp. 794–818 (cit. on p. 10).
- [BG72] G. K. Batchelor and J. T. Green. “The determination of the bulk stress in a suspension of spherical particles to order c^2 ”. In: *Journal of Fluid Mechanics* 56.03 (1972), p. 401 (cit. on p. 4).
- [BKS03] L. E. Becker, S. A. Koehler, and H. A. Stone. “On self-propulsion of micro-machines at low Reynolds number: Purcell’s three-link swimmer”. In: *Journal of Fluid Mechanics* 490 (2003). Publisher: Cambridge University Press, pp. 15–35 (cit. on p. 13).
- [BA73] H. C. Berg and R. A. Anderson. “Bacteria Swim by Rotating their Flagellar Filaments”. In: *Nature* 245 (1973), pp. 380–382 (cit. on p. 11).
- [BGN09] L. Berlyand, Y. Gorb, and A. Novikov. “Fictitious Fluid Approach and Anomalous Blow-up of the Dissipation Rate in a Two-Dimensional Model of Concentrated Suspensions”. In: *Archive for Rational Mechanics and Analysis* 193.3 (2009), pp. 585–622 (cit. on p. 5).
- [Bou+16] F. Bouchut, E.D. Fernández-Nieto, A. Mangeney, and G. Narbona-Reina. “A two-phase two-layer model for fluidized granular flows with dilatancy effects”. In: *Journal of Fluid Mechanics* 801 (2016). Publisher: Cambridge University Press, pp. 166–221 (cit. on p. 5).
- [BB88] J F Brady and G Bossis. “Stokesian Dynamics”. In: *Annual Review of Fluid Mechanics* 20 (1988), pp. 111–157 (cit. on pp. 4, 7).
- [Bre61] H. Brenner. “The slow motion of a sphere through a viscous fluid towards a plane surface”. In: *Chemical Engineering Science* 16.3-4 (1961), pp. 242–251 (cit. on p. 6).
- [CNP05] C. Cassar, M. Nicolas, and O. Pouliquen. “Submarine granular flows down inclined planes”. In: *Physics of Fluids* 17.10 (2005), p. 103301 (cit. on p. 10).
- [CM03] E Climent and M.R Maxey. “Numerical simulations of random suspensions at finite Reynolds numbers”. In: *International Journal of Multiphase Flow* 29.4 (2003), pp. 579–601 (cit. on p. 5).

- [Cox74] R. G. Cox. “The motion of suspended particles almost in contact”. In: *International Journal of Multiphase Flow* 1.2 (1974), pp. 343–371 (cit. on pp. 6, 15).
- [Cru+05] F. da Cruz, S. Emam, M. Prochnow, J-N. Roux, and F. Chevoir. “Rheophysics of dense granular materials: Discrete simulation of plane shear flows”. In: *Physical Review E* 72.2 (2005), p. 021309 (cit. on pp. 9, 10).
- [DG20] M. Duerinckx and A. Gloria. “On Einstein’s effective viscosity formula”. In: *arXiv:2008.03837 [math-ph]* (2020) (cit. on p. 4).
- [DBB87] L. Durlofsky, J. F. Brady, and G. Bossis. “Dynamic simulation of hydrodynamically interacting particles”. In: *Journal of Fluid Mechanics* 180 (1987). Publisher: Cambridge University Press, pp. 21–49 (cit. on pp. 4, 7).
- [Ein05] A. Einstein. “Eine neue Bestimmung der Moleküldimensionen [AdP 19, 289 (1906)]”. In: *Annalen der Physik* 14.S1 (2005), pp. 229–247 (cit. on p. 3).
- [Est+17] A. Esteghamatian, M. Bernard, M. Lance, A. Hammouti, and A. Wachs. “Micro/meso simulation of a fluidized bed in a homogeneous bubbling regime”. In: *International Journal of Multiphase Flow* 92 (2017), pp. 93–111 (cit. on p. 5).
- [FP08] Y. Forterre and O. Pouliquen. “Flows of Dense Granular Media”. In: *Annual Review of Fluid Mechanics* 40.1 (2008), pp. 1–24 (cit. on p. 9).
- [Gal+14a] S. Gallier, E. Lemaire, L. Lobry, and F. Peters. “A fictitious domain approach for the simulation of dense suspensions”. In: *Journal of Computational Physics* 256 (2014), pp. 367–387 (cit. on p. 7).
- [Gal+14b] S. Gallier, E. Lemaire, F. Peters, and L. Lobry. “Rheology of sheared suspensions of rough frictional particles”. In: *Journal of Fluid Mechanics* 757 (2014), pp. 514–549 (cit. on pp. 4, 5, 10).
- [GDR04] GDR MiDi. “On dense granular flows”. In: *The European Physical Journal E* 14.4 (2004), pp. 341–365 (cit. on pp. 3, 9).
- [Gér21] D. Gérard-Varet. “Derivation of the Batchelor-Green formula for random suspensions”. In: *Journal de Mathématiques Pures et Appliquées* 152 (2021), pp. 211–250 (cit. on p. 4).
- [GH20] D. Gérard-Varet and M. Hillairet. “Analysis of the Viscosity of Dilute Suspensions Beyond Einstein’s Formula”. In: *Archive for Rational Mechanics and Analysis* 238.3 (2020), pp. 1349–1411 (cit. on p. 4).
- [GH21] D. Gérard-Varet and R. M. Höfer. “Mild assumptions for the derivation of Einstein’s effective viscosity formula”. In: *Communications in Partial Differential Equations* 46.4 (2021), pp. 611–629 (cit. on p. 4).
- [Gom+20] G. Gompper, R. G. Winkler, T. Speck, et al. “The 2020 motile active matter roadmap”. In: *Journal of Physics: Condensed Matter* 32.19 (2020), p. 193001 (cit. on p. 12).

- [GM11] E. Guazzelli and J. F. Morris. *A physical introduction to suspension dynamics*. Vol. 45. Cambridge University Press, 2011 (cit. on p. 3).
- [GP18] E. Guazzelli and O. Pouliquen. “Rheology of dense granular suspensions”. In: *Journal of Fluid Mechanics* 852 (2018) (cit. on pp. 3, 10).
- [Hai+08] B. M. Haines, I. S. Aronson, L. Berlyand, and D. A. Karpeev. “Effective viscosity of dilute bacterial suspensions: a two-dimensional model”. In: *Physical Biology* 5.4 (2008), p. 046003 (cit. on p. 13).
- [HM12] B. M. Haines and A. L. Mazzucato. “A Proof of Einstein’s Effective Viscosity for a Dilute Suspension of Spheres”. In: *SIAM Journal on Mathematical Analysis* 44.3 (2012), pp. 2120–2145 (cit. on p. 4).
- [HE05] T. C. Halsey and D. Ertas. “Coherent Structures in Dense Granular Flows”. In: *arXiv:cond-mat/0506170* (June 2005) (cit. on p. 10).
- [Hey+17] J. Heyman, R. Delannay, H. Tabuteau, and A. Valance. “Compressibility regularizes the $\mu(I)$ -rheology for dense granular flows”. In: *Journal of Fluid Mechanics* 830 (2017), pp. 553–568 (cit. on p. 10).
- [HK15] M. Hillairet and T. Kelaï. “Justification of lubrication approximation: An application to fluid/solid interactions”. In: *Asymptotic Analysis* 95.3-4 (2015), pp. 187–241 (cit. on p. 19).
- [HT09] M. Hillairet and T. Takahashi. “Collisions in 3d fluid structure interactions problems”. In: *SIAM Journal on Mathematical Analysis* (2009), p. 25 (cit. on p. 6).
- [HW20] M. Hillairet and D. Wu. “Effective viscosity of a polydispersed suspension”. In: *Journal de Mathématiques Pures et Appliquées* 138 (2020), pp. 413–447 (cit. on p. 4).
- [JFP06] P. Jop, Y. Forterre, and O. Pouliquen. “A constitutive law for dense granular flows”. In: *Nature* 441.7094 (2006), pp. 727–730 (cit. on p. 10).
- [Kam19] K. Kamrin. “Non-locality in Granular Flow: Phenomenology and Modeling Approaches”. In: *Frontiers in Physics* 7 (2019) (cit. on p. 10).
- [KB04] E. Khruslov and L. Berlyand. “Homogenized Non-Newtonian Viscoelastic Rheology of a Suspension of Interacting Particles in a Viscous Newtonian Fluid”. In: *SIAM Journal on Applied Mathematics* 64.3 (2004), pp. 1002–1034 (cit. on p. 5).
- [LP09] E. Lauga and T. R. Powers. “The hydrodynamics of swimming microorganisms”. In: *Reports on Progress in Physics* 72.9 (2009). Publisher: IOP Publishing, p. 096601 (cit. on p. 12).
- [Li+20] Q. Li, M. Abbas, J. F. Morris, E. Climent, and J. Magnaudet. “Near-wall dynamics of a neutrally buoyant spherical particle in an axisymmetric stagnation point flow”. In: *Journal of Fluid Mechanics* 892 (2020) (cit. on p. 5).

- [Lig52] M. J. Lighthill. “On the squirming motion of nearly spherical deformable bodies through liquids at very small reynolds numbers”. In: *Communications on Pure and Applied Mathematics* 5.2 (1952), pp. 109–118 (cit. on p. 11).
- [LLC05] G. Lois, A. Lemaître, and J. M. Carlson. “Numerical tests of constitutive laws for dense granular flows”. In: *Physical Review E* 72.5 (2005), p. 051303 (cit. on pp. 9, 10).
- [LM03] S. Lomholt and M. R. Maxey. “Force-coupling method for particulate two-phase flow: Stokes flow”. In: *Journal of Computational Physics* 184.2 (2003), pp. 381–405 (cit. on p. 4).
- [Mar+14] R. Mari, R. Seto, J. F. Morris, and M. M. Denn. “Shear thickening, frictionless and frictional rheologies in non-Brownian suspensions”. In: *Journal of Rheology* 58.6 (2014), pp. 1693–1724 (cit. on pp. 5, 10).
- [Mau61] A D Maude. “End effects in a falling-sphere viscometer”. In: *British Journal of Applied Physics* 12.6 (1961), pp. 293–295 (cit. on p. 6).
- [Mau07] B. Maury. “A gluey particle model”. In: *ESAIM: Proceedings* 18 (2007). Ed. by J-F. Gerbeau and S. Labbé, pp. 133–142 (cit. on pp. 16, 20, 21).
- [Mau06] B. Maury. “A time-stepping scheme for inelastic collisions”. In: *Numerische Mathematik* 102.4 (2006), pp. 649–679 (cit. on pp. 16, 17).
- [MLT99] P Mills, D Loggia, and M Tixier. “Model for a stationary dense granular flow along an inclined wall”. In: *Europhysics Letters (EPL)* 45.6 (1999), pp. 733–738 (cit. on p. 10).
- [NG04] A. Najafi and R. Golestanian. “Simple swimmer at low Reynolds number: Three linked spheres”. en. In: *Physical Review E* 69.6 (2004), p. 062901 (cit. on p. 13).
- [NSM21] C. Ness, R. Seto, and R. Mari. “The physics of dense suspensions”. In: *arXiv:2105.04162 [cond-mat, physics:physics]* (2021) (cit. on p. 3).
- [NS20] B. Niethammer and R. Schubert. “A Local Version of Einstein’s Formula for the Effective Viscosity of Suspensions”. In: *SIAM Journal on Mathematical Analysis* 52.3 (2020), pp. 2561–2591 (cit. on p. 4).
- [NGP11] P.R. Nott, E. Guazzelli, and O. Pouliquen. “The suspension balance model revisited”. In: *Physics of Fluids* 23.4 (2011). Publisher: American Institute of Physics, p. 043304 (cit. on p. 5).
- [Pou+06] O Pouliquen, C Cassar, P Jop, Y Forterre, and M Nicolas. “Flow of dense granular material: towards simple constitutive laws”. In: *Journal of Statistical Mechanics: Theory and Experiment* 2006.07 (2006), P07020–P07020 (cit. on p. 10).
- [Pur77] E. M. Purcell. “Life at low Reynolds number”. In: *American Journal of Physics* 45.1 (1977). Publisher: American Association of Physics Teachers, pp. 3–11 (cit. on pp. 11–13).

- [RRD17] F. Radjai, J-N. Roux, and A. Daouadji. “Modeling Granular Materials: Century-Long Research across Scales”. In: *Journal of Engineering Mechanics* 143.4 (2017), p. 04017002 (cit. on p. 9).
- [RR02] F. Radjai and S. Roux. “Turbulentlike Fluctuations in Quasistatic Flow of Granular Media”. In: *Physical Review Letters* 89.6 (2002), p. 064302 (cit. on p. 10).
- [RHW18] M. Rahmani, A. Hammouti, and A. Wachs. “Momentum balance and stresses in a suspension of spherical particles in a plane Couette flow”. In: *Physics of Fluids* 30.4 (2018), p. 043301 (cit. on p. 5).
- [Sai18] D. Saintillan. “Rheology of Active Fluids”. In: *Annual Review of Fluid Mechanics* 50.1 (2018), pp. 563–592 (cit. on p. 13).
- [SW89a] A. Shapere and F. Wilczek. “Efficiencies of self-propulsion at low Reynolds number”. In: *Journal of Fluid Mechanics* 198 (1989). Publisher: Cambridge University Press, pp. 587–599 (cit. on p. 12).
- [SW89b] A. Shapere and F. Wilczek. “Geometry of self-propulsion at low Reynolds number”. In: *Journal of Fluid Mechanics* 198 (1989). Publisher: Cambridge University Press, pp. 557–585 (cit. on p. 12).
- [SP05] J. J. Stickel and R. L. Powell. “Fluid mechanics and rheology of dense suspensions”. In: *Annual Review of Fluid Mechanics* 37.1 (2005), pp. 129–149 (cit. on p. 10).
- [Tay51] G. I. Taylor. “Analysis of the swimming of microscopic organisms”. In: *Proceedings of the Royal Society of London. Series A. Mathematical and Physical Sciences* 209.1099 (1951). Publisher: Royal Society, pp. 447–461 (cit. on pp. 11, 13).
- [Ven11] J. Venel. “A numerical scheme for a class of sweeping processes”. In: *Numerische Mathematik* 118.2 (2011), pp. 367–400 (cit. on p. 20).
- [Wac09] A. Wachs. “A DEM-DLM/FD method for direct numerical simulation of particulate flows: Sedimentation of polygonal isometric particles in a Newtonian fluid with collisions”. In: *Computers & Fluids* 38.8 (2009), pp. 1608–1628 (cit. on p. 4).
- [Wac11] A. Wachs. “PeliGRIFF, a parallel DEM-DLM/FD direct numerical simulation tool for 3D particulate flows”. In: *Journal of Engineering Mathematics* 71.1 (2011), pp. 131–155 (cit. on p. 4).
- [WT06] D. Wan and S. Turek. “Direct numerical simulation of particulate flow via multigrid FEM techniques and the fictitious boundary method”. In: *International Journal for Numerical Methods in Fluids* 51.5 (2006), pp. 531–566 (cit. on p. 4).

Numerical simulation of suspensions: lubrication correction, including fluid correction.

Collaborators: Benoît Merlet (Labo. Paul Painlevé, Lille)- Flore Nabet (CMAP, Palaiseau) - T.N. Nguyen (PhD CMAP, Palaiseau) - Fabien Vergnet (LJLL, Paris)

Related publications:

[9] *An accurate method to include lubrication forces in numerical simulations of dense Stokesian suspensions.* With B. Merlet, and T. N. Nguyen. In: *Journal of Fluid Mechanics* 769 (2015), pp. 369–386

[10] *Numerical simulation of suspensions: lubrication correction, including fluid correction.* In: *Actes du colloque EDP-Normandie.* (2017)

[11] *Numerical simulation of rigid particles in Stokes flow: lubrication correction for general shape of particles.* With F. Nabet. *Math. Model. Nat. Phenom.*, 16 (2021), p. 45

Expected applications of the results presented in this chapter:

- *Rheology of suspensions: Taking lubrication into account in numerical simulations. Handling of non-spherical particles. Feedback on the flow.*
 - *Micro-swimmers and active suspensions: Make it possible to manage the large lubrication forces generated by the deformations of the swimmers.*
-

In this chapter, I present a new method that we have developed to **capture the lubrication phenomenon in numerical simulations**. First, recall that lubrication is generated by the flow of fluid in the gap between close particles. As explained in the introduction, it is a singular phenomenon when the distance between the particles tends to zero. It is therefore difficult to capture in numerical simulations. We focus here on the singularity in space: at a given time, for a given configuration, with possibly very close particles, we try to estimate as accurately as possible the effects of the fluid on the particles. Remember that, in view of the applications targeted, we need to develop a method which allows the simulation of **non-spherical particles** and which **transmits the effects of lubrication not only to the particles but also to the whole velocity and pressure fields in the fluid domain**.

We focus on the so-called Dirichlet to Neumann problem: the velocities of the particles are imposed, we try to calculate the velocity and pressure fields as well as the corresponding forces. This is a first step towards the numerical simulation of suspensions in which, conversely, the forces exerted on the system are known and the velocities of the particles are to be determined. Indeed, to calculate these unknown velocities, some methods are based on the inversion of the resistance matrix (which associates velocities to forces). The calculation of this matrix can be achieved via the resolution of several Dirichlet to Neumann problems. The study of dense suspensions in three dimensions leading to high dimensional numerical problems, some methods based on iterative solvers have also been developed. To implement these algorithms, one needs to define a matrix/vector product which, again, is based on a Dirichlet to Neumann type problem.

Let us first define the general Dirichlet to Neumann problem for N particles. We consider $\Omega = \mathbb{R}^3$ and denote by $(B_i)_{i=1,\dots,N}$ N rigid particles in Ω . We assume that the fluid domain $\mathcal{F} = \Omega \setminus \cup B_i$ is filled with a Newtonian fluid governed by Stokes equations with viscosity μ .

We suppose that the velocity on the boundary of each particle is given: the velocity of particle i is denoted by $\mathbf{u}_i^* \in H^{1/2}(\partial B_i)$. Each of the particles undergoes a rigid motion: $\mathbf{u}_i^*(\mathbf{x}) = \mathbf{V}_i + \mathbf{w}_i \wedge (\mathbf{x} - \mathbf{x}_i)$, where \mathbf{V}_i (resp. \mathbf{w}_i) is the translational (resp. rotational) velocity of particle i .

The problem is written as follows,

$$\left\{ \begin{array}{l} \text{Find } (\mathbf{u}, \mathbf{p}) \in H^1(\mathcal{F}) \times L_0^2(\mathcal{F}) \text{ such that} \\ -\mu \Delta \mathbf{u} + \nabla \mathbf{p} = 0, \quad \text{in } \mathcal{F}; \\ \operatorname{div} \mathbf{u} = 0, \quad \text{in } \mathcal{F}; \\ \mathbf{u} = \mathbf{u}_i^*, \quad \text{on } \partial B_i, \quad i = 1, \dots, N; \end{array} \right. \quad (2.1)$$

where $L_0^2(\mathcal{F}) = \{\mathbf{q} \in L^2(\mathcal{F}) : \int_{\mathcal{F}} \mathbf{q} = 0\}$.

Since we suppose that $\Omega = \mathbb{R}^3$, we add the following vanishing condition at infinity

$$\lim_{|(x,y,z)| \rightarrow \infty} \mathbf{u}(x, y, z) = 0.$$

This, together with the rigid movement of the particles \mathbf{u}_i^* , ensures that system (2.1) admits a unique solution that we denote by

$$(\mathbf{u}, \mathbf{p}) = \operatorname{St}(\mathbf{u}_1^*, \dots, \mathbf{u}_N^*).$$

To simplify the presentation, in the following, we will consider a "toy model", made of three aligned spherical particles of radius r_i , moving along the line of their centers:

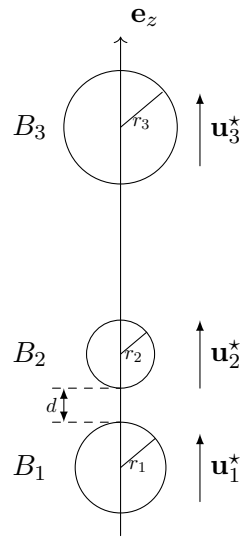


Fig. 2.1: Toy problem composed of 3 aligned particles. Notation.

Particles 1 and 2 are assumed to be close to each other and the third particle is assumed to be far away from the other two. The distance between the first two particles is denoted by d .

The velocities $(\mathbf{u}_1^*, \mathbf{u}_2^*, \mathbf{u}_3^*)$ of the particles are given with $\mathbf{u}_i^* = u_i \mathbf{e}_z$, $u_i \in \mathbb{R}$. One wants to compute the solution $(\mathbf{u}, p) = \text{St}(\mathbf{u}_1^*, \mathbf{u}_2^*, \mathbf{u}_3^*)$ and the corresponding forces exerted on the particles: $\mathbf{f} = (f_1, f_2, f_3) \in \mathbb{R}^3$ where $\mathbf{f}_i = f_i \mathbf{e}_z$ is the force exerted by the fluid on the i -th particle.

We suppose that a fluid solver, based on a direct method, is available (finite elements, finite volumes, ...). The size of the underlying mesh is denoted by h so that the solver converges when $h \rightarrow 0$.

When two particles are close, the singularity due to the lubrication in the gap imposes to construct a fine mesh between the particles (typically 5 to 8 cells in the gap). This makes the computations very expensive (h small, high number of degrees of freedom). Our aim is to propose a solution allowing to take into account the singularity, without having to refine between the particles.

2.1 Traditional method: correction of the forces

The most commonly used method to account for lubrication consists in computing the forces exerted on the particles with the fluid solver and then perform a correction step. It is based on the asymptotic expansion of the forces exerted on two close particles moving in an infinite domain.

► Two particles in an infinite domain: asymptotic expansion of the forces

Consider a single pair of particles immersed in an infinite surrounding fluid. It is assumed that they move along the line of their centers with velocities \mathbf{u}_1^* and \mathbf{u}_2^* . Using the linearity of Stokes equations, one can decompose the boundary conditions $(\mathbf{u}_1^*, \mathbf{u}_2^*)$ as (see figure 2.2):

$$\begin{aligned} (\mathbf{u}, p) = \text{St}(\mathbf{u}_1^*, \mathbf{u}_2^*) &= \frac{u_1^* - u_2^*}{2} \text{St}(\mathbf{e}_z, -\mathbf{e}_z) + \frac{u_1^* + u_2^*}{2} \text{St}(\mathbf{e}_z, \mathbf{e}_z) \quad (2.2) \\ &= \mathbf{u}_{2\text{parts}}^{\text{sing}} + \mathbf{u}_{2\text{parts}}^{\text{reg}} \end{aligned}$$

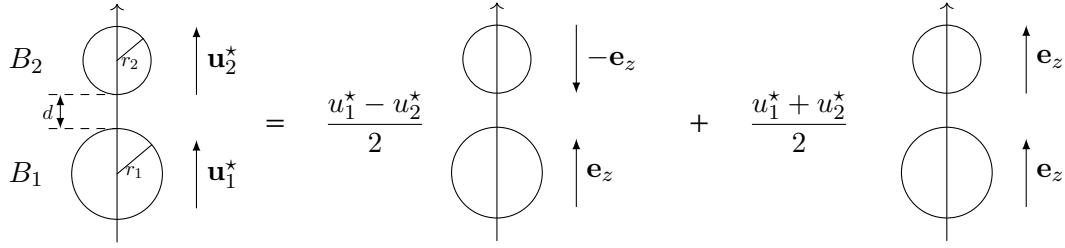


Fig. 2.2: Decomposition of the solution for 2 particles in singular and regular fields.

We can easily convince ourselves that $\text{St}(\mathbf{e}_z, \mathbf{e}_z)$ is regular when d goes to zero (the two particles move with the same velocity). Consequently, the singular behaviour comes from the first term of the sum which is proportional to the relative velocity $u_1^* - u_2^*$ of the particles.

Since [Cox74], the asymptotic expansion of the forces exerted on two isolated particles when the distance goes to zero is known. This expansion is available for any regular convex shape of the particle (close to the contact point) and any rigid movement of the particles. Let us denote by $(\mathbf{f}_1^{2\text{parts}}, \mathbf{f}_2^{2\text{parts}})$ the forces corresponding to the singular field $\mathbf{u}_{2\text{parts}}^{\text{sing}}$. Using the symmetry of the problem together with the linearity of Stokes equations, we write

$$\mathbf{f}_1^{2\text{parts}} = -\mathbf{f}_2^{2\text{parts}} = \frac{u_1^* - u_2^*}{2} \mathbf{f}^{2\text{parts}},$$

where $\mathbf{f}^{2\text{parts}}$ is computed from the field $\text{St}(\mathbf{e}_z, -\mathbf{e}_z)$. From Cox' expansion, we know that it behaves as:

$$\mathbf{f}^{2\text{parts}} \sim -6\pi\mu \frac{r_1^2 r_2^2}{(r_1 + r_2)^2} \frac{2}{d} \mathbf{e}_z \text{ when } d \rightarrow 0. \quad (2.3)$$

► **The Stokesian Dynamics correction [DBB87]**

So let us come back to our toy problem composed of 3 aligned particles. Suppose that, using a direct solver, we can compute the forces exerted on the particles $\mathbf{f}_h = (f_{1,h}, f_{2,h}, f_{3,h})$ for a not too small mesh size h . The question is to find a way to correct the numerical values obtained for the forces exerted on particles 1 and 2. Indeed, these particles being close, the solver is not able to catch the induced lubrication phenomenon for not too small values of h .

A widely used strategy has been proposed in [DBB87] in the context of Stokesian Dynamics simulations (which are non direct simulations). The founding remark is the

following: if two particles are embedded in an infinite fluid and **have the same given radius** r , then the solution $\text{St}(\mathbf{e}_z, -\mathbf{e}_z)$ only depends on the distance d . As a consequence, the corresponding forces $\mathbf{f}^{2\text{parts}}$ exerted on the particles can be written as a function of one variable: $d \rightarrow \mathbf{f}^{2\text{parts}}(d)$. Since it only depends on one parameter, it can easily be estimated using its asymptotic expansion (2.3) for small distances, together with a mean square approach for larger distances. Very precise computations are achieved off-line for a discrete set of distances to construct the approximation for any value of the distance.

From this approximation, the authors in [DBB87] propose to correct the forces computed by the fluid solver as follows:

$$\mathbf{f}_h^{SD} = \begin{pmatrix} f_{1,h} \\ f_{2,h} \\ f_{3,h} \end{pmatrix} + \frac{u_1^* - u_2^*}{2} \begin{pmatrix} \mathbf{f}^{2\text{parts}}(d) - \mathbf{f}_h^{2\text{parts}}(d) \\ -(\mathbf{f}^{2\text{parts}}(d) - \mathbf{f}_h^{2\text{parts}}(d)) \\ 0 \end{pmatrix}.$$

The numerical values of the forces exerted on particles 1 and 2 are corrected while no modification is done for particle 3. In order to correct the value of the forces on the first two particles, we use the corresponding precise approximation $\mathbf{f}^{2\text{parts}}(d)$: the two particles are considered as an isolated pair, immersed in an infinite fluid domain and the influence of the third particle is neglected. We also need to subtract the part of the singularity that would have been computed with the solver with precision h . Doing so, the correction goes to zero when h goes to zero and the method converges.

Note that this method can be rewritten as the sum of a singular part that is known analytically and a remaining regular part that is estimated online, using the solver with not too small values of h :

$$\begin{aligned} \mathbf{f}_h^{SD} &= \mathbf{f}^{\text{sing}} + \mathbf{f}_h^{\text{reg}} \\ &= \frac{u_1^* - u_2^*}{2} \begin{pmatrix} \mathbf{f}^{2\text{parts}}(d) \\ -\mathbf{f}^{2\text{parts}}(d) \\ 0 \end{pmatrix} + \begin{pmatrix} f_{1,h} - \frac{u_1^* - u_2^*}{2} \mathbf{f}_h^{2\text{parts}}(d) \\ f_{2,h} + \frac{u_1^* - u_2^*}{2} \mathbf{f}_h^{2\text{parts}}(d) \\ f_{3,h} \end{pmatrix} \end{aligned} \quad (2.4)$$

▷ Comments

The asymptotic expansion in [Cox74] is given for any rigid motion of the particles. As a consequence, the method can be extended to general suspensions in 3 dimension, with any number of particles. In that case, the contributions of all pairs of close particles are added together. It has been largely used for non direct simulations of suspensions (see e.g. [BB88; Lad88; Cic+94]) but also more recently in the force coupling method [YM10] or in the framework of direct simulation [Gal+14]. Note that, since the singular part is interpolated offline, the method is very efficient from a computational point of view.

It should also be noted that the correction (2.4) is accurate in many cases of interest, which has made the method successful. However, it is based on pairwise interactions: a particle in the neighborhood of two close particles is not affected by the correction. Moreover, the correction is computed supposing that the pairs of close particles are isolated from the other particles. Nevertheless, the interactions between two particles do depend on the presence and on the position of other particles. Many-body interactions are not correctly included in the correction step. As a consequence, the correction eliminates the diagonal leading order term $O(1/d)$ of the error (effect of a pair of close particles on itself) but does not affect the non-diagonal terms (effect of a pair on the other particles and vice versa). Let us consider a system of three particles B_1 , B_2 , B_3 , the first two being close one to another and the third at a finite distance as in figure 2.3. If the

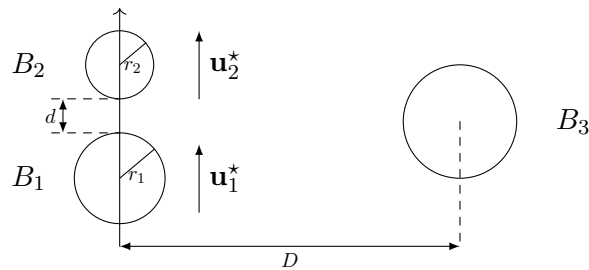


Fig. 2.3: Interaction between a pair of close particles and a distant third particle.

particles B_1 and B_2 have opposite velocities then the velocity field at distance $O(D)$ has a horizontal component of order dV/D^2 resulting in a force of order dV/D^2 on B_3 (where $dV = u_2^* - u_1^*$ is the relative velocity of the two particles). As a consequence, the influence of the remaining error has negligible influence when we consider relatively small hydrodynamic forces (i.e. when the close particles have nearly identical velocities: dV is small). On the other hand, the correction may be inadequate when hydrodynamic

forces have to balance large non-hydrodynamic forces (as it happens, for example, when we consider micro-scale swimmers: the internal forces generate high relative velocities). In these cases, there is a need for numerical methods which are accurate even in the presence of large forces. These methods need to take into account the many-body interactions.

To finish, let's recall that, as stated in the introduction, current research in the field of suspension rheology focuses on suspensions made of non-spherical particles and on the study of quantities derived from the velocity and pressure fields in the fluid. The proposed method does not allow to answer these requests. First, no correction is performed on the numerical velocity and pressure fields. Moreover, it cannot easily be used for non-monodisperse suspensions. Indeed, the off-line computations have to be done using very precise three dimensional simulations, which is very costly (fine meshes are needed to obtain precise results for close particles). Until now, it has only been achieved in case of monodisperse suspensions, for which the forces only depend on a single parameter. In the case of polydisperse suspensions, the forces would depend on two parameters: $(d, \gamma) \rightarrow \mathbf{f}_{2\text{parts}}(d, \gamma)$ with $\gamma = \frac{r_1^2 r_2^2}{(r_1 + r_2)^2}$ (see equation 2.3). Although possible, this precise two-parameter approximation is very time demanding and it has never been achieved until now. Finally, let us recall that the method is based on the calculation of the total force exerted on the particles. These forces are highly dependent on the shape and orientation of the particles, which makes it difficult to extend the method to non-spherical particles.

For these reasons, we proposed with Benoît Merlet a new method, to take into account the effect of lubrication on the flow [9]. The method natively takes into account the multi-particle nature of the interactions. However, it still relies on an offline interpolation and is therefore restricted to monodisperse suspensions. Then, I have adapted [10] the method to take into account more general shapes (regular and convex) of particles. To do so, the tabulations are replaced by explicit asymptotic expansions. With Flore Nabet, we then modified the asymptotic expansions to be more efficient from a numerical point of view. We describe, analyze and test the corresponding method in [11]. These works are described in the following section.

2.2 A new method: singular/regular splitting of the velocity and pressure fields.

▷ **The idea: a singular/regular decomposition of the flow**

Suppose you compute an approximation $(\mathbf{u}_h, \mathbf{p}_h)$ of $(\mathbf{u}, \mathbf{p}) = \text{St}(\mathbf{u}_1^*, \dots, \mathbf{u}_N^*)$ using a direct solver based on a mesh with size h . This discretization induces an error $\|\mathbf{u} - \mathbf{u}_h\|_{\mathbf{u}}$, $\|\mathbf{p} - \mathbf{p}_h\|_{\mathbf{p}}$ for given norms, that can be estimated as follows

$$\|\mathbf{u} - \mathbf{u}_h\|_{\mathbf{u}} \leq C_1 \|(\mathbf{u}, \mathbf{p})\| h^{\alpha_1}, \quad \|\mathbf{p} - \mathbf{p}_h\|_{\mathbf{p}} \leq C_2 \|(\mathbf{u}, \mathbf{p})\| h^{\alpha_2},$$

where α_1 and α_2 depend on the chosen method and discretization space as well as on the norm used for the error.

The founding remark of the method we propose is the following: the norm $\|(\mathbf{u}, \mathbf{p})\|$ of the solution depends on the distance d and blows up when d decreases. Consequently, h being given, it is generally observed that the error also blows up when the distance decreases. Let us consider, for example, the configuration given in Figure 2.4 with $r_1 = 0.07$, $r_2 = 0.1$, $\mathbf{u}_1^* = \mathbf{e}_x$, $\mathbf{u}_2^* = -\mathbf{e}_x$. The numerical tests are implemented in

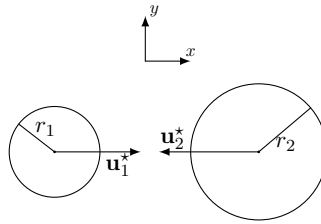


Fig. 2.4: Spherical particles moving along the line of their centers.

two dimensions with FreeFEM [Hec12]. As in dimension three, the solution of the problem in two dimensions is singular. The lubrication force behaves in this case as $\ln(d)$. We discretize the velocity and pressure fields using the finite elements $\mathbb{P}^1\text{-iso}\mathbb{P}^2$ and \mathbb{P}^1 respectively. Since we do not know the exact solution to the problem, we compare our results with a reference solution $(\mathbf{u}^{\text{ref}}, \mathbf{p}^{\text{ref}})$ computed on a very fine mesh (the corresponding reference solution was plotted in the introduction figure 1.2). The tests are run for three different distances between the particles: $d = r_2/10$, $d = r_2/20$, $d = r_2/30$. We display on Figure 2.5 the fine mesh used to compute the reference solution, together

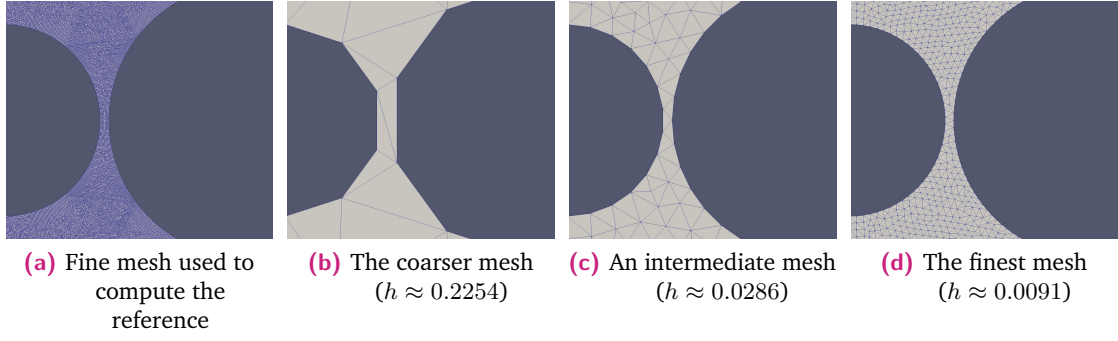


Fig. 2.5: Different meshes used for the computation.

with three of the meshes used for the computations. We plot the absolute error between the approximate solution and the reference solution (in H_0^1 -norm for each component of the velocity and in L^2 -norm for the pressure). The configuration being given (i.e. d being

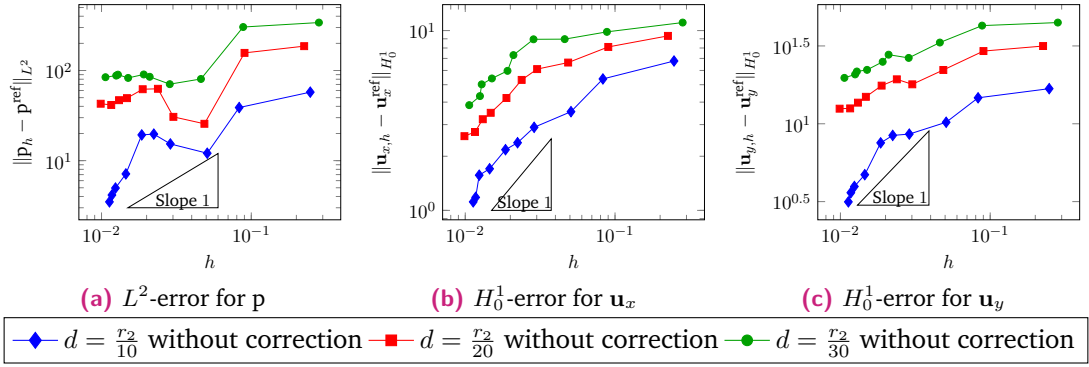


Fig. 2.6: Absolute error as a function of h for 3 different distances for two spherical particles.

given), one can observe the convergence rate of the method. However, one can see that the y -intercept of the lines is increasing when the distance goes to zero.

The idea behind the method we propose is the following: replace the estimate of (\mathbf{u}, p) by the estimate of another "regular" field $(\mathbf{u}^{\text{reg}}, p^{\text{reg}})$ whose norm would not depend on the distance. To do so, we are going to take advantage of the knowledge we have on the singularity, in order to decompose the field it into a sum of a singular part (exploding with distance) and a regular part (bounded independently of the distance):

$$(\mathbf{u}, p) = (\mathbf{u}^{\text{sing}}, p^{\text{sing}}) + (\mathbf{u}^{\text{reg}}, p^{\text{reg}}).$$

This decomposition is similar to that of the forces (2.4) in the Stokesian Dynamics case, but we now decompose the whole velocity and pressure fields.

Suppose now that the singular field is known. Then, to solve the original problem (2.1), it remains to approximate the solution to the following regular problem:

$$\left\{ \begin{array}{l} \text{Find } (\mathbf{u}^{\text{reg}}, \mathbf{p}^{\text{reg}}) \in H^1(\mathcal{F}) \times L_0^2(\mathcal{F}) \text{ such that} \\ -\Delta \mathbf{u}^{\text{reg}} + \nabla \mathbf{p}^{\text{reg}} = \Delta \mathbf{u}^{\text{sing}} - \nabla \mathbf{p}^{\text{sing}}, \quad \text{in } \mathcal{F}; \\ \text{div } \mathbf{u}^{\text{reg}} = -\text{div } \mathbf{u}^{\text{sing}}, \quad \text{in } \mathcal{F}; \\ \mathbf{u}^{\text{reg}} = \mathbf{u}_i^* - \mathbf{u}^{\text{sing}} \text{ on } \partial B_i, \quad i = 1 \dots N. \end{array} \right. \quad (2.5)$$

To make the method work, it is necessary to construct a suitable singular field $(\mathbf{u}^{\text{sing}}, \mathbf{p}^{\text{sing}})$ such that:

- $(\mathbf{u}^{\text{sing}}, \mathbf{p}^{\text{sing}})$ is known analytically or can be computed precisely offline;
- the corresponding solution $(\mathbf{u}^{\text{reg}}, \mathbf{p}^{\text{reg}})$ to (2.5) is bounded regardless of the distance.

Doing so, the right-hand side of (2.5) can be computed precisely and the solution $(\mathbf{u}^{\text{reg}}, \mathbf{p}^{\text{reg}})$ may be approximated without the error increasing when the distance decreases. To finish, suppose that \mathbf{u}^{sing} is computed exactly and that $\mathbf{u}_h^{\text{reg}}$ is an approximation of \mathbf{u}^{reg} with precision h . Then, the approximated solution to the initial problem with precision h writes $\mathbf{u}_h^{\text{new}} = \mathbf{u}^{\text{sing}} + \mathbf{u}_h^{\text{reg}}$ and the corresponding error is

$$\|\mathbf{u} - \mathbf{u}_h^{\text{new}}\|_{\mathbf{u}} = \|(\mathbf{u}^{\text{sing}} + \mathbf{u}^{\text{reg}}) - (\mathbf{u}^{\text{sing}} + \mathbf{u}_h^{\text{reg}})\|_{\mathbf{u}} = \|\mathbf{u}^{\text{reg}} - \mathbf{u}_h^{\text{reg}}\|_{\mathbf{u}} \leq C_1 \|(\mathbf{u}^{\text{reg}}, \mathbf{p}^{\text{reg}})\| h^{\alpha_1}.$$

The norm $\|(\mathbf{u}^{\text{reg}}, \mathbf{p}^{\text{reg}})\|$ is bounded independently of the distance and the same result holds for the approximation of the pressure field. The decomposition into singular and regular fields therefore improves the global error estimation. It should be noted, however, that the constants C_1 and C_2 depend on the shape of the fluid domain and therefore on the distance. They could blow up when the distance vanishes. We will show in the numerical results that this is not a problem in practice.

To sum up, the method we propose is the following:

- Analytical computation of the singular field $(\mathbf{u}^{\text{sing}}, \mathbf{p}^{\text{sing}})$,
- Computation of $(\mathbf{u}_h^{\text{reg}}, \mathbf{p}_h^{\text{reg}})$, numerical approximation of the solution to (2.5), without refining the mesh,
- Solution to the initial problem: $(\mathbf{u}_h^{\text{new}}, \mathbf{p}_h^{\text{new}}) = (\mathbf{u}^{\text{sing}}, \mathbf{p}^{\text{sing}}) + (\mathbf{u}_h^{\text{reg}}, \mathbf{p}_h^{\text{reg}})$.

It now remains to describe how to calculate a singular field that satisfies the requirements, which we present in the following.

Before going further, let's make a remark on a method known as the Singular Complement Method [ACS00; CH03]. This numerical method, in the context of variational problems with singular solutions, also takes advantage of a decomposition in a singular and a regular field of the solution. In that context, the fact that the solution is *singular* has to be understood in the sense that it does not belong to the Hilbert space needed to obtain optimal convergence of the numerical algorithms. One can think for example to the Laplace problem in domains with reentrant corners [CH03]. Note that this kind of singular behaviour is different from the one we consider. Indeed, in our case, for a given distance, the solution belongs to the usual Hilbert spaces for Stokes problems, but we say that its behaviour is *singular* when the distance tends to zero in the sense that its norm in this space blows up.

▷ Decomposition of the boundary condition [9]

The first idea to choose the singular field is to transpose to the whole fluid field the correction proposed in the Stokesian Dynamics framework. This is the method we proposed in [9] with Benoît Merlet, as part of Thanh Nhan Nguyen's PhD thesis (supervised by Benoît Merlet).

Let us first recall that, for a single pair of particles in an infinite domain, the singular part of the field is generated by the relative velocity between the two particles (see equation (2.2)). We denote in the following

$$(\mathbf{u}_{2\text{parts}}^{\text{rel}}, \mathbf{p}_{2\text{parts}}^{\text{rel}}) = \frac{u_1^* - u_2^*}{2} \text{St}(\mathbf{e}_z, -\mathbf{e}_z)$$

the solution for **two particles in an infinite domain** with velocities $\pm(u_1^* - u_2^*)/2\mathbf{e}_z$. The upper-script "rel" stands for *relative* velocities.

Let us consider again our toy problem composed of 3 particles. The singularity is induced by the relative velocity between particles 1 and 2, which are close to each other. The solution $(\mathbf{u}, \mathbf{p}) = \text{St}(\mathbf{u}_1^*, \mathbf{u}_2^*, \mathbf{u}_3^*)$ is then decomposed as (see figure 2.7):

$$(\mathbf{u}, \mathbf{p}) = \text{St}(\mathbf{u}_1^*, \mathbf{u}_2^*, \mathbf{u}_3^*) = (\mathbf{u}_{2\text{parts}}^{\text{rel}}, \mathbf{p}_{2\text{parts}}^{\text{rel}}) + (\mathbf{u}^{\text{reg}}, \mathbf{p}^{\text{reg}}). \quad (2.6)$$

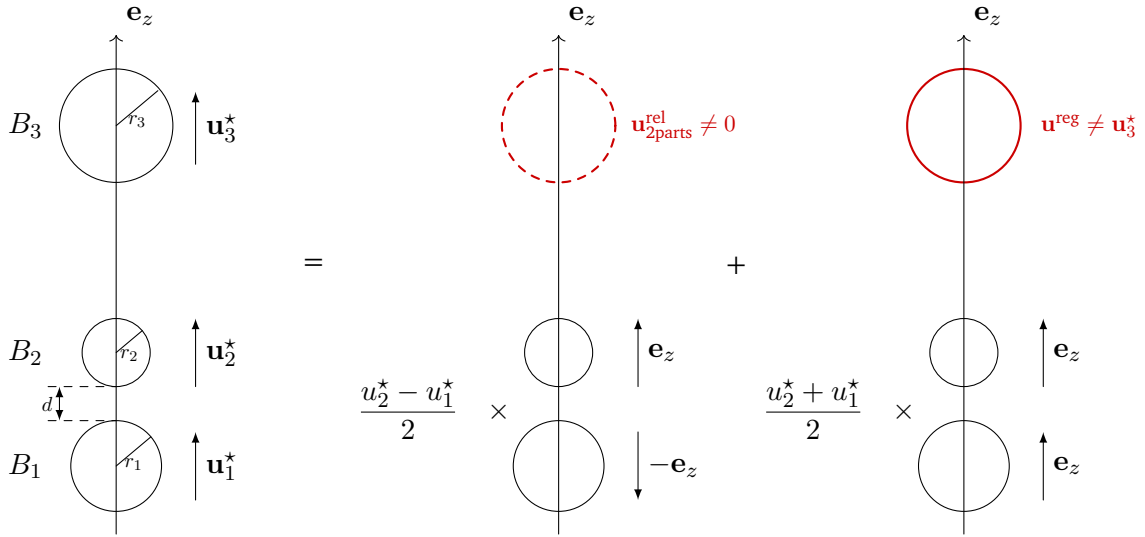


Fig. 2.7: Decomposition of the solution for 2 particles in singular and regular fields.

The singular/regular decomposition (2.6) is the field counterpart of the decomposition of forces (2.4): $(\mathbf{u}_{2\text{parts}}^{\text{rel}}, \mathbf{p}_{2\text{parts}}^{\text{rel}})$ contains the singular part of the solution while the remaining part $(\mathbf{u}^{\text{reg}}, \mathbf{p}^{\text{reg}})$ is regular. The field $(\mathbf{u}_{2\text{parts}}^{\text{rel}}, \mathbf{p}_{2\text{parts}}^{\text{rel}})$ is computed considering that particles 1 and 2 are isolated in an infinite domain: it does not vanish on ∂B_3 . Then, unlike the method based on the correction of the forces, the contribution of the singularity between particles 1 and 2 is now transmitted to particle 3 through the boundary condition that the regular field \mathbf{u}^{reg} must satisfy on ∂B_3 (see (2.5)).

In view of the decomposition (2.6), it now remains to estimate analytically $(\mathbf{u}_{2\text{parts}}^{\text{rel}}, \mathbf{p}_{2\text{parts}}^{\text{rel}})$.

► Two particles in an infinite domain: a tabulated singular field [9]

The first method to estimate the singular field we proposed is described in [9]. As for the Stokesian Dynamics correction, since $\text{St}(\mathbf{e}_z, -\mathbf{e}_z)$ only depend on one parameter (if the

particles have the same radius), we proposed a method to approximate offline a, accurate approximation of this singular field, as a function of the distance:

$$d \rightarrow \text{St}(\mathbf{e}_z, -\mathbf{e}_z) \approx (\mathbf{u}_{2\text{parts}}^{\pm 1}, \mathbf{p}_{2\text{parts}}^{\pm 1})(d).$$

The approximation procedure is based on the decomposition of the flow on a vectorial spherical harmonic basis. The coordinates of the pressure and velocity singular fields in this basis only depend on one parameter (the distance) and can be accurately approximated off-line using interpolation techniques.

This approximation at hand, decomposition (2.6) leads to the following approximation of the solution to our three particles problem:

$$\begin{aligned} (\mathbf{u}, \mathbf{p}) = \text{St}(\mathbf{u}_1^*, \mathbf{u}_2^*, \mathbf{u}_3^*) &= (\mathbf{u}_{2\text{parts}}^{\text{rel}}, \mathbf{p}_{2\text{parts}}^{\text{rel}}) + (\mathbf{u}^{\text{reg}}, \mathbf{p}^{\text{reg}}) \\ &\approx \frac{u_1^* - u_2^*}{2} (\mathbf{u}_{2\text{parts}}^{\pm 1}, \mathbf{p}_{2\text{parts}}^{\pm 1})(d) + (\mathbf{u}_h^{\text{reg}}, \mathbf{p}_h^{\text{reg}}). \end{aligned}$$

The singular field is computed using the offline approximation and $\mathbf{u}_h^{\text{reg}}$ is the approximation of \mathbf{u}^{reg} solution to (2.5).

The method is tested in [9] for a cluster of 4 particles. We showed that it behaves better than the Stokesian Dynamics correction. We also illustrated in [9] the efficiency of the method to compute the displacement of the three-sphere swimmer of Najafi and Golestanian (see chapter 5, figure 5.1), for which high hydrodynamic forces are generated, due to the relative velocities of the spheres.

By proceeding in this way, we meet several of the needs expressed in the introduction:

- we have access to **corrected velocity and pressure fields**, taking into account the lubrication phenomenon;
- the **multi-particle character** of the phenomenon is taken into account (a singularity induces a correction on all particles);
- the method allows to deal with large hydrodynamic forces generated by micro-swimmers.

On the other hand, the offline approximation of the coordinates of the singular fields requires, as for the Stokesian Dynamics, to deal with a singular field depending only on one parameter. It thus limits again the applications to **mono-disperse suspensions**.

▷ **Two particles in an infinite domain: an explicit asymptotic expansion [10,11]**

To overcome this limitation, I proposed in [10] to use an explicit asymptotic expansion of the solution for two particles in an infinite domain, valid for more general forms of particles. Indeed, it is clear that in decomposition (2.6), it is not necessary to compute the whole field $(\mathbf{u}_{2\text{parts}}^{\text{rel}}, p_{2\text{parts}}^{\text{rel}})$: an asymptotic expansion of this field is sufficient to run the method. In that case, the remaining regular part will then be part of $(\mathbf{u}^{\text{reg}}, p^{\text{reg}})$.

In [11], we propose with Flore Nabet a singular field $(\mathbf{u}_{2\text{parts}}^{\text{sing}}, p_{2\text{parts}}^{\text{sing}})$ for the 2 particle problem and we prove that the remaining field is regular:

$$(\mathbf{u}_{2\text{parts}}^{\text{rel}}, p_{2\text{parts}}^{\text{rel}}) = (\mathbf{u}_{2\text{parts}}^{\text{sing}}, p_{2\text{parts}}^{\text{sing}}) + (\mathbf{u}_{2\text{parts}}^{\text{reg}}, p_{2\text{parts}}^{\text{reg}}), \quad (2.7)$$

with $(\mathbf{u}_{2\text{parts}}^{\text{reg}}, p_{2\text{parts}}^{\text{reg}})$ bounded independently of the distance. This singular field is an adaptation of the asymptotic expansion proposed by Hillairet and Kelai in [HK15]. It has been modified to make it more tractable from a numerical point of view. Our estimations for $(\mathbf{u}_{2\text{parts}}^{\text{reg}}, p_{2\text{parts}}^{\text{reg}})$ are based on the estimations proved in [HK15] which are used as an intermediate result. The modifications we propose have two goals:

- Avoid too many oscillations in the singular field. Indeed, we will need to compute precisely the right-hand side of (2.5) to solve the problem for $(\mathbf{u}^{\text{reg}}, p^{\text{reg}})$. Too many oscillations makes this step of the method difficult. We modify the expression of the singular field proposed in [HK15] in the gap between the particles to deal with this problem.
- Reduce the computational cost and make it possible to parallelize the computation of the right-hand side in case of multiple singularities. To do so, the velocity and pressure fields are designed to cancel outside the gap between the particles, which was not the case in [HK15]. In case of multi-particle simulations, each singularity can then be computed independently and affects only the boundary condition on the two particles concerned, making it possible to use parallelisation.

In order to assess the benefit of the singular/regular decomposition on the accuracy of the numerical simulations, we consider again the two dimensional case of two spherical particles for which the errors without correction was reported on figure 2.6. The asymptotic expansion of the solution can be computed in two dimensions, so that one can use the decomposition method to compute the solution to the problem. We plot on figure 2.8 the errors we obtain using the decomposition method. To make the comparison easier,

the errors obtained without correction are reproduced on the same graph. It can be seen that the error now nearly no longer depends on the distance.

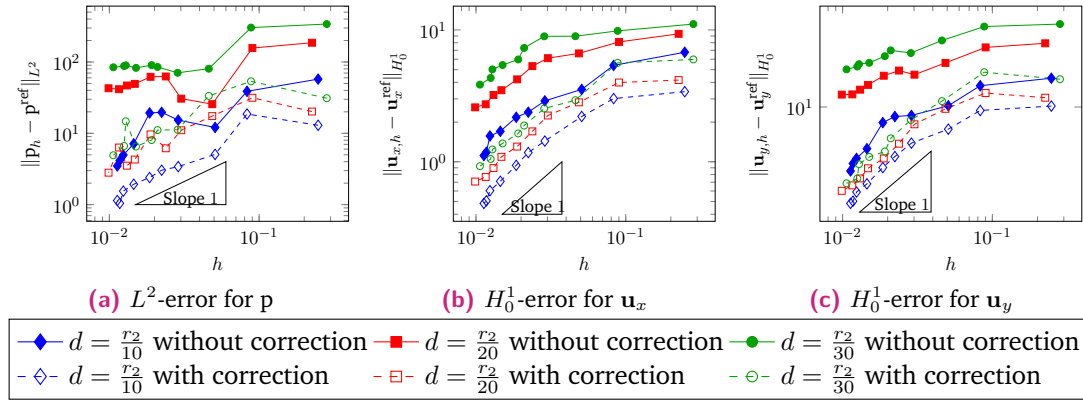


Fig. 2.8: Absolute error with and without decomposition as a function of h for 3 different distances for two spherical particles.

Of course, this implies a computational effort to compute accurately the right hand side of problem (2.5) online. Indeed, we have to consider singular source terms on a coarse mesh. To do so, one can for example consider the singular field as a continuous function and use precise quadrature formula to compute the corresponding integrals. As this method proved to be quite expensive, we chose to project the singular field on a fine mesh (typically the one used for the computation of the reference solution) and to compute the integrals using the fine mesh.

So let us now come back to our 3 particles toy problem. Decomposition (2.6) together with the two particles asymptotic expansion (2.7) suggests the following singular/regular decomposition of the flow:

$$(\mathbf{u}, \mathbf{p}) = \text{St}(\mathbf{u}_1^*, \mathbf{u}_2^*, \mathbf{u}_3^*) = (\mathbf{u}_{2\text{parts}}^{\text{sing}}, \mathbf{p}_{2\text{parts}}^{\text{sing}}) + (\mathbf{u}^{\text{reg,new}}, \mathbf{p}^{\text{reg,new}}).$$

We proved in [11] that, using this singular field, the remaining field $(\mathbf{u}^{\text{reg,new}}, \mathbf{p}^{\text{reg,new}})$ is bounded independently of the distance. The techniques used in the proof are adapted from those used in [HK15] for the two particle case. Note that, although the singular field is non-zero only on the boundary of the two particles involved, it influences the whole solution, through the solution of the non-local problem (2.5) for $(\mathbf{u}^{\text{reg}}, \mathbf{p}^{\text{reg}})$.

The main difference with the method we proposed in [9] is that the singular field is now reduced to the asymptotic expansion of the solution for the isolated pair of particles

(instead of the whole solution, tabulated). The main advantage is that we have at our disposal a formula for this asymptotic field, which is valid for various forms of particles and any rigid movement. As a consequence, unlike the interpolation method in [9], this new method should be used for much more general configurations than our toy problem. Unfortunately, explicit computations of the singular field were carried to the end only for the case of two spherical particles (with different radius) undergoing a relative motion of translation along the axes joining their centers. We propose in [11] to take advantage of these explicit computations in more general cases:

- In case of spherical particles undergoing a more general rigid relative motion, we choose to neglect the lubrication effects due to tangential relative velocities or rotations, which are in fact less singular than the normal translations. We then consider the relative normal velocities of the two bodies at the contact point and proceed as already detailed.
- In case of non-spherical particles, in order to take advantage of the previous computations, we approximate the non-spherical boundaries by the osculating circle at the contact point and proceed as in the previous case.

Using these approximations, one can now deal with more general shapes for the particles, undergoing general rigid movements. Note that in that case, due to the previous approximations, the norm of $(\mathbf{u}^{\text{reg}}, \mathbf{p}^{\text{reg}})$ now depends again on the distance but in a less singular way than the original field (\mathbf{u}, \mathbf{p}) . Several two dimensional tests are run in [11]. In particular, we considered the configuration displayed on figure 2.9, composed of three aligned non-spherical particles undergoing general rigid velocities. We choose $\mathbf{V}_1 = (1, 5)$, $\mathbf{V}_2 = (-1, -2)$, $\mathbf{V}_3 = (1.5, -5)$, $\boldsymbol{w}_1 = 3$, $\boldsymbol{w}_2 = 5$, $\boldsymbol{w}_3 = 10$, $r_2 = 1/20$ and the radius of the osculating circles at the contact points are $r_1 = 1/15$ and $r_3 = (1.3)^2/20$.

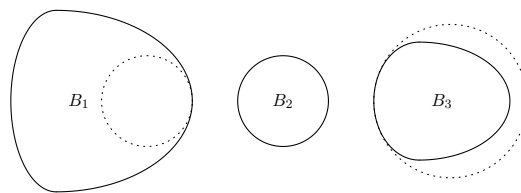


Fig. 2.9: Configuration for the 3 non-spherical particles. Particles, together with their osculating circles at the contact point.

The convergence of the method is illustrated on Figure 2.10. We can see that the two previous simplifications did not prevent to catch the lubrication effects: the errors are much less distance dependent when using the new method than when solving the initial problem.

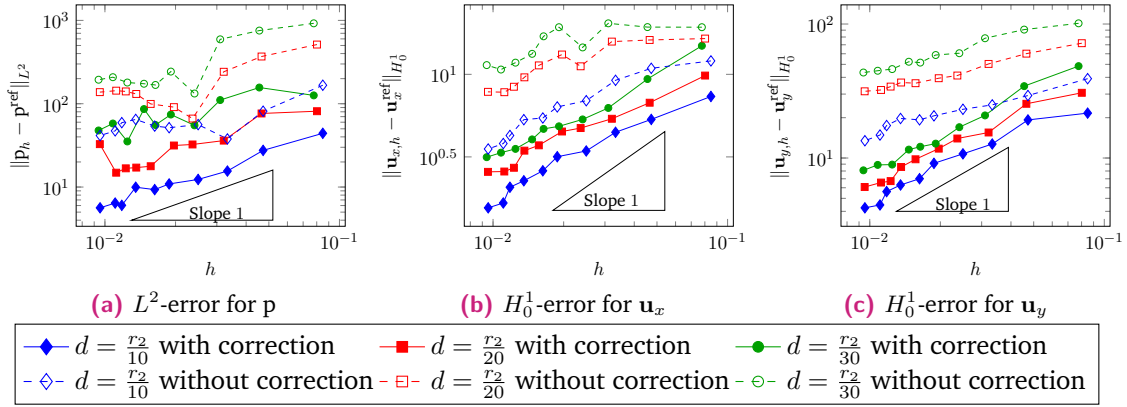


Fig. 2.10: Absolute error in function of h for 3 aligned non-spherical particles undergoing general rigid motions. The distance d between two neighbouring particles is varied.

The procedure can easily be extended to general three dimensional configurations with N particles: we showed that one can simply add the singularities due to all pairs of close particles in the singular field. Finally, compared to the tabulated singular field proposed in [9], this method allows us to meet a new need expressed in the introduction:

- we can now take lubrication into account in numerical simulations of suspensions for **various shapes of particles** (strictly convex close to the contact point).
- Note also that the asymptotic expansion in [HK15] is available for any boundary condition $\mathbf{u}_i^* \in H^{1/2}(\partial B_i)$ satisfying the incompressibility condition $\int_{\partial B_i} \mathbf{u}_i^* \cdot \mathbf{n} = 0$. As a consequence, our method generalizes to non-rigid boundary conditions and could be used for example to take lubrication into account in simulations of deformable particles or bubbles for example.

On-going work - Prospects

The method presented in this chapter allows us to take lubrication into account in numerical simulations, meeting two needs arising from recent research on the rheology of suspensions: capture the lubrication effects on the whole fluid flow and deal with the case of non-spherical particles.

- The method was validated in [21] for two dimensional academic tests. The numerical tests were achieved using finite element direct method, based on a mesh fitting the boundary of the particles. As for the three dimensional case, the simulations of suspensions are particularly costly, and we are led to use fictitious domain methods. This avoids remeshing at each time step. Some of these methods, based on the use of Cartesian meshes, also allow the use of fast solvers. Following [21], we therefore worked with Fabien Vergnet (as part of a **post-doctorate funded by the ANR RheoSUNN**) to **adapt the method to the 3d fluid/particle solver CAFES [FG12]** which is based on a fictitious domain method. One of the main difficulties is to define the singular field inside the particles. We have to take care that the remaining $\mathbf{u} - \mathbf{u}^{\text{sing}}$ field is regular, including inside the particles. This work is ongoing, in collaboration with Flore Nabet and Fabien Vergnet (who is now lecturer at the LJLL).
- Including this method in three dimensional numerical computations will allow us to perform new rheological studies, that cannot be achieved with the existing codes. This is part of **ANR RheoSUNN's** project which aims to design a code that meets the current challenges in this domain. Indeed, the key point to make a breakthrough in the understanding of some recently observed phenomena is to compute the velocity and pressure fields in the whole fluid domain, modelling carefully the multi-body lubrication and its feedback on the flow for general forms of particles. The method described in this chapter meets these requirements. With Georges Gautier, from the FAST laboratory and member of the ANR, we would like to recruit and co-supervise a PhD student at the end of the project, in order to **carry out new rheological studies with the code resulting from the project**.
- A longer term project would be to **extend this decomposition method in order to take into account lubrication in boundary element simulations** (BEM methods). Indeed, I had the opportunity to take part in the development of a BEM solver for Stokes (see chapter 3). This kind of numerical method, discretizing precisely the

boundary of the particles, can be of great help in the fine study of the lubrication phenomenon between solids or in the simulation of rigid or elastic micro-swimmers. A good consideration of lubrication in these simulations is essential to obtain accurate results. It would therefore be interesting to think about an extension to this new framework of the decomposition method presented in this chapter. In the case of a Dirichlet to Neumann problem, the unknown in BEM formulations is the local surface force exerted by the fluid on the particle boundary. The idea would be to obtain an asymptotic expansion of this surface force field in the gap between the particles. Then we can decompose the surface unknown in the same way as we decomposed the fluid field in the case of a volume discretization. Note that a BEM method coupled with a tabulation of the local force field was proposed in [ZI09].

References

- [ACS00] F. Assous, P. Ciarlet, and J. Segré. “Numerical Solution to the Time-Dependent Maxwell Equations in Two-Dimensional Singular Domains: The Singular Complement Method”. In: *Journal of Computational Physics* 161.1 (2000), pp. 218–249 (cit. on p. 39).
- [BB88] J F Brady and G Bossis. “Stokesian Dynamics”. In: *Annual Review of Fluid Mechanics* 20 (1988), pp. 111–157 (cit. on p. 34).
- [CH03] P. Ciarlet and J. He. “The Singular Complement Method for 2d scalar problems”. In: *Comptes Rendus Mathématique* 336.4 (2003), pp. 353–358 (cit. on p. 39).
- [Cic+94] B. Cichocki, B. U. Felderhof, K. Hinsen, E. Wajnryb, and J. Blawdziewicz. “Friction and mobility of many spheres in Stokes flow”. In: *The Journal of Chemical Physics* 100.5 (1994). Publisher: American Institute of Physics, pp. 3780–3790 (cit. on p. 34).
- [Cox74] R. G. Cox. “The motion of suspended particles almost in contact”. In: *International Journal of Multiphase Flow* 1.2 (1974), pp. 343–371 (cit. on pp. 32, 34).
- [DBB87] L. Durlofsky, J. F. Brady, and G. Bossis. “Dynamic simulation of hydrodynamically interacting particles”. In: *Journal of Fluid Mechanics* 180 (1987). Publisher: Cambridge University Press, pp. 21–49 (cit. on pp. 32, 33).
- [FG12] B. Fabrèges and L. Gouarin. *CAFES (CArtesian Finite Element Solver)*. 2012. URL: <https://github.com/gouarin/cafes> (visited on Sept. 1, 2021) (cit. on p. 46).
- [Gal+14] S. Gallier, E. Lemaire, L. Lobry, and F. Peters. “A fictitious domain approach for the simulation of dense suspensions”. In: *Journal of Computational Physics* 256 (2014), pp. 367–387 (cit. on p. 34).
- [Hec12] F. Hecht. “New development in FreeFem++”. In: *J. Numer. Math.* 20.3-4 (2012), pp. 251–265 (cit. on p. 36).
- [HK15] M. Hillairet and T. Kelaï. “Justification of lubrication approximation: An application to fluid/solid interactions”. In: *Asymptotic Analysis* 95.3-4 (2015), pp. 187–241 (cit. on pp. 42, 43, 45).
- [Lad88] A. J. C. Ladd. “Hydrodynamic interactions in a suspension of spherical particles”. In: *The Journal of Chemical Physics* 88.8 (1988), pp. 5051–5063 (cit. on p. 34).
- [YM10] K. Yeo and M. R. Maxey. “Simulation of concentrated suspensions using the force-coupling method”. In: *Journal of Computational Physics* 229.6 (2010), pp. 2401–2421 (cit. on p. 34).
- [ZI09] G. Zhu and M. S. Ingber. “Accurate treatment of lubrication forces between rigid spheres in viscous fluids using a traction-corrected boundary element method”. In: *Engineering Analysis with Boundary Elements* 33.4 (2009), pp. 467–473 (cit. on p. 47).

New tools for Boundary Element Methods for Stokes.

Collaborators: François Alouges (CMAP, Palaiseau) - Matthieu Aussal (CMAP, Palaiseau) - Franck Pigeonneau (Saint-Gobain Recherche) - Antoine Sellier (LadHyX, Palaiseau)

Related publications:

[12] *Application of the Sparse Cardinal Sine Decomposition to 3D Stokes Flows.* With F. Alouges, M. Aussal, F. Pigeonneau, and A. Sellier. In: *International Journal of Computational Methods and Experimental Measurements*. 5.3 (2017), pp. 387–394

[13] *Motion of a solid particle in a bounded viscous flow using the Sparse Cardinal Sine Decomposition.* With F. Alouges and A. Sellier. In: *Meccanica* 55 (2020), pp. 403–419

Expected applications of the results presented in this chapter:

- *Rheology of suspensions: fast BEM solver for numerical simulation of suspensions. The fine description of the boundaries allows a good consideration of close interactions between solids.*
 - *Micro-swimmers and active suspensions: Numerical computation of optimal strokes. BEM is a good framework to simulate the deformation of elastic swimmers.*
-

As mentioned in the introduction, there is a great need for numerical simulation to better understand the rheology of suspensions. This requires codes allowing the simulation of many particles, possibly close to each other in the case of dense suspensions.

Existing numerical rheological studies are mostly based on the so-called "non-direct" simulation methods. In that case, the flow is not resolved and the positions of the particles are obtained by modelling the hydrodynamic forces acting on them. It is only recently that direct methods, solving Stokes PDEs without adding any model, have been used to simulate dense suspensions. In 2014, it was shown in [Gal+14b; Gal+14a] that current computational resources allow the use of direct solvers to perform rheological studies. In that work, the authors implement a fictitious domain method based on a finite difference discretization. More recently, in [Yan+20], a boundary element method (BEM) has been used to perform HPC simulations of dense suspensions composed of spherical particles.

It seems clear that **numerical simulation of suspensions based on direct methods** has an important role to play in the better understanding of their behaviour. Until a few years ago, I worked mainly with direct methods based on a three dimensional mesh of the domain (think e.g. of finite element, finite difference or finite volume methods). These methods can be divided into two classes. The first one is based on meshes fitting the boundaries of the particles. In that case, the geometry is respected but it requires remeshing of the fluid domain at time iteration. Although immense progress has been made in recent years on remeshing techniques, these methods are still little used for the study of suspension rheology. The second class of methods is based on a global mesh of the whole fluid and solid domain, not fitting the boundary of the particles. These methods have the advantage, for example, to avoid remeshing the fluid domain at each time step and to allow the use of fast solvers in the case of a global Cartesian mesh. One of their disadvantages is the difficulty to correctly take into account the geometry of the particles, without losing accuracy when transferring the information from the particles to the global mesh. Several strategies have been implemented to overcome this difficulty (see e.g. [ALR05; FGM13; Wac+15]).

In 2015, Franck Pigeonneau (Saint-Gobain Recherche in 2015, now at CEMEF, Sophia Antipolis, MINES ParisTech) and Antoine Sellier (LadHyX, Ecole Polytechnique) were working with a boundary element solver to simulate bubbles in glass. They had a very accurate BEM solver but it did not allow to take into account many particles. Compared to fictitious domain solvers, one of the great advantages of BEM solvers is that they are based on a two dimensional mesh of the particle boundary (see figure 3.1). The geometry of the latter is thus accurately taken into account and the number of unknowns is limited.

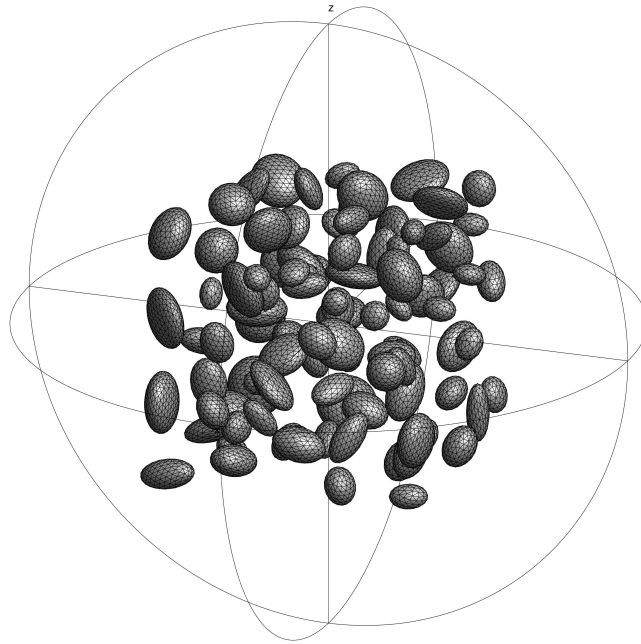


Fig. 3.1: Suspension of 100 ellipsoids in three dimensions. Example of two dimensional mesh of the surface of the particles used in BEM simulations.

However, they had to face a well-known difficulty of BEM methods: the matrices of the discrete system are full matrices and it is essential to design fast solvers to be able to solve the problems when the number of unknowns increases (which is fatally the case when the number of particles increases since the boundary of these particles is meshed). To meet the needs of Saint-Gobain Research, they were looking for a fluid solver that was able to deal with many entities in the fluid.

At the same time, at CMAP, François Alouges and Matthieu Aussal were working on a fast solver (the SCSD) to solve Helmholtz and Maxwell's equations using BEM. We had in mind to extend this fast solver to the Stokes equations. Our objective was to use the BEM solver for the numerical simulation of suspensions and micro-swimmers at low Reynolds number. From the point of view of the simulation of dense suspensions (whether rigid particles or bubbles), I think for example that the accurate meshing of the geometry in BEM methods, could make it possible to better take into account and understand the phenomena of lubrication when the particles are close.

We therefore set up **project with Saint Gobain** whose objective was to test the interest and efficiency of the SCSD for the simulation of moving entities (rigid or not) in a Stokes fluid.

We obviously had to face the two usual difficulties of **Boundary Element Methods**: the **implementation of fast solvers to compute the solution of the full system**, but also the **computation of singular integrals** involved in the coefficients of the matrices. To solve these two problems, François Alouges and Matthieu Aussal had developed new methods for Helmholtz equations. Their work naturally extended to Maxwell equations thanks to formulations based on Helmholtz kernel (see e.g. [BCS02] for such a formulation). In [11,12], we further extended their methods to deal with Stokes problem. The main difficulty was that, unlike Helmholtz kernel which is radial, Stokes kernel is entirely three-dimensional. One consequence is that the techniques developed for Helmholtz problem did not generalize directly to Stokes problem.

Finally, it should be noted that the **numerical simulation of suspensions has some features that are not usual** in many applications of BEM (compared for example to the Helmholtz and Maxwell domains of application). Indeed, we must keep in mind in the following that:

- **The domain over which we have to solve the equations changes at each time step.** This is very different for example from the study of the diffraction of a wave on a given solid, for which we want to vary the incident direction on the solid. Indeed, in that case, the domain is fixed and so is the matrix to be inverted: the problem amounts to inverting the same matrix for many different second members. In the case of suspensions, the fluid domain changes at each time step and so does the matrix to be inverted. Thus, the pre-processing of the matrix that is needed to obtain a fast matrix/vector product must be redone at each iteration. As a consequence, the computational time needed for this pre-processing step should be optimized.
- **The domain consists of several solids that may be close to each other and for which the distance is not controlled.** Thus, the mesh of the boundary is made of several distinct connected surfaces and the points of two of these surfaces may be arbitrarily close. This remark is of great importance in the design of a method approximating the singular integrals. Again, this is specific to the fact that we consider several moving entities.

In the following, I begin with an introduction to Boundary Element Methods for the readers that are not used to these methods. Then, for each of the two difficulties encountered (designing a fast solver and computing singular integrals), I present the problems that arise and the methods developed by François Alouges and Matthieu Aussal

to solve them in the case of Helmholtz and Maxwell equations. Finally, I explain how we adapted these methods to Stokes equations.

3.1 Introduction to Boundary Element Methods (BEM)

To better understand the issues at hand, we present in this section the main features of Boundary Element Methods. In order to make the presentation easier to read, we focus on the three dimensional Laplace problem and say a word about Stokes problem at the end of the section. I refer to [Bon99] for an introduction to boundary element methods and to [Poz92] for a reference book on boundary element methods for Stokes equation.

▷ Green's functions

The *free-space Green's function* of a given linear partial differential equation problem, may also appear in the literature under the name of *fundamental solution*. It is the solution to the corresponding distribution equation with a source at point \mathbf{x} . Thus, Laplace Green's function, also known as Newton kernel or Newton potential, is solution to the following distribution equation:

$$-\Delta_{\mathbf{y}}G(\mathbf{x}, \mathbf{y}) = \delta_{\mathbf{x}}(\mathbf{y}).$$

If $T(\mathbf{x}, \mathbf{y}) \cdot \mathbf{n}(\mathbf{y})$ is the corresponding flux in direction $\mathbf{n}(\mathbf{y})$ at point \mathbf{y} we have

$$\begin{aligned} G(\mathbf{x}, \mathbf{y}) &= \frac{1}{4\pi|\mathbf{x} - \mathbf{y}|}, \\ T(\mathbf{x}, \mathbf{y}) \cdot \mathbf{n}(\mathbf{y}) &= \nabla_{\mathbf{y}}G(\mathbf{x}, \mathbf{y}) \cdot \mathbf{n}(\mathbf{y}) = \frac{(\mathbf{x} - \mathbf{y}) \cdot \mathbf{n}(\mathbf{y})}{4\pi|\mathbf{x} - \mathbf{y}|^3}. \end{aligned} \tag{3.1}$$

Kernel G is also called the *single layer potential* while T is the *double-layer potential*.

▷ Boundary integral representation

Suppose u is solution to Laplace equation outside a domain Ω :

$$-\Delta u = 0 \quad \text{in } \mathbb{R}^3 \setminus \Omega.$$

If Γ is the boundary of Ω , we have the following *boundary integral representation* of u :

$$\begin{aligned} \forall \mathbf{x} \in (\mathbb{R}^3 \setminus \Omega) \setminus \Gamma, \quad u(\mathbf{x}) &= \int_{\Gamma} T(\mathbf{x}, \mathbf{y}) \cdot \mathbf{n}(\mathbf{y}) u(\mathbf{y}) d\mathbf{y} - \int_{\Gamma} G(\mathbf{x}, \mathbf{y}) \frac{\partial u}{\partial \mathbf{n}}(\mathbf{y}) d\mathbf{y}, \\ \forall \mathbf{x} \in \Gamma, \quad \frac{u(\mathbf{x})}{2} &= \int_{\Gamma} T(\mathbf{x}, \mathbf{y}) \cdot \mathbf{n}(\mathbf{y}) u(\mathbf{y}) d\mathbf{y} - \int_{\Gamma} G(\mathbf{x}, \mathbf{y}) \frac{\partial u}{\partial \mathbf{n}}(\mathbf{y}) d\mathbf{y}, \end{aligned} \quad (3.2)$$

where \mathbf{n} is the exterior normal to Ω and $\frac{\partial u}{\partial \mathbf{n}} = \nabla u \cdot \mathbf{n}$.

From the first equation, we see that u is known everywhere in $\mathbb{R}^3 \setminus \Omega$ as soon as u together with $\frac{\partial u}{\partial \mathbf{n}}$ are known on the boundary Γ . The values of u and $\frac{\partial u}{\partial \mathbf{n}}$ on the boundary can be determined from the second equation together with boundary conditions on Γ .

Suppose for example one wants to solve the exterior Dirichlet to Neumann problem:

$$\begin{aligned} -\Delta u &= 0 \quad \text{in } \mathbb{R}^3 \setminus \Omega, \\ u &= u^0 \quad \text{on } \Gamma, \end{aligned}$$

with decreasing properties at infinity and $u^0 \in H^{1/2}(\Gamma)$. In that case, u is known on the boundary Γ and we can compute $\frac{\partial u}{\partial \mathbf{n}}$ on Γ solving the following boundary equation:

$$\forall \mathbf{x} \in \Gamma, \quad \int_{\Gamma} G(\mathbf{x}, \mathbf{y}) \frac{\partial u}{\partial \mathbf{n}}(\mathbf{y}) d\mathbf{y} = \int_{\Gamma} T(\mathbf{x}, \mathbf{y}) \cdot \mathbf{n}(\mathbf{y}) u^0(\mathbf{y}) d\mathbf{y} - \frac{u^0(\mathbf{x})}{2}. \quad (3.3)$$

Equation (3.3) is called the *boundary integral equation* and has to be understood as an equality in $H^{1/2}(\Gamma)$. This equation is specific to the Dirichlet to Neumann problem: there exists many integral equations, depending on the problem one wants to solve and the prescribed boundary conditions.

► Boundary element method

Let us now explain how the Boundary Element Method works. It is based on finite element discretizations of boundary integral equations. To describe the method, we focus on the Laplace Dirichlet to Neumann problem and the boundary integral equation (3.3).

Finite element discretization

The boundary Γ is discretized using a surface mesh Γ_h where h is the size of the elements constituting the mesh. In the following we consider flat triangles elements (see figure 3.2) but other kind of elements can be chosen (e.g. quadratic triangles). The unknown

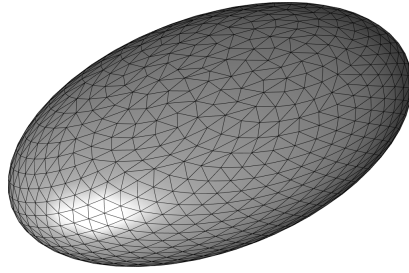


Fig. 3.2: Surface of an ellipsoid: mesh composed of flat triangular elements.

$\lambda = \frac{\partial u}{\partial \mathbf{n}} \in H^{-1/2}(\Gamma)$ as well as the boundary condition $u^0 \in H^{1/2}(\Gamma)$ are discretized using Lagrange finite elements spaces V_h and W_h on this mesh:

$$\lambda_h = \sum_{j=1}^{N_{dof}} \lambda_j \phi_j, \quad u_h^0 = \sum_{j=1}^{N_{BC}} u_j^0 \psi_j, \quad (3.4)$$

where $(\phi_j)_{j=1 \dots N_{dof}}$ (resp. $(\psi_j)_{j=1 \dots N_{BC}}$) is the finite element basis of V_h (resp. W_h). The number of degrees of freedom N_{dof} is the dimension of the space V_h to which the unknown λ_h belongs.

The boundary integral equation (3.3) is discretized as: find $\lambda_h \in V_h$ such that

$$\int_{\Gamma_h} G(\mathbf{x}, \mathbf{y}) \lambda_h(\mathbf{y}) d\mathbf{y} = \int_{\Gamma_h} T(\mathbf{x}, \mathbf{y}) \cdot \mathbf{n}(\mathbf{y}) u_h^0(\mathbf{y}) d\mathbf{y} - \frac{u_h^0(\mathbf{x})}{2}, \quad (3.5)$$

"for all $\mathbf{x} \in \Gamma$ " in a sense that remains to be specified.

Collocation method.

To solve the discrete boundary integral equation (3.5) for $\mathbf{x} \in \Gamma$ one can use the so-called *collocation method*. It consists in choosing *collocation points* $(\mathbf{x}_i)_i$ to evaluate the equation. In order to obtain as many equations as there are unknowns, we have to choose N_{dof} collocation points $(\mathbf{x}_i)_{i=1 \dots N_{dof}}$. Most often, the degrees of freedom of the Lagrange finite elements are used. The method is then to solve the following N_{dof} equations: find $\lambda_h \in V_h$ such that

$$\forall i = 1 \dots N_{dof}, \quad \int_{\Gamma_h} G(\mathbf{x}_i, \mathbf{y}) \lambda_h(\mathbf{y}) d\mathbf{y} = \int_{\Gamma_h} T(\mathbf{x}_i, \mathbf{y}) \cdot \mathbf{n}(\mathbf{y}) u_h^0(\mathbf{y}) d\mathbf{y} - \frac{u_h^0(\mathbf{x}_i)}{2}.$$

This can be rewritten, using decomposition (3.4): find $(\lambda_j)_{j=1\dots N_{dof}}$ such that

$$\forall i = 1 \dots N_{dof}, \quad \sum_{j=1}^{N_{dof}} \left(\int_{\Gamma_h} G(\mathbf{x}_i, \mathbf{y}) \phi_j(\mathbf{y}) d\mathbf{y} \right) \lambda_j = \sum_{j=1}^{N_{BC}} \left(\int_{\Gamma_h} T(\mathbf{x}_i, \mathbf{y}) \cdot \mathbf{n}(\mathbf{y}) \psi_j(\mathbf{y}) d\mathbf{y} \right) u_j^0 - \frac{1}{2} \sum_{j=1}^{N_{BC}} \psi_j(\mathbf{x}_i) u_j^0.$$

This in turn can be rewritten as the following matrix problem: find $\boldsymbol{\lambda} \in \mathbb{R}^{N_{dof}}$ such that

$$S^c \boldsymbol{\lambda} = D^c \mathbf{U}^0 - \frac{1}{2} I^c \mathbf{U}^0, \quad (3.6)$$

where $\boldsymbol{\lambda} = (\lambda_j)_j \in \mathbb{R}^{N_{dof}}$, $\mathbf{U}^0 = (u_j^0)_j \in \mathbb{R}^{N_{BC}}$ and the matrices S^c , D^c and I^c are given by

$$\begin{aligned} S_{ij}^c &= \int_{\Gamma_h} G(\mathbf{x}_i, \mathbf{y}) \phi_j(\mathbf{y}) d\mathbf{y}, \quad 1 \leq i, j \leq N_{dof}, \\ D_{ij}^c &= \int_{\Gamma_h} T(\mathbf{x}_i, \mathbf{y}) \cdot \mathbf{n}(\mathbf{y}) \psi_j(\mathbf{y}) d\mathbf{y} \quad 1 \leq i \leq N_{dof}, \quad 1 \leq j \leq N_{BC}, \\ I_{ij}^c &= \psi_j(\mathbf{x}_i) \quad 1 \leq i \leq N_{dof}, \quad 1 \leq j \leq N_{BC}. \end{aligned} \quad (3.7)$$

Note that the matrix S^c is dense and non symmetric. In general a direct solver is used to solve the system.

Variational method.

The second method to solve (3.3) is to consider the equality in $H^{1/2}(\Gamma)$ in a variational framework: find $\lambda = \frac{\partial u}{\partial \mathbf{n}} \in H^{-1/2}(\Gamma)$ such that

$$\forall v \in H^{-1/2}(\Gamma), \quad \int_{\Gamma} \left(\int_{\Gamma} G(\mathbf{x}, \mathbf{y}) \lambda(\mathbf{y}) d\mathbf{y} \right) v(\mathbf{x}) d\mathbf{x} = \int_{\Gamma} \left(\int_{\Gamma} T(\mathbf{x}, \mathbf{y}) \cdot \mathbf{n}(\mathbf{y}) u^0(\mathbf{y}) d\mathbf{y} \right) v(\mathbf{x}) d\mathbf{x} - \int_{\Gamma} \frac{u^0(\mathbf{x})}{2} v(\mathbf{x}) d\mathbf{x}.$$

Then, approximating λ and v in V_h and u^0 in W_h , the corresponding discrete problem writes, with evident notations: find $\lambda_y \in V_h$ such that

$$\forall v_h \in V_h, \quad \int_{\Gamma} \left(\int_{\Gamma} G(\mathbf{x}, \mathbf{y}) \lambda_h(\mathbf{y}) d\mathbf{y} \right) v_h(\mathbf{x}) d\mathbf{x} = \int_{\Gamma} \left(\int_{\Gamma} T(\mathbf{x}, \mathbf{y}) \cdot \mathbf{n}(\mathbf{y}) u_h^0(\mathbf{y}) d\mathbf{y} \right) v_h(\mathbf{x}) d\mathbf{x} - \int_{\Gamma} \frac{u_h^0(\mathbf{x})}{2} v_h(\mathbf{x}) d\mathbf{x}.$$

Finally, decomposing on the basis $(\phi_j)_{j=1\dots N_{dof}}$ (resp. $(\psi_j)_{j=1\dots N_{BC}}$) of V_h (resp. W_h) the problem becomes: find $\boldsymbol{\lambda} \in \mathbb{R}^{N_{dof}}$ such that

$$\begin{aligned} \forall \mathbf{v} \in \mathbb{R}^{N_{dof}}, \quad & \sum_{i,j} \left(\int_{\Gamma} \int_{\Gamma} G(\mathbf{x}, \mathbf{y}) \phi_i(\mathbf{x}) \phi_j(\mathbf{y}) \, dy d\mathbf{x} \right) v_i \lambda_j = \\ & \sum_{i,j} \left(\int_{\Gamma} \int_{\Gamma} T(\mathbf{x}, \mathbf{y}) \cdot \mathbf{n}(\mathbf{y}) \phi_i(\mathbf{x}) \psi_j(\mathbf{y}) \, dy d\mathbf{x} \right) v_i u_j^0 - \frac{1}{2} \sum_{i,j} \left(\int_{\Gamma} \phi_i(\mathbf{x}) \psi_j(\mathbf{x}) \, d\mathbf{x} \right) v_i u_j^0, \end{aligned}$$

which can be rewritten using matrices as

$$\forall \mathbf{v} \in \mathbb{R}^{N_{dof}}, \quad \mathbf{v}^T S^v \boldsymbol{\lambda} = \mathbf{v}^T D^v \mathbf{U}^0 - \frac{1}{2} \mathbf{v}^T I^v \mathbf{U}^0,$$

where the matrices S^v , D^v and I^v are given by

$$\begin{aligned} S_{ij}^v &= \int_{\Gamma_h} \int_{\Gamma_h} G(\mathbf{x}, \mathbf{y}) \phi_j(\mathbf{y}) \phi_i(\mathbf{x}) \, dy d\mathbf{x}, \quad 1 \leq i, j \leq N_{dof}, \\ D_{ij}^v &= \int_{\Gamma_h} \int_{\Gamma_h} T(\mathbf{x}, \mathbf{y}) \cdot \mathbf{n}(\mathbf{y}) \psi_j(\mathbf{y}) \phi_i(\mathbf{x}) \, dy d\mathbf{x} \quad 1 \leq i \leq N_{dof}, \quad 1 \leq j \leq N_{BC}, \\ I_{ij}^v &= \int_{\Gamma_h} \phi_i(\mathbf{x}) \psi_j(\mathbf{x}) \, d\mathbf{x}, \quad 1 \leq i \leq N_{dof}, \quad 1 \leq j \leq N_{BC}. \end{aligned} \tag{3.8}$$

The problem is finally equivalent to solving the following linear system:

$$S^v \boldsymbol{\lambda} = D^v \mathbf{U}^0 - \frac{1}{2} I^v \mathbf{U}^0. \tag{3.9}$$

Again, the matrix S^v we obtained in this variational framework is full. However, it is now symmetric, which allows the use of non-direct iterative solvers. Note that D^v and I^v are also symmetric (and square) if one uses the same basis to discretize $H^{1/2}$ and $H^{-1/2}$ (e.g. P^1 finite elements). Moreover, in this variational framework, theoretical results of convergence can be obtained when the size of the triangles of the mesh goes to zero.

The two main difficulties in implementing BEM methods.

- The first difficulty in solving BEM problems is that it comes down to **solving dense systems**. A direct resolution based on a factorization of the matrix would cost $O(N_{dof}^3)$ and require the storage of the matrix. This is impossible for large values of N_{dof} . An iterative resolution reduces the cost to $O(N_{dof}^2)$ and avoids the storage of the matrix. However, it remains too slow for large values of N_{dof} . There is therefore a great need to design fast algorithms to solve such systems. This problem will be addressed in the next section 3.2.

- The second difficulty is the computation of the matrix itself. Indeed, its coefficients are obtained from integrals which are singular when \mathbf{x} and \mathbf{y} are close. The **approximation of these singular integrals** is a difficult problem and it is essential, in order to obtain accurate results, to develop adapted methods. We will deal with this problem in section 3.3.

▷ Extension to Stokes' problem

Let us come back for a moment to Stokes' problem. The implementation of a BEM method for this problem is similar to the one presented for the Laplace problem. The main (and important!) difference is that it consists in four equations, for which the unknown is a set of four scalar fields. The free-space Stokes problem writes

$$\begin{aligned} -\mu \Delta \mathbf{u} + \nabla p &= \mathbf{f}, \\ \nabla \cdot \mathbf{u} &= 0, \end{aligned}$$

where the velocity \mathbf{u} and the force \mathbf{f} are both in \mathbb{R}^3 while the pressure p is in \mathbb{R} . This leads to three fundamental solutions (one for each of the three directions of the force):

$$\begin{aligned} -\mu \Delta_{\mathbf{y}} \mathbf{u}_j(\mathbf{x}, \mathbf{y}) + \nabla_{\mathbf{y}} p_j(\mathbf{x}, \mathbf{y}) &= \delta_{\mathbf{x}}(\mathbf{y}) \mathbf{e}_j, \\ \nabla \cdot \mathbf{u}_j(\mathbf{x}, \mathbf{y}) &= 0. \end{aligned}$$

The solution writes

$$\mathbf{u}_j(\mathbf{x}, \mathbf{y}) = \mathbf{G}_j(\mathbf{x}, \mathbf{y})/8\pi\mu, \quad p_j(\mathbf{x}, \mathbf{y}) = \Pi_j(\mathbf{x}, \mathbf{y})/8\pi,$$

where $\mathbf{G}_j(\cdot, \cdot) = (G_{ij}(\cdot, \cdot))_{i=1\dots 3} : \mathbb{R}^3 \times \mathbb{R}^3 \rightarrow \mathbb{R}^3$ and $\Pi_i(\cdot, \cdot) : \mathbb{R}^3 \times \mathbb{R}^3 \rightarrow \mathbb{R}$. The Stokes kernel $\mathbf{G} = (G_{ij})_{ij}$, also called *Stokeslet*, can be seen as a 3×3 matrix given by:

$$G_{ij}(\mathbf{x}, \mathbf{y}) = \frac{\delta_{ij}}{|\mathbf{x} - \mathbf{y}|} + \frac{(x_i - y_j)(x_j - y_j)}{|\mathbf{x} - \mathbf{y}|^3}, \quad 1 \leq i, j \leq 3. \quad (3.10)$$

The corresponding pressure is $\Pi_j(\mathbf{x}, \mathbf{y}) = 2 \frac{x_j}{|\mathbf{x} - \mathbf{y}|^3}$, $1 \leq j \leq 3$.

We define $\mathbf{T}_j(\mathbf{x}, \mathbf{y}) = \sigma_1(\mathbf{G}_j, \Pi_j) \in \mathbb{R}^{3 \times 3}$ where $\sigma_\mu(\mathbf{v}, \mathbf{q}) = \mu(\nabla \mathbf{v} + \nabla^T \mathbf{v}) - \mathbf{q} \text{Id}$ is the stress tensor for viscosity μ .

We have $\mathbf{T}_j(\mathbf{x}, \mathbf{y}) = [T_{ijk}(\mathbf{x}, \mathbf{y})]_{i,k=1\dots 3}$

$$T_{ijk}(\mathbf{x}, \mathbf{y}) = -6 \frac{(x_i - y_i)(x_j - y_j)(x_k - y_k)}{|\mathbf{x} - \mathbf{y}|^5}, \quad 1 \leq i, j, k \leq 3. \quad (3.11)$$

The tensor $\mathbf{T} = (T_{ijk})_{ijk}$ is called the *Stresslet*.

The boundary integral representation (3.2) as well as the integral equation (3.3) can be generalized to Stokes' problem using the Stokeslet and Stresslet tensors (see [Poz92] for details about BEM for Stokes).

The natural Neumann boundary term in the case of Stokes equations is $\boldsymbol{\lambda} = \sigma_\mu(\mathbf{u}, \mathbf{p})\mathbf{n}(\mathbf{y}) \in [H^{-1/2}(\Gamma)]^3$. This one plays for Stokes problem the role of $\frac{\partial u}{\partial \mathbf{n}}$ for Laplace problem. Consider (\mathbf{u}, \mathbf{p}) , solution to Stokes equations outside a domain Ω . The boundary integral representation (3.2) generalizes to Stokes problem: the velocity and pressure fields are known everywhere outside Ω , as soon as \mathbf{u} , together with $\boldsymbol{\lambda}$ are known on its boundary.

So suppose now that one wants to solve the exterior Stokes Dirichlet to Neumann problem:

$$\begin{aligned} -\mu \Delta \mathbf{u} + \nabla \mathbf{p} &= 0 \quad \text{in } \mathbb{R}^3 \setminus \Omega, \\ \nabla \cdot \mathbf{u} &= 0 \quad \text{in } \mathbb{R}^3 \setminus \Omega, \\ \mathbf{u} &= \mathbf{u}^0 \quad \text{on } \Gamma, \end{aligned}$$

with decreasing properties at infinity and where $\mathbf{u}^0 \in (H^{1/2}(\Gamma))^3$. The solution is known everywhere provided $\boldsymbol{\lambda} = \sigma(\mathbf{u}, \mathbf{p})\mathbf{n}(\mathbf{y})$ is known on Γ . The corresponding vector boundary equation now writes: find $\boldsymbol{\lambda} \in [H^{-1/2}(\Gamma)]^3$, such that

$$\begin{aligned} \forall j = 1 \dots 3, \forall \mathbf{x} \in \Gamma, \quad \frac{1}{8\pi\mu} \int_{\Gamma} \sum_{1 \leq i \leq 3} G_{ij}(\mathbf{x}, \mathbf{y}) \lambda_i(\mathbf{y}) d\mathbf{y} = \\ \frac{1}{8\pi} \int_{\Gamma} \sum_{1 \leq i, k \leq 3} u_i^0(\mathbf{y}) T_{ijk}(\mathbf{x}, \mathbf{y}) \mathbf{n}_k(\mathbf{y}) d\mathbf{y} - \frac{u_j^0(\mathbf{x})}{2}. \end{aligned} \quad (3.12)$$

Note that, a priori, due to the vector nature of the problem, the second integral is only defined in the sense of Cauchy principal values. The discretization using finite elements on Γ follows the same lines as for the Laplace problem. Here, each coordinate λ_i of $\boldsymbol{\lambda}$ must be discretized on Γ while equation (3.12) provides three equations on Γ . As a consequence, the corresponding vector problem for Stokes equations can be seen as a 3×3 block problem.

3.2 First challenge: fast resolution of dense systems. The Sparse Cardinal Sine Decomposition method (SCSD) adapted to Stokes.

In this section, we focus on the resolution of the variational system (3.9) using an iterative algorithm. As already said, matrix S^v (3.8) is full and one needs to design fast algorithms to solve the system. I first present the general idea on which fast algorithms for this type of system are based. I then describe the method on which the one we propose for the Stokes kernel is based: the Sparse Cardinal Sine Decomposition (SCSD). This method was designed by François Alouges and Matthieu Aussal for radial kernels. I finally explain how we have extended it to Stokes kernels.

▷ Separation of variables

Let us consider a generic scalar kernel K (think for example to Laplace kernel G (3.1), or to one of the coefficients G_{ij} of the Stokeslet (3.10)). As far as an iterative algorithm is used to solve the linear system, one needs to design a fast algorithm to compute the matrix-vector product $\mathbf{V} = S^v \boldsymbol{\lambda} \in \mathbb{R}^{N_{dof}}$:

$$\forall m = 1 \dots N_{dof}, \quad V_m = \sum_{j=1}^{N_{dof}} \left(\int_{\Gamma_h} \int_{\Gamma_h} K(\mathbf{x}, \mathbf{y}) \phi_j(\mathbf{y}) \phi_m(\mathbf{x}) d\mathbf{y} d\mathbf{x} \right) \lambda_j.$$

Consider a quadrature formula $(\mathbf{x}_k, w_k)_{k=1 \dots N_{int}}$ where $(\mathbf{x}_k)_{k=1 \dots N_{int}}$ is the set of integration points on Γ_h and $\mathbf{w} = (w_k)_{k=1 \dots N_{int}}$ the corresponding weights. The problem comes down to the computation of $\tilde{\mathbf{V}}$ approximating \mathbf{V} where

$$\forall m = 1 \dots N_{dof}, \quad \tilde{V}_m = \sum_{j=1}^{N_{dof}} \left(\sum_{k=1}^{N_{int}} \sum_{l=1}^{N_{int}} w_k w_l K(\mathbf{x}_k, \mathbf{x}_l) \phi_j(\mathbf{x}_l) \phi_m(\mathbf{x}_k) \right) \lambda_j.$$

This can again be re-written as

$$\tilde{\mathbf{V}} = \Phi_{\mathbf{w}}' \mathbf{K} \Phi_{\mathbf{w}} \boldsymbol{\lambda},$$

where $\Phi_{\mathbf{w}} = (w_l \phi_j(\mathbf{x}_l))_{lj}$ is the $N_{int} \times N_{dof}$ integration matrix, and $\mathbf{K} = (K(\mathbf{x}_k, \mathbf{x}_l))_{kl}$ is a $N_{int} \times N_{int}$ matrix. Matrix $\Phi_{\mathbf{w}}$ being sparse, the computation of $\tilde{\mathbf{V}}$ requires only one full matrix-vector product (by matrix \mathbf{K}).

We are thus finally led to design a fast algorithm for the computation of $\mathbf{g} = \mathbf{K}\mathbf{f}$:

$$\forall k, \quad g_k = \sum_l K(\mathbf{x}_k, \mathbf{x}_l) f_l, \quad (3.13)$$

where $\mathbf{f} = (f_l)_l$ is given. Note that, the kernels we consider only depend on $\mathbf{x} - \mathbf{y}$: $K(\mathbf{x}, \mathbf{y}) = K(\mathbf{x} - \mathbf{y})$. Consequently, \mathbf{g} is the discrete convolution of \mathbf{f} by kernel K . This discrete convolution product requires a priori $O(N^2)$ operations to be computed.

The fast algorithms designed to achieve this computation are based on a common idea: the **separation of variables** (together with hierarchical computations). The point of separating the variables is easy to understand if we consider the kernel $K(\mathbf{x}, \mathbf{y}) = K(\mathbf{x} - \mathbf{y}) = |\mathbf{x} - \mathbf{y}|^2$. In that case, one can separate the variables writing

$$K(\mathbf{x}_k - \mathbf{x}_l) = |\mathbf{x}_k - \mathbf{x}_l|^2 = |\mathbf{x}_k|^2 - 2\mathbf{x}_k \cdot \mathbf{x}_l + |\mathbf{x}_l|^2. \quad (3.14)$$

The corresponding discrete convolution product writes

$$\forall k, \quad g_k = \sum_l K(\mathbf{x}_k - \mathbf{x}_l) f_l = |\mathbf{x}_k|^2 \sum_l f_l - 2\mathbf{x}_k \cdot \sum_l \mathbf{x}_l f_l + \sum_l |\mathbf{x}_l|^2 f_l$$

and can be computed in $O(N)$ iterations instead of $O(N^2)$.

Then, the challenge to design fast BEM algorithm is to obtain counterparts of (3.14), separating the variables \mathbf{x} and \mathbf{y} for the considered kernel (Laplace, Stokes...).

Before going further, let us say a word about the hierarchical matrix method (H-matrix method). This kind of acceleration method has been successfully used to deal with integral equations. It is based on a sum of low rank matrices (algebraic counterpart of the separation of variables) for which the matrix-product vector is particularly fast. As a consequence, this method is very efficient in the case of multi right-members computations, for which a single factorization is needed before performing many matrix-vector products. However, the computation of the factorization in low-rank matrices is quite expensive. Let us recall that, in case of numerical simulation of suspensions, the domain changes at each time step and the factorization must be recalculated each time. As a consequence, the H-matrix method does not seem to be suited for our application.

▷ The Fast Multipole Method (FMM)

Let us describe the classical and well-known Fast Multipole Method. It was developed about 40 years ago in order to realize fast matrix-vector products for full matrices resulting from BEM discretizations. It gave rise to a large amount of research since then. The method takes advantage of the "smoothness" in the kernel due to the distance: the mesh is subdivided in panels and nearby panels are clustered to compute their contributions to distant point panels. The method is accelerated using a hierarchical decomposition of the mesh.

Let us first describe the idea behind the mono-level FMM. Consider C_1 and C_2 two parts of the boundary with M_i center of C_i . When M_1 is sufficiently far from M_2 , the idea is to find an approximation of kernel K of the following type:

$$K(\mathbf{x} - \mathbf{y}) \approx \sum_q \tilde{F}^q(\mathbf{M}_1 \mathbf{x}) T^q(\mathbf{M}_2 \mathbf{M}_1) F^q(\mathbf{M}_2 \mathbf{y}), \quad \forall \mathbf{x} \in C_1, \mathbf{y} \in C_2. \quad (3.15)$$

This formula can be understood as follows: first, F^q carries the information from \mathbf{y} to M_2 , then, T ensures the transfer of this information from M_2 to M_1 and finally, \tilde{F}^q spreads the information from M_1 to \mathbf{x} . Doing so, the variables \mathbf{x} and \mathbf{y} are separated.

Suppose now that we do have such a formula and denote by I_{C_m} the set of indices l for which \mathbf{x}_l is in C_m : $I_{C_m} = \{l, \mathbf{x}_l \in C_m\}$. The term in the matrix-vector product resulting from the interaction between C_1 and C_2 can then be computed as

$$\begin{aligned} \forall k \in I_{C_1}, \quad g_k^{C_2} &:= \sum_{l \in I_{C_2}} K(\mathbf{x}_k - \mathbf{x}_l) f_l dy \\ &\approx \sum_q \tilde{F}^q(\mathbf{M}_2 \mathbf{x}_k) T^q(\mathbf{M}_1 \mathbf{M}_2) \left[\sum_{l \in I_{C_2}} F^q(\mathbf{M}_1 \mathbf{x}_l) f_l \right]. \end{aligned}$$

As expected, the variables are separated (see figure 3.3).

The mono-level Multipole Method consists in decomposing the mesh into cells $(C_m)_{m \in \{1 \dots M\}}$, to compute the interactions between each pair of cells and aggregate all the results to obtain $(g_k)_k$. Close interactions are computed exactly. To estimate the contributions of distant cells, the computations are driven as follows: choose a cell C_2 , compute the sum $(\sum_{l \in I_{C_2}} F^q(\mathbf{M}_1 \mathbf{x}_l) f_l)$ that do not depend on \mathbf{x}_k and then, for all cells C far from C_2 , compute $(g_k^{C_2})_{k \in I_C}$ using the previous approximation formula. Doing so, we obtain an algorithm much faster than $O(N^2)$.

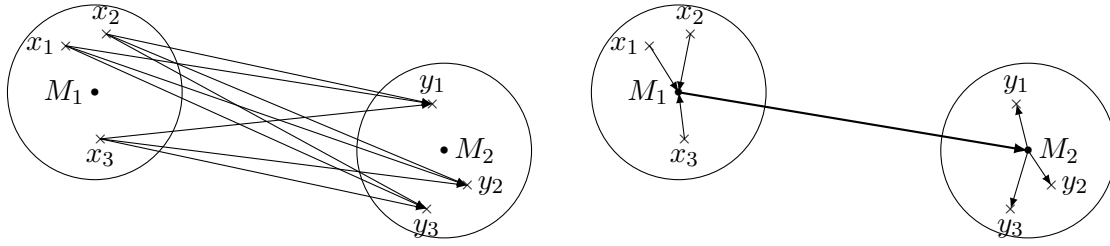


Fig. 3.3: Without FMM (left) and variable separation with FMM (right).

The Fast Multiple Method (FMM) is based on this procedure, which is accelerated using a "divide and conquer" like algorithm through a hierarchical decomposition of the mesh. This provides an overall method with complexity $O(N \log(N))$. Developed about 40 years ago, the FMM method has given rise to a great amount of research since then, leading to great expertise in the field. It should be noted that it is based on formula (3.15), which must be derived independently for each kernel. First described in [GR88b; GR88a] for the Laplace kernel, the method was extended to Helmholtz/Maxwell problem in [CRW93]. Note also that involved numerical implementation are customary when programming FMM methods.

► **The Sparse Cardinal Sine Decomposition (SCSD) for radial kernels [Alouges, Aussal]**

A new method to deal with radial kernels has been proposed in [AA15] by François Alouges and Matthieu Aussal. Suppose that K is decomposed as

$$K(\mathbf{x}) = \sum_{q=1}^M \alpha_q e^{i\mathbf{x} \cdot \boldsymbol{\xi}_q}. \quad (3.16)$$

Then, from the definition of $(g_k)_k$ (3.13), we obtain

$$\forall k, \quad g_k = \sum_{l=1}^N K(\mathbf{x}_k - \mathbf{x}_l) f_l = \sum_{q=1}^M e^{i\mathbf{x}_k \cdot \boldsymbol{\xi}_q} \left[\alpha_q \left(\sum_{l=1}^N e^{-i\mathbf{x}_l \cdot \boldsymbol{\xi}_q} f_l \right) \right]. \quad (3.17)$$

Note that here, we have taken advantage of the properties of the convolution product in Fourier space to separate the variables. Indeed, the definition of $(g_k)_k$ can be seen as a discrete counterpart of $g = K \star f$. Then, from equation (3.16), the $(\alpha_q)_q$ can be seen as a discrete Fourier transform of K and finally, equation (3.17) can be understood as a discrete counterpart of $\hat{g} = \widehat{K \star f} = \hat{K} \hat{f}$.

Finally, we see that, to design a fast method, one can try to decompose K as in (3.16), with M as small as possible.

Following the previous remark, the first idea is to use a discrete Fourier transform of $(K(\mathbf{x}_k))_k$ to obtain (3.16) and then FFT algorithms to compute the matrix-vector product. To do so, K being known on Γ , it first has to be projected on a regular 3D grid and the algorithm can be summarized as

$$\begin{aligned}
 K^{grid} &\leftarrow (K(\mathbf{x}_k))_k, & f^{grid} &\leftarrow (f(\mathbf{x}_l))_l && \text{(Interpolation from } \Gamma \text{ to the regular grid)} \\
 g^{grid} &= \text{IFFT}(\text{FFT}(K^{grid}) \text{FFT}(f^{grid})) && && \text{(FFT on the regular grid)} \\
 (g_k)_k &\leftarrow g^{grid} && && \text{(Interpolation from the regular grid to } \Gamma)
 \end{aligned} \tag{3.18}$$

Again, the separation of variables, together with the hierarchical nature of the FFT algorithm provides a fast algorithm. As with the FMM algorithm, close interactions must be corrected to be accurate. Unlike FMM, this new algorithm does not depend on the kernel since the decomposition is performed by the FFT. Moreover, its implementation is easier than that of FMM, provided one has a FFT algorithm at hand. On the other hand, one of the difficulties comes from the 3D interpolation step: as K is singular, one may need very fine interpolation grids in order to obtain a good accuracy. This may lead to large values of M in decomposition (3.16), which deteriorates the speed of the algorithm.

F. Alouges and M. Aussal proposed in [AA15] to exploit the rotational invariance of the kernels they considered (Helmoltz, Maxwell or Laplace) to obtain a precise decomposition (3.16) with small M . This new method allows, the precision and the distance for close interactions being given, to choose the smallest M and the best coefficients $\alpha = (\alpha_q)_q$, and points $\xi = (\xi_q)_q$ in (3.16). This improves the speed of the algorithm while controlling the precision. As the $(\xi_q)_q$ do not form a regular grid, one now need to use Non Uniform FFT (NUFFT) and the algorithm writes:

$$\begin{aligned}
 (\alpha, \xi) &= \text{SCSD}(K) && \text{(Computation of } \alpha, \xi) \\
 (g_k)_k &= \text{INUFFT}_\xi(\alpha \text{NUFFT}_\xi(f)) && \text{(NUFFT on the grid } \xi)
 \end{aligned}$$

To choose α and ξ , the authors in [AA15] start by writing K as the inverse Fourier transform of its Fourier transform \hat{K} :

$$K(\mathbf{x}) = \frac{1}{(2\pi)^3} \int_{\mathbb{R}^3} \hat{K}(\xi) e^{i\mathbf{x}\cdot\xi} d\xi. \quad (3.19)$$

The idea is then to find a precise quadrature formula on \mathbb{R}^3 adapted to the radial kernel and involving a number of points as small as possible. The two steps of the procedure are:

1. The authors first note that, if $K(\mathbf{x}) = \text{sinc}(|\mathbf{x}|) = \frac{\sin(|\mathbf{x}|)}{|\mathbf{x}|}$, $\hat{K}(\mathbf{x}) = \frac{1}{4\pi} \delta_{S^2}$ and one has

$$K(\mathbf{x}) = \text{sinc}(|\mathbf{x}|) = \frac{1}{4\pi(2\pi)^3} \int_{S^2} e^{i\mathbf{x}\cdot\xi} d\xi \approx \sum_{q=1}^M \omega_q e^{i\mathbf{x}\cdot\xi_q},$$

where $(\omega_q, \xi_q)_q$ is a quadrature formula on S^2 . In that case, the integration domain is reduced to S^2 which limits the number of points needed.

2. Then, if the kernel is radial $K(\mathbf{x}) = K(|\mathbf{x}|)$, so is its Fourier transform $\hat{K}(\xi) = \hat{K}(|\xi|)$ and one has:

$$\begin{aligned} K(\mathbf{x}) &= \frac{1}{(2\pi)^3} \int_{\mathbb{R}^3} \hat{K}(\xi) e^{i\mathbf{x}\cdot\xi} d\xi \\ &= \frac{1}{(2\pi)^3} \int_{\mathbb{R}} \int_{S^2} \hat{K}(\lambda \tilde{\xi}) e^{i\mathbf{x}\cdot\lambda \tilde{\xi}} \lambda^2 d\lambda d\tilde{\xi} \\ &= \frac{1}{(2\pi)^3} \int_{\mathbb{R}} \hat{K}(\lambda) \lambda^2 \left(\int_{S^2} e^{i\mathbf{x}\cdot\lambda \tilde{\xi}} d\tilde{\xi} \right) d\lambda \\ &= 4\pi \int_{\mathbb{R}} \text{sinc}(\lambda|\mathbf{x}|) \hat{K}(\lambda) \lambda^2 d\lambda \\ &\approx \sum_p \beta_p \text{sinc}(\lambda_p |\mathbf{x}|) \end{aligned}$$

where $(\beta_p, \lambda_p)_p$ is a one dimensional quadrature formula for the weighted integral.

The key point of the method is then to choose the quadrature formula $(\beta_p, \lambda_p)_p$ in step 2 in order to optimize both the error and the number of points. Then, putting together steps 1 and 2 provides a discretization for (3.19) and one finally obtain coefficients $\alpha = (\alpha_q)_q$, and points $\xi = (\xi_q)_q$ for (3.16). The corresponding points $\xi = (\xi_q)_q$ are distributed on concentric spheres, the radii $(\lambda_p)_p$ of these spheres are optimized for the considered kernel, in order to minimize the error.

The grid for the decomposition (3.16) is not uniform and is adapted to the rotational invariance of K . It results in a very precise approximation of the Kernel, since it comes from an adapted 1 dimensional quadrature formula in the radial variable. The Cardinal Sine Decomposition (step 2) is Sparse, in the sense that the number of points M is chosen as small as possible to ensure a given tolerance for the error. This, together with the use of Non-Uniform FFT, provides a fast algorithm for radial kernels. The method is quite simple to implement and only depend on the kernel through the knowledge of its Fourier transform.

To finish, note that the decomposition is achieved in such a way that (3.16) uniformly holds. To do so, the number of points in this decomposition depends on two parameters. First, the number of points chosen for the quadrature on S^2 in step 1 depends on the radius R_{max} of the largest sphere in the final decomposition, which itself depends on the size of the domain. Then, the cardinal sine decomposition in step 2 converges very slowly when $|x|$ is small (similarly to the decomposition of 1 in sine functions). Then, the number of points in this decomposition depends on R_{min} which is the minimal radius for which the interactions between two points will be treated using SCSD (for smaller distances, classical but non fast computations are implemented). The radius R_{min} is thus chosen in order to obtain a compromise between the computation time (and storage) of the close interactions and the number of points of the sparse decomposition.

▷ [SCSD adapted to Stokes kernel \[12, 13\]](#)

In [12, 13], we extended the SCSD algorithm to Stokes kernel. Let us first recall that Stokes problem is a vector problem in 3d. For example, the Stokeslet can be described by 9 scalar kernels in 3d: $\mathbf{G} = (G_{ij})_{1 \leq i, j \leq 3}$ (3.10). A straightforward approach to design fast algorithms for the Stokes kernel is to use the existing fast algorithms on each of these scalar kernels. For example, one can use this approach to extend the FFT fast algorithm (3.18) to the Stokeslet. Unfortunately, this will lead to a total of 18 FFTs and IFFTs which is inefficient. In [Wan+06], the authors propose an alternative scheme, requiring 6 FFTs and IFFTs to achieve the matrix-vector product.

Concerning FFM and SCSD, the methods do not extend straightforwardly to Stokes problem. Indeed, FMM is highly kernel dependent and SCSD is restricted to radial kernels. To overcome this difficulty, the idea is to rewrite the kernels as sums and/or derivatives of kernels for which the methods are available. For example, fast FMM algorithms for the Stokes kernel, based on harmonic or biharmonic FMMs has been developed. In [TG08], the authors present a new decomposition for which harmonic FMMs can be used as

"black-boxes" to compute the matrix-product vector. The method leads to 4 harmonic FMM calls with twice the initial number of sources for both the Stokeslet and the Stresslet (the algorithm is then optimized so that the cost is approximately that of three FMM calls with the initial number of sources).

In the same spirit, we proposed and tested in [12, 13] an extension of the SCSD to Stokes kernels. The idea is to decompose the kernels in sums and/or derivatives of *radial* kernels, for which the SCSD method can be applied. For example, one can decompose the Stokeslet (3.10) as:

$$\begin{aligned} \mathbf{G}(\mathbf{x}) &= \mathbf{G}_1(\mathbf{x}) + \mathbf{G}_2(\mathbf{x}) \\ &= 2\frac{\text{Id}}{|\mathbf{x}|} + \left(\frac{\mathbf{x} \otimes \mathbf{x}}{|\mathbf{x}|^3} - \frac{\text{Id}}{|\mathbf{x}|} \right). \end{aligned}$$

First, \mathbf{G}_1 being radial, we can apply the SCSD technique to compute the corresponding matrix-vector product. Concerning \mathbf{G}_2 , we remark that it is the Hessian matrix of the radial function $g_2 : \mathbf{x} \mapsto -|\mathbf{x}|$. Achieving the SCSD of g_2 and differentiating twice its SCSD decomposition yields an approximation of \mathbf{G}_2 . The matrix-product vector for the Stokeslet then reduces to two SCSD decompositions and two NUFFT and INUFFT calls. In a similar fashion, the Cartesian components of the Stresslet are written as sums and derivatives of radial functions, leading to 2 SCSD decompositions and 4 NUFFT and INUFFT calls.

In [12], academic computational examples permit us to compare the SCSD method against a usual direct BEM solver in terms of both accuracy and convergence. For example, solving a Dirichlet to Neumann problem on the mesh of an ellipsoid (as plotted on Figure 3.2), we show that for a sufficiently small tolerance, the SCSD has the same order of convergence for the error (versus the size of the mesh) than the direct BEM method. Moreover, the CPU time is shown to behave as $O(N \log(N))$, while, as expected, it behaves as $O(N^2)$ for the direct BEM method. The results are plotted on Figure 3.4.

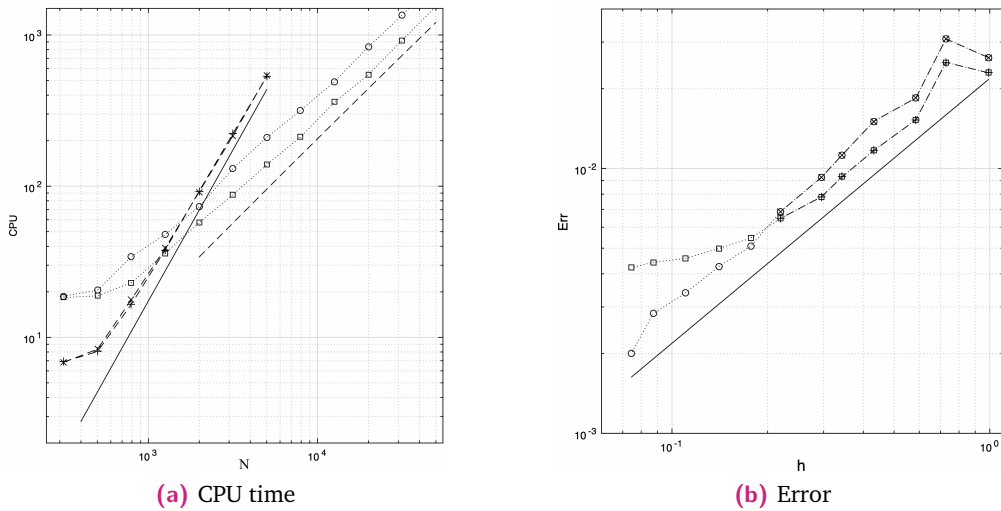


Fig. 3.4: Error and CPU time for the Dirichlet to Neumann problem for a given tolerance ϵ . BEM with $\epsilon = 10^{-3}$ (+) or $\epsilon = 10^{-4}$ (x) and SCSD for $\epsilon = 10^{-3}$ (◊) and $\epsilon = 10^{-4}$ (◦). Functions $N \log(N)$ (dashed line) and N (solid line for error) or N^2 (solid line for CPU time) are also plotted.

3.3 Second challenge: Singular and near-singular integrals for the Stokes kernel. A semi-analytic method.

Let us now focus on the computation of the coefficients of matrices S^c and S^v involved in collocation (3.7) and variational (3.8) discretizations. The integrals to be computed to solve the problem are

$$I^K(\mathbf{x}) = \int_{\Gamma} K(\mathbf{x} - \mathbf{y})\phi(\mathbf{y})d\mathbf{y}, \quad \text{for } \mathbf{x} \in \Gamma,$$

where K is a kernel which is singular when \mathbf{y} tends to \mathbf{x} . Note that, in case of a variational approximation, only the internal singular integral in (3.8) is treated, the external integral being calculated by means of Gauss points.

If we consider applications involving only one solid (e.g. submarine, plane...), the surface Γ is made of one connected region. Suppose now we want to simulate the dynamics of particles or drops that can approach each other. In that case, the surface Γ is made of N connected regions Γ_n , $1 \leq n \leq N$: $\Gamma = \cup_{n=1..N}\Gamma_n$, each particle/bubble corresponding to

one of these connected region. We suppose that each connected region Γ_n is sufficiently regular. We then need to compute the integrals

$$I_n^K(\mathbf{x}) = \int_{\Gamma_n} K(\mathbf{x} - \mathbf{y})\phi(\mathbf{y})d\mathbf{y} \quad \text{for } \mathbf{x} \in \Gamma, \quad n = 1 \dots N.$$

One can then face two possibilities (see figure 3.5. For better readability, this figure and the following ones refer to two-dimensional problems, the generalization to 3d problems is straightforward.):

- **Singular integral.** In case $\mathbf{x} \in \Gamma_n$, the corresponding integral is singular.
- **Near singular integral.** In case $\mathbf{x} \in \Gamma_m$ for m different from n , the integral is no more singular. However, if \mathbf{x} is close to Γ_n , the high variations of the kernel close to \mathbf{x} make it difficult to compute the integral. It is therefore necessary to develop specific strategies to obtain accurate estimations. Such near-singular integrals arise when the two surfaces Γ_n and Γ_m are close to each other.

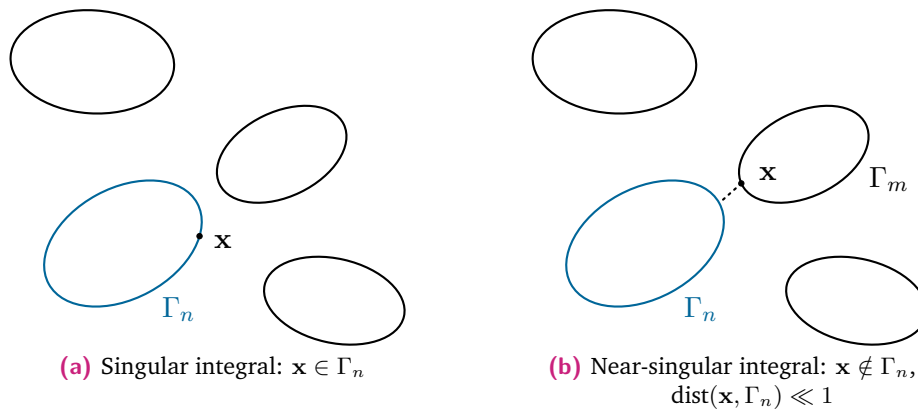


Fig. 3.5: Integral on a connected component Γ_n of the boundary.

Singular integrals is known to be a difficult problem in BEM formulations. To simulate the dynamics of suspensions, it also becomes essential to calculate precisely the numerous near-singular integrals while maintaining the performance of fast solvers.

▷ **Description of the problem.**

The singularities encountered for Stokes problem are similar to those involved in Laplace problem. Indeed, when $\mathbf{y} \rightarrow \mathbf{x}$,

$$G_{ij}(\mathbf{x} - \mathbf{y}) = \frac{\delta_{ij}}{|\mathbf{x} - \mathbf{y}|} + \frac{(x_i - y_i)(x_j - y_j)}{|\mathbf{x} - \mathbf{y}|^3} = O\left(\frac{1}{|\mathbf{x} - \mathbf{y}|}\right)$$

$$T_{ij}(\mathbf{x} - \mathbf{y})\mathbf{n}(\mathbf{y}) = -6\frac{(x_i - y_i)(x_j - y_j)}{|\mathbf{x} - \mathbf{y}|^5}(\mathbf{x} - \mathbf{y}) \cdot \mathbf{n}(\mathbf{y}) = O\left(\frac{1}{|\mathbf{x} - \mathbf{y}|^3}(\mathbf{x} - \mathbf{y}) \cdot \mathbf{n}(\mathbf{y})\right)$$

Case of singular integrals ($\mathbf{x} \in \Gamma_n$): the single-layer potential G .

The singular integrals related to the single-layer potential are **converging** singular integrals. Indeed, let $\mathbf{x} \in \Gamma_n$ be given and let us consider $I(\mathbf{x}) = \int_{\Gamma_n} 1/|\mathbf{x} - \mathbf{y}|d\mathbf{y}$. If the surface is regular, there exists a diffeomorphism sending the Γ -neighbourhood of \mathbf{x} onto $B^2(0, 1)$, where $B^2(0, 1)$ is the two-dimensional ball of radius 1 and centered at $(0, 0)$. Then, studying the convergence of $I(\mathbf{x})$ amounts to studying the convergence of the 2 dimensional integral $\int_{B^2(0,1)} 1/|\mathbf{y}|d\mathbf{y}$. Using a polar change of coordinates, we have

$$\int_{B^2(0,1)} \frac{1}{|\mathbf{y}|}d\mathbf{y} = \int_0^{2\pi} \int_0^1 \frac{1}{\rho} \rho d\rho d\theta < +\infty, \quad (3.20)$$

which proves that the integral is converging.

Case of singular integrals ($\mathbf{x} \in \Gamma_n$): the double-layer potential T .

In general, the integrals involving the double layer potential in vector problems has to be understood in the Cauchy principle value sense. In case of Stokes double layer kernel, one can factor the term $(\mathbf{x} - \mathbf{y}) \cdot \mathbf{n}(\mathbf{y})$ into the integrand (which in not the case in general). We show in the following that this makes the corresponding integral more regular than expected.

Let us suppose that Γ_n is sufficiently regular (which is the case for suspensions if we consider regular rigid particles). Consider (\mathbf{x}, \mathbf{y}) the arc on Γ_n joining \mathbf{x} and \mathbf{y} (see figure 3.6). There exists $\boldsymbol{\xi} \in (\mathbf{x}, \mathbf{y})$ such that $\mathbf{y} - \mathbf{x} = |\mathbf{y} - \mathbf{x}|\tau(\boldsymbol{\xi})$ where $\tau(\boldsymbol{\xi})$ is tangent to the arc at point $\boldsymbol{\xi}$. Using the fact that $\tau(\mathbf{y}) \cdot \mathbf{n}(\mathbf{y}) = 0$ together with the regularity of the surface we write:

$$(\mathbf{y} - \mathbf{x}) \cdot \mathbf{n}(\mathbf{y}) = |\mathbf{y} - \mathbf{x}|\tau(\boldsymbol{\xi}) \cdot \mathbf{n}(\mathbf{y}) = |\mathbf{y} - \mathbf{x}|(\tau(\boldsymbol{\xi}) - \tau(\mathbf{y})) \cdot \mathbf{n}(\mathbf{y}) = O(|\mathbf{x} - \mathbf{y}|^2).$$

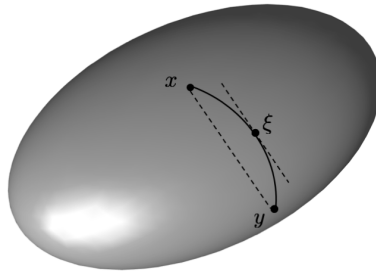


Fig. 3.6: Regularization of the second-layer potential. Notation.

From these computations we obtain that

$$T_{ij}(\mathbf{x} - \mathbf{y})\mathbf{n}(\mathbf{y}) \underset{y \rightarrow x}{\sim} \frac{C_{\mathbf{x}}}{|\mathbf{x} - \mathbf{y}|},$$

when \mathbf{y} tends to \mathbf{x} . Finally, if Γ_n is sufficiently regular, T_{ij} is singular as $1/|\mathbf{x} - \mathbf{y}|$ and then, as before, the corresponding integral converges.

Case of singular integrals ($\mathbf{x} \in \Gamma_n$): regularization of the second-layer potential.

We show in the following that the integral involving the second-layer potential can be regularized.

To do so, let us first compute $\int_{\Gamma_n} T_{ij}(\mathbf{x} - \mathbf{y})\mathbf{n}(\mathbf{y})d\mathbf{y}$ when Γ_n is a closed connected surface and $\mathbf{x} \in \Gamma_n$. We consider the Stokes problem associated to the punctual source $\delta_{\mathbf{x}}\mathbf{e}_i$. Then, the map $\mathbf{y} \rightarrow T_{ij}(\mathbf{x} - \mathbf{y})\mathbf{n}(\mathbf{y})d\mathbf{y}$ for $\mathbf{y} \in \Gamma_n$ is the corresponding local force exerted on the surface by the fluid located on the side of \mathbf{n} . Let us now consider a ball centered at point $\mathbf{x} \in \Gamma_n$ with radius ϵ . The surface of the ball inside Γ_n is denoted by S_ϵ . We also denote by Γ_ϵ , the trace of the ball on Γ_n (see figure 3.7).

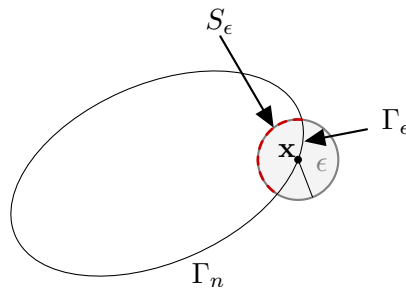


Fig. 3.7: Computation of $\int_{\Gamma_n} T_{ij}(\mathbf{x} - \mathbf{y})\mathbf{n}(\mathbf{y})d\mathbf{y}$. Notation.

Since we proved that the integral converges, we have

$$\int_{\Gamma_n} T_{ij}(\mathbf{x} - \mathbf{y})\mathbf{n}(\mathbf{y})d\mathbf{y} = \lim_{\epsilon \rightarrow 0} \int_{\Gamma_n \setminus \Gamma_\epsilon} T_{ij}(\mathbf{x} - \mathbf{y})\mathbf{n}(\mathbf{y})d\mathbf{y}.$$

Using the fact that \mathbf{x} is not inside $(\Gamma_n \setminus \Gamma_\epsilon) \cup S_\epsilon$, we know that the global force exerted on this surface by the fluid located on the side of \mathbf{n} is zero: $\int_{(\Gamma_n \setminus \Gamma_\epsilon) \cup S_\epsilon} T_{ij}(\mathbf{x} - \mathbf{y})\mathbf{n}(\mathbf{y})d\mathbf{y} = 0$. This gives

$$\begin{aligned} \int_{\Gamma_n} T_{ij}(\mathbf{x} - \mathbf{y})\mathbf{n}(\mathbf{y})d\mathbf{y} &= - \lim_{\epsilon \rightarrow 0} \int_{S_\epsilon} T_{ij}(\mathbf{x} - \mathbf{y})\mathbf{n}(\mathbf{y})d\mathbf{y} \\ &= 6 \lim_{\epsilon \rightarrow 0} \int_{S_\epsilon} \frac{(x_i - y_i)(x_j - y_j)(\mathbf{x} - \mathbf{y}) \cdot \mathbf{n}(\mathbf{y})}{|\mathbf{x} - \mathbf{y}|^5}. \end{aligned}$$

Using the fact that $|\mathbf{y} - \mathbf{x}| = \epsilon$ and $\mathbf{y} - \mathbf{x} = \epsilon\mathbf{n}(\mathbf{y})$ on S_ϵ , and supposing that the surface is regular at point \mathbf{x} , we finally obtain

$$\int_{\Gamma_n} T_{ij}(\mathbf{x} - \mathbf{y})\mathbf{n}(\mathbf{y})d\mathbf{y} = 6 \lim_{\epsilon \rightarrow 0} \int_{S_\epsilon} \frac{\epsilon^3 n_i n_j \mathbf{n}(\mathbf{y}) \cdot \mathbf{n}(\mathbf{y})}{\epsilon^5} = \frac{6}{\epsilon^2} \lim_{\epsilon \rightarrow 0} \int_{S_\epsilon} n_i n_j = 4\pi \delta_{ij}.$$

Using this result, we can now proceed to the regularization of the second-layer integral. For any test function ϕ , we rewrite the corresponding singular integral as

$$\int_{\Gamma_n} T_{ij}(\mathbf{x} - \mathbf{y})\mathbf{n}(\mathbf{y})\phi(\mathbf{y})d\mathbf{y} = \int_{\Gamma_n} T_{ij}(\mathbf{x} - \mathbf{y})\mathbf{n}(\mathbf{y})(\phi(\mathbf{y}) - \phi(\mathbf{x}))d\mathbf{y} + \frac{\phi(\mathbf{x})}{4\pi} \delta_{ij}.$$

Since $T_{ij}(\mathbf{x} - \mathbf{y})\mathbf{n}(\mathbf{y}) \sim \frac{C_{\mathbf{x}}}{|\mathbf{x} - \mathbf{y}|}$ for $\mathbf{y} \rightarrow \mathbf{x}$, the integral in the right-hand side is now regular and can be computed using Gauss quadrature. This method is called the **singularity subtraction method**.

Case of near singular integrals ($\mathbf{x} \notin \Gamma_n$ and $\text{dist}(\mathbf{x}, \Gamma_n)$ small)

Let us first consider the double-layer potential T . In case $\mathbf{x} \notin \Gamma_n$, the term $(\mathbf{x} - \mathbf{y}) \cdot \mathbf{n}(\mathbf{y})$ in the integrand do not allow anymore to reduce the singularity and T now behaves as $1/|\mathbf{x} - \mathbf{y}|^2$ when \mathbf{y} is close to \mathbf{x} . Using the singularity subtraction method, we can reduce this singularity to $1/|\mathbf{x} - \mathbf{y}|$. As a consequence, both G and T behave as $1/|\mathbf{x} - \mathbf{y}|$ when \mathbf{x} is close to Γ_n . Although these integrals are not singular ($\mathbf{x} \notin \Gamma_n$), their high variations in the neighborhood of \mathbf{x} make it essential to set up specific methods to compute them accurately.

Summary.

$\mathbf{x} \in \Gamma_n$ Singular integral		$\mathbf{x} \notin \Gamma_n$ and $\text{dist}(\mathbf{x}, \Gamma_n)$ small Near-singular integral	
G_{ij}	T_{ij}	G_{ij}	T_{ij}
$O(1/ \mathbf{x} - \mathbf{y})$	$O(1/ \mathbf{x} - \mathbf{y})$	$O(1/ \mathbf{x} - \mathbf{y})$	$O(1/ \mathbf{x} - \mathbf{y} ^2)$
	Singularity subtraction $\hookrightarrow O(1)$		Singularity subtraction $\hookrightarrow O(1/ \mathbf{x} - \mathbf{y})$
\hookrightarrow singular but converging	\hookrightarrow regular	\hookrightarrow Near singular	
Approximation via specific methods	Classical quadrature	Approximation via specific methods	

The question is now to find a way to compute the remaining singular and near-singular integrals as accurately as possible.

▷ **Approximation of the singular and near-singular integrals.**

Approximation of the singular integrals: a well documented problem.

The calculation of singular integrals has been the subject of much research since Cruse's original work [Cru69] and many efficient methods have been developed. Suppose that $\mathbf{x} \in \Gamma_n$ and that $\Gamma_{n,h}$ is a discretization of Γ_n into elements τ . If K is a singular kernel and ϕ a finite element basis function (constant, linear or polynomial with higher degree) the corresponding singular integral can be approximated by

$$\int_{\Gamma_n} K(\mathbf{x} - \mathbf{y})\phi(\mathbf{y})d\mathbf{y} \approx \int_{\Gamma_{n,h}} K(\mathbf{x} - \mathbf{y})\phi(\mathbf{y})d\mathbf{y} = \sum_{\tau \in \Gamma_{n,h}} \int_{\tau} K(\mathbf{x} - \mathbf{y})\phi(\mathbf{y})d\mathbf{y}.$$

The problem then comes back to evaluate the integrals over the elements τ . The integral is singular if τ is the element that contains \mathbf{x} . It is also necessary to pay attention to its computation for the elements τ that do not contain \mathbf{x} but are close to it.

Several methods have been proposed to evaluate these local integrals. Some of them are based on an adequate change of variable: as in (3.20), using polar (or more subtle) coordinates make the integrand regular. It can then be evaluated by classical quadrature. Another group of methods consists in proposing a new quadrature formula, adapted to the singularity. One can also compute analytically the integrals, for specific singularities, geometries and test functions ϕ . We refer to [RC92; HS94; Bon99; SS11] and references therein for an overview of the available methods. These methods for singular integrals are known to be quite cumbersome to implement. Moreover, to make the changes of variable or analytical computations work, they are in general restricted to the case where τ is the element that contains \mathbf{x} or one of its neighbours (see figure 3.8).

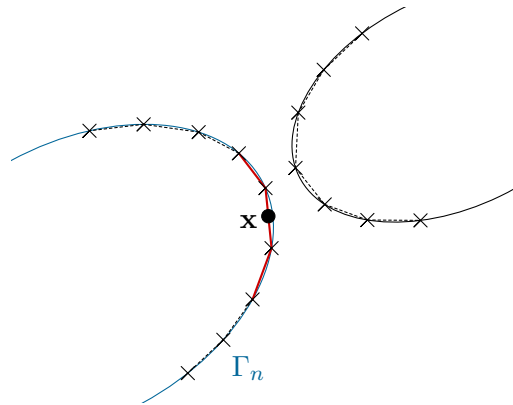


Fig. 3.8: Computation of a singular integral on Γ_n : corrections are achieved on the element τ that contains \mathbf{x} and adjacent elements (red solid line).

Case of near singular integrals: an active domain of research

As we have just seen, the specific techniques developed for the singular case do not extend to the general case $\mathbf{x} \notin \Gamma_n$. However, some elements of Γ_n are close to \mathbf{x} and require specific treatments to be computed accurately (see figure 3.9).

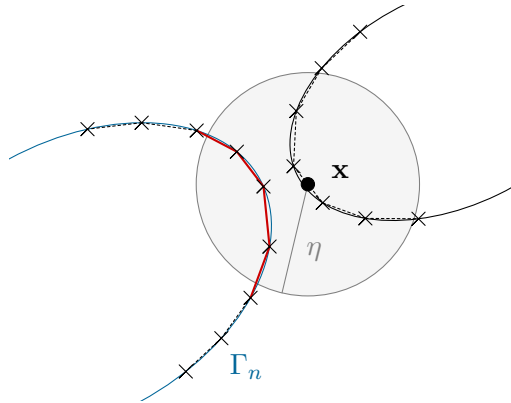


Fig. 3.9: Computation of a near-singular integral on Γ_n : the close elements require specific treatments to be computed accurately (red solid line, $\text{dist}(\mathbf{x}, \tau) \leq \eta$).

Developing methods to compute accurate estimations of near-singular integrals is an active domain of research. If some efficient methods have been developed in 2 dimensions (see e.g. [HO08; BWV15]), the 3 dimensional case remains delicate. To illustrate the difficulty of the problem, I mention here three classes of methods that have been proposed (the list is not exhaustive, see the cited articles and references therein for an overview of the problem):

- First, some *numerical approximation methods* have been developed to estimate near-singular integrals (see e.g. [YBZ06; KT14]). Although accurate, these methods require a specific numerical work for each singular point (quadrature, grid, expansion of the kernel...) and their cost increase rapidly if too many near-singular integrals have to be computed. Moreover, the techniques developed are not adapted to be integrated in fast BEM solvers. In [KT16], the authors propose a very accurate numerical approximation and an accelerated implementation in case of spheroidal bodies is detailed. Very recently, more general fast algorithms for quadrature methods in three dimensions have been proposed (see e.g. [WK19; ZV21; MRZ21]).
- Another interesting class of methods to estimate the near singular integrals is the so-called *semi-analytic methods*. The "semi-analytic" term refers to the fact that, in case of variational approximation, only the internal integral in (3.8) is approximated by an analytical calculation, the external integral being then calculated by means of Gauss points. Such a semi-analytic method was proposed in [BYW16] for harmonic kernels and has been recently extended to Stokes Kernels in [TB19;

Bea20]. These semi-analytic methods are based on a decomposition of the integral in a numerical approximation using a *global* gaussian quadrature and a correcting term that is computed analytically. Doing so, the overall method do not require specific treatments near the singularities and do not increase the complexity of fast solvers. The correction term highly depends on the local geometry close to the singularity (tangent vectors, surface gradient and laplacian of scalar functions, surface divergence of a vector function, mean curvature...). The authors describe how to compute all the needed quantities when a local Monge parameterization of the surface is known close to the singularity.

- Note that a *fully analytic method* has also been proposed in [LS12]: the whole double integrals (3.8) arising in the variational method are explicitly computed in the specific case of flat triangular elements, coplanar or in parallel planes, and constant test functions. This last method can then be used for non neighboring triangles but in a specific geometrical configuration.

▷ **A semi-analytic method for both singular and near-singular integrals.**

In the following I describe the method we have set up to deal with singular and near-singular integrals for Stokes equations. This method belongs to the class of semi-analytical methods which is particularly adapted to the simulations of suspensions. Indeed, compared to numerical approximations, the analytical computation of the singular terms allows to take into account more easily both singular and near-singular integrals. This is essential to deal with close particles. Moreover, these methods are based on a first classical computation of the integrals followed by a sparse correction. Consequently, we will see that they have the great advantage of being easy to couple with fast solvers.

The semi-analytical method on which we rely was developed by François Alouges and Matthieu Aussal for Maxwell and Helmholtz equations. While in [TB19; Bea20], the semi-analytical correction was achieved at the continuous level, the analytical computations proposed by François Alouges and Matthieu Aussal are performed for a mesh composed of **flat triangles** and for low order finite elements. Although the method is restricted to specific discretizations, it has the advantage of leading to simple and easily implementable expressions, whatever the geometry of the particle.

In what follows, I first describe the method developed by François Alouges and Matthieu Aussal and then explain how we extended it to the Stokes kernel. These works have not been published yet.

A new semi-analytic method. [Alouges, Aussal]

In this method, all connected components of the boundary Γ are treated together: we want to evaluate integrals

$$\int_{\Gamma} K(\mathbf{x} - \mathbf{y})\phi(\mathbf{y})d\mathbf{y},$$

where K is a singular kernel and ϕ a finite element basis function. If Γ_h is a discretization of Γ into elements τ , these integrals are approximated by

$$\int_{\Gamma} K(\mathbf{x} - \mathbf{y})\phi(\mathbf{y})d\mathbf{y} \approx \int_{\Gamma_h} K(\mathbf{x} - \mathbf{y})\phi(\mathbf{y})d\mathbf{y} = \sum_{\tau \in \Gamma_h} \int_{\tau} K(\mathbf{x} - \mathbf{y})\phi(\mathbf{y})d\mathbf{y}.$$

Suppose that a classical quadrature formula $(\mathbf{y}_p, \omega_p)_{p=1\dots P}$ is chosen in a reference triangle and extended to any triangle τ : $(\mathbf{y}_p^{\tau}, \omega_p^{\tau})_{p=1\dots P}$. Then François Alouges and Matthieu Aussal proposed to approximate the integral as follows:

$$\begin{aligned} \int_{\Gamma} K(\mathbf{x} - \mathbf{y})\phi(\mathbf{y})d\mathbf{y} \approx & \sum_{\tau \in \Gamma_h} \sum_p \omega_p^{\tau} K(\mathbf{x} - \mathbf{y}_p^{\tau})\phi(\mathbf{y}_p^{\tau}) \\ & + \sum_{\substack{\tau \in \Gamma_h \\ d(\mathbf{x}, \tau) \leq \eta}} \left[\int_{\tau} K(\mathbf{x} - \mathbf{y})\phi(\mathbf{y})d\mathbf{y} - \sum_p \omega_p^{\tau} K(\mathbf{x} - \mathbf{y}_p^{\tau})\phi(\mathbf{y}_p^{\tau}) \right]. \end{aligned}$$

The whole integral is first computed numerically and then, for each element close to the singular point \mathbf{x} , the quadrature approximation is replaced by the exact value of the corresponding integral (which must be computed analytically). From an analytical point of view, this formula can then be rewritten as the sum of two terms: classical quadratures for triangles far from point \mathbf{x} and exact integrals for triangles close to this point.

However, from an implementation point of view, it is important to consider the formula as it is presented here: first, a classical quadrature formula is performed **on all triangles of the mesh** and then the values on the triangles close to the singularity point are corrected.

The reason for doing this is that, in this way, the first term corresponds to the usual full matrix/vector product in BEM: it can be computed using existing fast solvers, without taking the singularity into account. Any modification in this term (removal of triangles, local modification of integration points...) may lead to a loss of efficiency of the code and require the modification of existing fast solvers. On the other hand, the second

term (correction term) is sparse and therefore has no impact on the efficiency of the method in terms of computation time. Note also that, although this correction may seem numerically inaccurate due to possible rounding errors, experience shows that it does not affect the accuracy of the method.

Finally, it should be noted that the correction is calculated regardless whether \mathbf{x} is in the same connected component as τ or not (see figure 3.10). Doing so, both singular and near-singular integrals are taken into account in the same way.

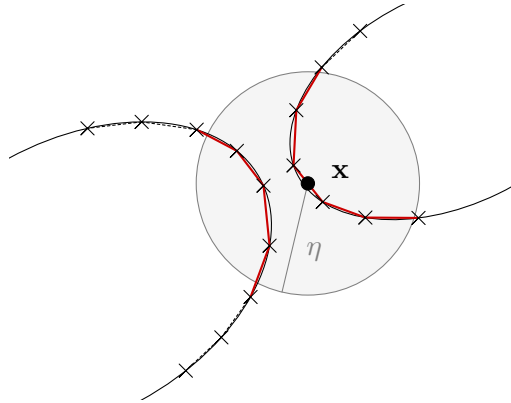


Fig. 3.10: Semi-analytical correction. Point \mathbf{x} being given, the correction is achieved for all close elements (red solid line, $\text{dist}(\mathbf{x}, \tau) \leq \eta$): both singular and near-singular integrals are taken into account.

This method is easy to implement and, being based on a mesh discretization, it does not require fine knowledge on the geometry of Γ . It is also flexible in the sense that the correction may take into account only a part of the kernel (e.g. its singular part). For example, the knowledge of the explicit correction for the Laplace kernel $1/r$ can be used to correct the Helmholtz/Maxwell kernel e^{ikr}/r . In the same way, the correction term may not take into account the entire test function. For example, in case of a P^1 finite element discretization, the test function in τ can be written $\phi(\mathbf{y}) = a + \mathbf{b} \cdot (\mathbf{y} - \mathbf{x})$ with $a \in \mathbb{R}$ and $\mathbf{b} \in \mathbb{R}^3$. In that case, the constant term a generates a larger singularity than the term proportional to $\mathbf{y} - \mathbf{x}$: one can choose to correct only this part of the integral.

Exact computations for the Laplace Kernel.

The method can be applied to a kernel K provided one can compute analytically the integrals

$$\int_{\tau} K(\mathbf{x} - \mathbf{y})\phi(\mathbf{y})d\mathbf{y},$$

where τ is an element of the mesh, ϕ is a test function and \mathbf{x} is an arbitrary point close to τ (but not necessarily belonging to τ).

Let us consider the single and double layer Laplace Kernels:

$$G(x, y) = \frac{1}{4\pi r} \quad \text{and} \quad T(x, y) = \frac{1}{4\pi} \nabla_{\mathbf{y}} \left(\frac{1}{r} \right) \cdot \mathbf{n}(y),$$

where $\mathbf{r} = \mathbf{y} - \mathbf{x}$ and $r = |\mathbf{r}| = |\mathbf{y} - \mathbf{x}|$.

Exact computations for these kernels has already been carried out but are not easy to find in the literature. In the following, we show how to calculate them in the **case of finite element approximations P^0 and P^1 on flat triangles** (see e.g. [New86] for similar computations for quadrilateral elements). As already mentioned, the integrals calculated in the Laplace case also allow to deal with Helmholtz and Maxwell kernels. Moreover, they will be useful to extend the method to Stokes kernel. This extension will be described in a second step.

Let's start by listing the singular integrals that need to be calculated.

First of all, the point \mathbf{x} being given, we recall that any finite element function P^1 in τ can be written $\phi(y) = a + \mathbf{b} \cdot (\mathbf{y} - \mathbf{x})$ with $a \in \mathbb{R}$ and $\mathbf{b} \in \mathbb{R}^3$. Therefore, we can deal with both P^0 and P^1 finite elements provided we calculate the singular integrals for the two test functions $\phi_0 = 1$ and $\phi_1 = \mathbf{y} - \mathbf{x} = \mathbf{r}$.

Moreover, consider the case of kernel T and the affine test function ϕ_1 . Recalling that τ is supposed to be a flat triangle we see that $\mathbf{r} \cdot \mathbf{n}$ is constant in τ and we set $\delta := \mathbf{r} \cdot \mathbf{n}$ (see figure 3.11).

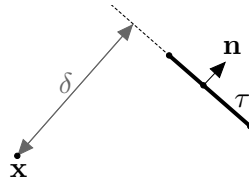


Fig. 3.11: Analytical computations. Notation.

Then, we can write

$$\begin{aligned} \int_{\tau} (T(r) \cdot \mathbf{n}) \mathbf{r} &= \int_{\tau} (\nabla_{\mathbf{y}} G(r) \cdot \mathbf{n}) \mathbf{r} = \int_{\tau} (G'(r) \nabla_{\mathbf{y}} \mathbf{r} \cdot \mathbf{n}) \mathbf{r} = \int_{\tau} G'(r) \frac{\mathbf{r}}{r} \cdot \mathbf{n} \mathbf{r} \\ &= \delta \int_{\tau} \nabla_{\mathbf{y}} G(r) d\mathbf{y} = \delta \int_{\tau} \nabla_{\mathbf{y}} \left(\frac{1}{r} \right) d\mathbf{y}. \end{aligned}$$

So one finally needs to compute analytically the following integrals:

test function	$\phi_0 = 1$	$\phi_1 = \mathbf{r}$
Kernel G	$I_1(\mathbf{x}) = \int_{\tau} \frac{1}{r} d\mathbf{y}$	$I_2(\mathbf{x}) = \int_{\tau} \frac{\mathbf{r}}{r} d\mathbf{y}$
Kernel T	$I_0(\mathbf{x}) = \int_{\tau} \nabla_{\mathbf{y}} \left(\frac{1}{r} \right) \cdot \mathbf{n}(\mathbf{y}) d\mathbf{y}$	$I_3(\mathbf{x}) = \int_{\tau} \nabla_{\mathbf{y}} \left(\frac{1}{r} \right) d\mathbf{y}$

To compute these integrals, the first step is to compute I_0 . Then, the three other integrals are expressed as sums of $I_0(\mathbf{x})$ and boundary terms which can easily be integrated analytically.

- **Computation of $I_0(\mathbf{x})$.** To compute I_0 , let us first recall that $I_0(\mathbf{x}) = 4\pi \int_{\tau} T(r) \cdot \mathbf{n}(\mathbf{y})$. Then, let us recall that, by definition, $T(r) \cdot \mathbf{n}(\mathbf{y})$ corresponds to the natural boundary condition of the studied PDE (for example, the normal flux for Laplace equation). Now, consider the tetrahedron \mathcal{T} with base τ and vertex \mathbf{x} (see figure 3.12 for notation).

Using the fact that $\Delta_{\mathbf{y}} G = 0$ in $\mathcal{T} \setminus B(\mathbf{x}, \varepsilon)$ and integrating by part we have

$$0 = \int_{\mathcal{T} \setminus B(\mathbf{x}, \varepsilon)} \Delta_{\mathbf{y}} \left(-\frac{1}{r} \right) = \int_{\partial\{\mathcal{T} \setminus B(\mathbf{x}, \varepsilon)\}} \nabla_{\mathbf{y}} \left(-\frac{1}{r} \right) \cdot \mathbf{n}(\mathbf{y}).$$

Then, we note that $\nabla_{\mathbf{y}} \left(\frac{1}{r} \right) \cdot \mathbf{n} = 0$ on $\partial\{\mathcal{T} \setminus B(\mathbf{x}, \varepsilon)\}$, except on τ and S_{ε} . This, together with $\mathbf{r} \cdot \mathbf{n} = -r$ on S_{ε} , gives:

$$I_0(\mathbf{x}) = \int_{\tau} \nabla_{\mathbf{y}} \left(-\frac{1}{r} \right) \cdot \mathbf{n}(\mathbf{y}) = - \int_{S_{\varepsilon}} \nabla_{\mathbf{y}} \left(-\frac{1}{r} \right) \cdot \mathbf{n}(\mathbf{y}) = \int_{S_{\varepsilon}} \frac{1}{r^2} = \frac{1}{\varepsilon^2} \int_{S_{\varepsilon}} d\sigma = \omega,$$

where ω is the solid angle of τ viewed from point \mathbf{x} .

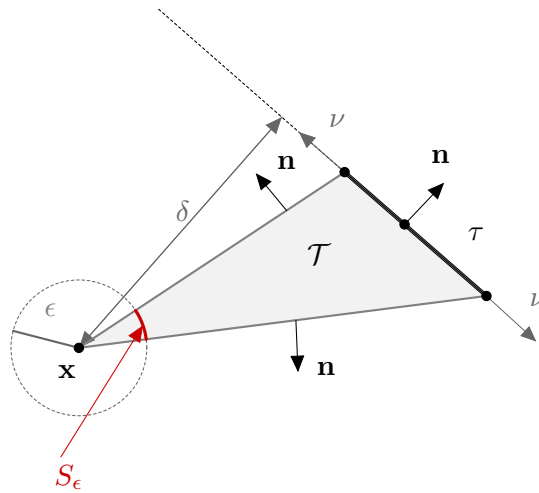


Fig. 3.12: Analytical computation of $I_0(\mathbf{x})$. Notation.

- **Computation of $I_1(\mathbf{x})$, $I_2(\mathbf{x})$ and $I_3(\mathbf{x})$.** The idea is to rewrite the integrand as the sum of the tangential derivative of a given function (in the plane containing τ) and a rest:

$$\begin{aligned} \frac{1}{r} &= \Delta_{\mathbf{y},2d} r - \frac{(\mathbf{n} \cdot \mathbf{r})^2}{r^3}, \\ \frac{\mathbf{r}}{r} &= \nabla_{\mathbf{y}} r = \nabla_{\mathbf{y},2d} r + \left(\int_{\tau} \nabla_{\mathbf{y}} r \cdot \mathbf{n} \right) \mathbf{n}, \\ \nabla_{\mathbf{y}} \left(\frac{1}{r} \right) &= \nabla_{\mathbf{y},2d} \left(\frac{1}{r} \right) + \left(\int_{\tau} \nabla_{\mathbf{y}} \left(\frac{1}{r} \right) \cdot \mathbf{n} \right) \mathbf{n}, \end{aligned}$$

where the subscript "2d" denotes derivatives tangent to τ . The integral on τ of the tangential derivative is then integrated by part which leads to boundary terms that can be analytically computed. The remaining terms can be expressed as functions of $I_0(\mathbf{x})$. As already mentioned, these calculations are known but difficult to find in the literature. We refer again to [New86] for similar computations in the case of quadrangular elements. In order to limit the technical aspects of the manuscript, I have chosen not to details further the computations for the Laplace kernel. The techniques are very similar to those we used to extend the method to Stokes kernel. The latter constitute the original contribution of our work and are detailed in the following.

Extension to Stokes single-layer potential and constant test functions [Alouges, Aussal, Lefebvre-Lepot].

With François Alouges and Matthieu Aussal we extended the previous method to Stokes single layer kernel $\mathbf{G} = (G_{ij})_{ij}$ defined in equation (3.10), page 58. Note that the treatment of the single layer singularity is sufficient in two cases we have in mind, for which the double layer \mathbf{T} (3.11) does not appear in the formulations:

- Simulation of a unique body in an infinite Stokes flow [12]. In that case, since there is only one particle, there are no near singular integrals to deal with. The singular integrals for the double layer can be regularized using the singularity subtraction method. Therefore, it is sufficient to treat the singular integrals related to \mathbf{G} .
- Computation of the resistance matrix for several rigid bodies such as in suspensions [13]. In that case, close rigid bodies can interact and both singular and near-singular integrals have to be taken into account. For example in [13], we consider the behaviour of a solid particle close to a wall so that a precise computation of the near-singular integrals is needed (see figure 3.13). The resistance matrix provides the forces, the velocities being known and is computed by solving some Dirichlet to Neumann problems. The corresponding boundary integral formulation only requires the inversion of \mathbf{G} (see the corresponding integral equation (3.12)). Moreover, the term involving the second layer potential at the right-hand side vanishes, due to the fact that one considers rigid given velocities. Therefore, in this case, it is sufficient to treat the singular and near-singular integrals related to \mathbf{G} .

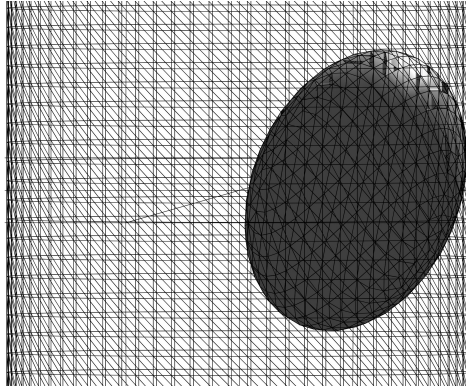


Fig. 3.13: Ellipsoidal particle close to the boundary of a cylinder [13].

As far as \mathbf{G} is concerned, the integrals to be computed are $\int_{\tau} \mathbf{G}(\mathbf{r})\phi(\mathbf{y})d\mathbf{y} \in \mathbb{R}^3$ where ϕ is a *vectorial* P^1 finite-element test function. Since \mathbf{G} behaves as $1/|\mathbf{x} - \mathbf{y}|$, the singular

part of these integrals are due to the constant term \mathbf{a} in ϕ where $\phi(\mathbf{y}) = \mathbf{a} + \mathbf{B}(\mathbf{y} - \mathbf{x})$. We therefore choose to restrict the correction to this leading term and we refer to this in the following as the P^0 correction for P^1 test functions. It had been checked numerically that it was sufficient for the Laplace kernel.

So finally we need to compute analytically $\int_{\tau} \mathbf{G}(\mathbf{r}) d\mathbf{y}$, where \mathbf{G} is the Stokes single layer kernel. To do so, we express this integral as a sum of boundary terms and of singular integrals already computed for the Laplace kernel. From expression (3.10) for \mathbf{G} , we first write

$$\int_{\tau} \mathbf{G}(\mathbf{r}) = 2 \int_{\tau} \frac{\text{Id}}{r} - \int_{\tau} \left(\frac{\text{Id}}{r} - \frac{\mathbf{x} \otimes \mathbf{x}}{r^3} \right) = 2I_1(\mathbf{x}) \text{Id} - \int_{\tau} \nabla_{\mathbf{y}}^2(r),$$

so that it remains to compute $I_4(\mathbf{x}) = \int_{\tau} \nabla_{\mathbf{y}}^2(r)$. We proceed as for the Laplace kernel: we write $\nabla_{\mathbf{y}}^2(r) = \nabla_{\mathbf{y}}(\mathbf{r}/r)$ and the gradient is decomposed into a tangential and normal part. The tangential part is integrated by parts on τ . If ν denotes the exterior normal to the edges of τ (in the plane containing τ , see figure 3.12), we obtain:

$$\begin{aligned} I_4(\mathbf{x}) &= \int_{\tau} \nabla_{\mathbf{y}} \left(\frac{\mathbf{r}}{r} \right) = \int_{\tau} \nabla_{\mathbf{y},2d} \left(\frac{\mathbf{r}}{r} \right) + \int_{\tau} \mathbf{n} \otimes \left[\nabla_{\mathbf{y}} \left(\frac{\mathbf{r}}{r} \right) \mathbf{n} \right] \\ &= \int_{\partial\tau} \nu \otimes \frac{\mathbf{r}}{r} + \int_{\tau} \mathbf{n} \otimes \left[\nabla_{\mathbf{y}} \left(\frac{\mathbf{r}}{r} \right) \mathbf{n} \right] \\ &= \int_{\partial\tau} \nu \otimes \frac{\mathbf{r}}{r} + \int_{\tau} \mathbf{n} \otimes \left[\frac{\mathbf{n}}{r} - \frac{\mathbf{r} \cdot \mathbf{n} \mathbf{r}}{r^3} \right] \\ &= \int_{\partial\tau} \nu \otimes \frac{\mathbf{r}}{r} + \int_{\tau} \frac{\mathbf{n} \otimes \mathbf{n}}{r} - \int_{\tau} \frac{\mathbf{r} \cdot \mathbf{n} \mathbf{n} \otimes \mathbf{r}}{r^3} \end{aligned}$$

Using the fact that \mathbf{n} is constant on τ , that $\mathbf{r} \cdot \mathbf{n} = h$ on τ and that ν is constant on each edge of τ we finally have

$$I_4(\mathbf{x}) = \sum_{a \in \partial\tau} \nu_a \otimes \int_a \frac{\mathbf{r}}{r} + \mathbf{n} \otimes \mathbf{n} I_1(\mathbf{x}) - h \mathbf{n} \otimes I_3(\mathbf{x})$$

and the boundary integrals can be computed exactly.

In [13], the regularization we propose has been tested on the configuration described in figure 3.13, for different distances between the spheroid and the boundary of the cylinder. In particular, we check that the near-singular integrals are well taken into account when the distance is small. To do so, the method is validated in the case a spherical particle: the results are in nice agreement with the literature (see Figure 3.14). Moreover, for small distances, we can observe the decrease of the falling velocity when the particle is very close to the wall, sign of the effects of lubrication.

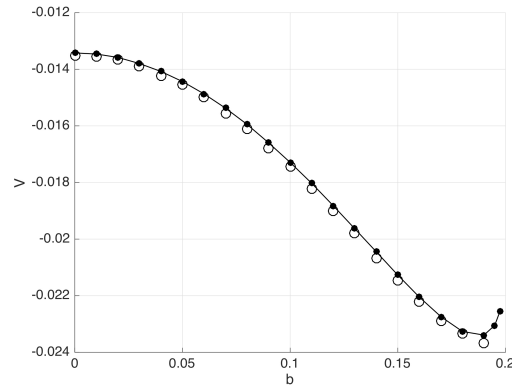


Fig. 3.14: Settling velocity of a spherical particle in a cylinder, as a function of the distance b to the center of the cylinder. In white circles, the results from [TPG92]. In black, our results, using the semi-analytical regularization we proposed.

The method is then used in [13] to investigate the settling motion of a spheroid in a fluid confined by a cylindrical tube. For volume-equivalent and equal-density spheroids the computed settling motion is found to deeply depend not only upon the particle center of volume location but also upon the particle orientation and slenderness ratio.

Let me finish this section with comments about the method:

- *The computations are adapted to mesh discretization based on flat triangles.* As a consequence, it cannot be used to deal with singular integrals in BEM codes based on different surface discretizations (think for example to quadrilateral or curved elements). However, it provides an easily implementable method for those who make the choice flat triangle panels for the discretization.
- *The corrections are computed for constant test functions.* First, note that this is not a limitation since the full P^1 correction could be achieved by writing the corresponding integrand $\mathbf{G}(\mathbf{r})\mathbf{r}$ as a sum of $\nabla^3 r^3$ and other terms already computed. However, as already said, since \mathbf{G} behaves as $1/|\mathbf{x} - \mathbf{y}|$, the P^0 correction for P^1 test functions may be sufficient from a numerical point of view. It has been checked that, for the Laplace kernel and P^1 test functions, taking the non-constant part of the test function into account did not improve the convergence. Concerning Stokes kernel, we tested the convergence for P^1 test functions and P^0 correction. To do so, we considered an ellipsoid in an infinite domain. Suppose that (\mathbf{u}_0, p_0) is the (explicitly known) fundamental solution to the Stokes problem for a punctual

source term inside the ellipsoid. Then, $(\mathbf{u}_0, \sigma(\mathbf{u}_0, \mathbf{p}_0))$ satisfies on the boundary Γ of the ellipsoid the following integral representation:

$$\forall j = 1 \dots 3, \forall \mathbf{x} \in \Gamma, \quad u_j^0(\mathbf{x}) = \frac{1}{4\pi} \int_{\Gamma} \sum_{i,k} u_i^0(\mathbf{y}) T_{ijk}(\mathbf{x}, \mathbf{y}) \mathbf{n}_k(\mathbf{y}) dy - \frac{1}{4\pi\mu} \int_{\Gamma} \sum_i G_{ij}(\mathbf{x}, \mathbf{y}) \sigma(\mathbf{u}_0, \mathbf{p}_0)(\mathbf{y}) dy.$$

We computed numerically the right-hand side of this equality for a P^1 discretization and plotted the $L^2(\Gamma)$ error with \mathbf{u}_0 when the size h of the mesh decrease. The

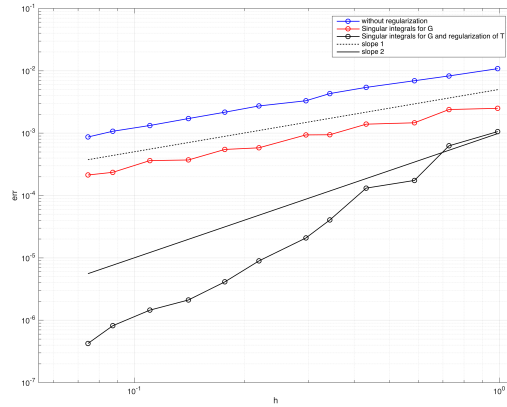
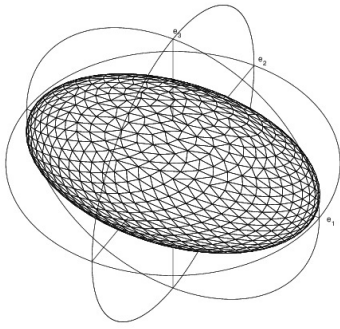


Fig. 3.15: Convergence for the Integral representation. Mesh of the ellipsoid for 1 000 vertices (left) and error versus the size of the elements h (right) for different regularizations of the integrals: no regularization (blue), singular integrals for \mathbf{G} (red), singular integrals for \mathbf{G} and singularity subtraction for \mathbf{T} (black).

numerical results on figure 3.15 show that, correcting both \mathbf{T} with the singularity subtraction method and \mathbf{G} with the P^0 semi-analytic method for the singular integrals, we obtain an $O(h^2)$ convergence.

- *The corrections are computed for the single-layer potential.* In view of the applications we have in mind, this is, in my opinion, the main limitation of the current computations. For example, in case of numerical simulations of suspensions, the double layer potential is part of the boundary integral formulation. As the particles may be close to each other, it is essential to deal with both the corresponding singular and near-singular integrals. However, we have seen that, while the singularity subtraction method is sufficient to regularize singular integrals, this is not the case

for near-singular integrals. It is therefore essential to develop a method to deal with the singularities related to the double layer potential.

To solve this problem, let us see how we can extend the semi-analytical method we proposed. In the case of a P^0 -correction, it leads to the analytical computation of the integrals $\int_{\tau} [\mathbf{T}_j(\mathbf{x}, \mathbf{y}) \mathbf{n}(\mathbf{y})] d\mathbf{y} \in \mathbb{R}^3$, where \mathbf{T}_j is defined in (3.11), page 59. To do this, we can for example follow the computations achieved to compute $I_0(\mathbf{x})$ for the Laplace Kernel (see figure 3.12). We recall that $\mathbf{T}_j(\mathbf{x}, \mathbf{y}) \mathbf{n}(\mathbf{y}) = \sigma_1(\mathbf{G}_j, \Pi_j) \mathbf{n}(\mathbf{y}) \in \mathbb{R}^3$ where σ_1 is the stress tensor for viscosity $\mu = 1$ and (\mathbf{G}_j, Π_j) is the solution to the Stokes problem with $\mu = 1$ and the source term $\delta_{\mathbf{x}}(\mathbf{y}) \mathbf{e}_j$ (see again page 59). Integrating by part Stokes equation on the tetrahedron \mathcal{T} and following the same computations as for $I_0(\mathbf{x})$ we obtain

$$\int_{\tau} [\mathbf{T}_j(\mathbf{x}, \mathbf{y}) \mathbf{n}(\mathbf{y})] d\mathbf{y} = - \int_{S_{\varepsilon}} [\mathbf{T}_j(\mathbf{x}, \mathbf{y}) \mathbf{n}(\mathbf{y})] d\mathbf{y}.$$

Using the fact that $\mathbf{r} \cdot \mathbf{n} = r = \varepsilon$ on S_{ε} , we have that $\mathbf{T}_j \mathbf{n} = \left(\frac{\mathbf{r}_i \mathbf{r}_j}{\varepsilon^4} \right)_{i=1 \dots 3}$ on S_{ε} and we finally obtain

$$\int_{\tau} [\mathbf{T}_j(\mathbf{x}, \mathbf{y}) \mathbf{n}(\mathbf{y})]_i d\mathbf{y} = - \frac{1}{\varepsilon^4} \int_{S_{\varepsilon}} \mathbf{r}_i \mathbf{r}_j = - \int_{S_1} \mathbf{r}_i \mathbf{r}_j.$$

Unfortunately, unlike the radial case, this last integral cannot be easily calculated (we recall that S_1 is the part of the sphere defining the solid angle of τ viewed from point \mathbf{x}). The integral being regular, a solution could be to approach it numerically using a classical quadrature method.

On-going work - Prospects

- We currently have at hand a BEM code taking advantage of the implementation of the SCSD for Stokes and dealing with singular integrals for the corresponding single layer. With François Alouges and Antoine Sellier, we are currently testing the code's ability to perform **numerical simulation of suspensions composed of rigid particles**. We first tested its behaviour on the case of two close ellipsoids by calculating the corresponding resistance matrices. We checked that the results were comparable to those obtained with Antoine Sellier's very accurate BEM code (direct solver, collocation discretization and P2 finite elements). We also investigated the behaviour of the code for a cluster of 100 particles whose density was varied (see figure 3.16). For the different configurations, we solved a Dirichlet to Neumann

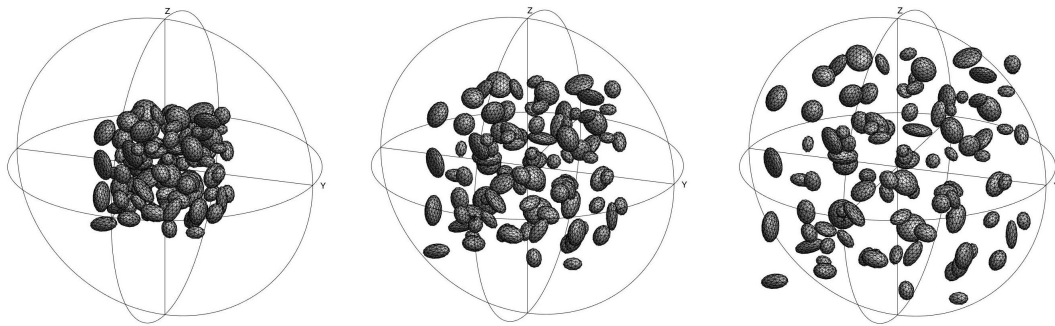


Fig. 3.16: Configurations involving 100 particles. The parameter β measures the minimal distance d_{min} between the particles: for $\beta = 0$, $d_{min} = 0.12421$ (left), for $\beta = 0.5$, $d_{min} = 0.96323$ (center) and for $\beta = 1$, $d_{min} = 1.7874$ (right). The length of the axes of the ellipsoids is in $[0.5, 2]$.

problem and studied both CPU time and convergence (see figure 3.17). It has to be emphasized that for this Dirichlet to Neumann problem, the CPU time as well as the error depend little on the distance between the particles. The code, thanks to a precise discretization of the surface and to the semi-analytical treatment of singular integrals, allows a good consideration of close interactions for the studied configurations. **These first results are very encouraging on the relevance of the numerical approach for the study of the rheology of suspensions.**

- As already mentioned, to go further in the numerical simulation of suspension, it becomes essential to **improve the treatment of near-singular integrals**. Indeed, near-singular integrals has to be considered as soon as two particles are close to

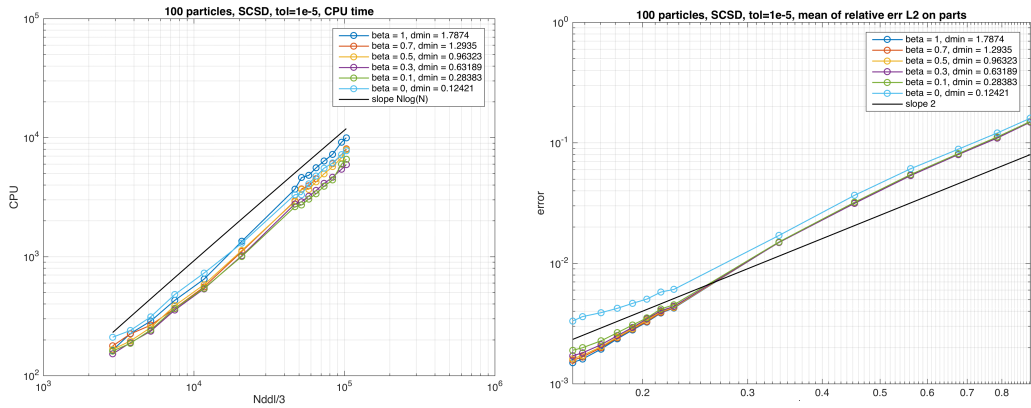


Fig. 3.17: Configurations involving 100 particles. Dirichlet to Neumann problem, with Stokeslet sources inside the particles. CPU time versus the number of degrees of freedom (left) and L^2 error versus the size of the discretization elements (right).

each other. It will be essential in the future to deal with the case of singularities arising from Stokes double layer potential, which is not done in the current code. There are several options for doing this. Among these, it would be interesting to try to extend the semi-analytical method we have implemented for the single layer potential.

- It would be interesting to develop, as for FMM, a **multi-level implementation of the SCSD fast algorithm**, based on a decomposition of the mesh into cells. The current implementation corresponds to a single-level implementation. Its cost is related to both the minimum distance R_{min} below which a direct calculation is chosen and the maximum distance in the domain R_{max} . In case of a multi-level implementation, each pair of cells corresponds to a different pair (R_{min}, R_{max}) . One option would be to perform as many SCSD decompositions as there are pairs (R_{min}, R_{max}) . Then the interactions between each pair of cells could be computed using the appropriate decomposition.
- As proposed in chapter 2, **extending the singular/regular decomposition method to BEM solvers** could be of great interest to better take into account lubrication in the simulations.
- To finish, a very motivating application of BEM methods is the **simulation of low Reynolds number swimmers or active suspensions**. This domain of application is discussed in chapter 5.

References

- [AA15] F. Alouges and M. Aussal. “The sparse cardinal sine decomposition and its application for fast numerical convolution”. In: *Numerical Algorithms* 70.2 (2015), pp. 427–448 (cit. on pp. 63–65).
- [ALR05] P. Angot, H. Lomonède, and I. Ramière. “A general fictitious domain method with non-conforming structured meshes”. In: *Finite Volume for Complex Applications IV, Problems and Perspectives*, Ed. F. Benkhaldoun, D. Ouazar, S. Raghay-Hermes Science (2005), pp. 261–272 (cit. on p. 50).
- [BWV15] A. Barnett, B. Wu, and S. Veerapaneni. “Spectrally Accurate Quadratures for Evaluation of Layer Potentials Close to the Boundary for the 2D Stokes and Laplace Equations”. In: *SIAM Journal on Scientific Computing* 37.4 (2015), B519–B542 (cit. on p. 75).
- [Bea20] J. T. Beale. “Neglecting discretization corrections in regularized singular or nearly singular integrals”. In: *arXiv preprint arXiv:2004.06686* (Apr. 2020) (cit. on p. 76).
- [BYW16] J. T. Beale, W. Ying, and J. R. Wilson. “A Simple Method for Computing Singular or Nearly Singular Integrals on Closed Surfaces”. In: *Communications in Computational Physics* 20.3 (2016), pp. 733–753 (cit. on p. 75).
- [Bon99] M. Bonnet. *Boundary Integral Equation Methods for Solids and Fluids*. Wiley, 1999 (cit. on pp. 53, 74).
- [BCS02] A. Buffa, M. Costabel, and C. Schwab. “Boundary element methods for Maxwell’s equations on non-smooth domains”. In: *Numerische Mathematik* 92.4 (2002), pp. 679–710 (cit. on p. 52).
- [CRW93] R. Coifman, V. Rokhlin, and S. Wandzura. “The fast multipole method for the wave equation: a pedestrian prescription”. In: *IEEE Antennas and Propagation Magazine* 35.3 (1993), pp. 7–12 (cit. on p. 63).
- [Cru69] T. A. Cruse. “Numerical solutions in three dimensional elastostatics”. In: *International Journal of Solids and Structures* 5.12 (1969), pp. 1259–1274 (cit. on p. 73).
- [FGM13] B. Fabreges, L. Gouarin, and B. Maury. “A smooth extension method”. In: *Comptes Rendus Mathématique* 351.9 (2013), pp. 361–366 (cit. on p. 50).
- [Gal+14a] S. Gallier, E. Lemaire, L. Lobry, and F. Peters. “A fictitious domain approach for the simulation of dense suspensions”. In: *Journal of Computational Physics* 256 (2014), pp. 367–387 (cit. on p. 50).
- [Gal+14b] S. Gallier, E. Lemaire, F. Peters, and L. Lobry. “Rheology of sheared suspensions of rough frictional particles”. In: *Journal of Fluid Mechanics* 757 (2014), pp. 514–549 (cit. on p. 50).

- [GR88a] L. Greengard and V. Rokhlin. *On the Efficient Implementation of the Fast Multipole Algorithm*. Tech. rep. Section: Technical Reports. YALE UNIV NEW HAVEN CT DEPT OF COMPUTER SCIENCE, 1988 (cit. on p. 63).
- [GR88b] L. Greengard and V. Rokhlin. “The rapid evaluation of potential fields in three dimensions”. In: *Vortex Methods*. Ed. by C. Anderson and C. Greengard. Lecture Notes in Mathematics. Berlin, Heidelberg: Springer, 1988, pp. 121–141 (cit. on p. 63).
- [HS94] W. Hackbusch and S. A. Sauter. “On numerical cubatures of nearly singular surface integrals arising in BEM collocation”. In: *Computing* 52.2 (1994), pp. 139–159 (cit. on p. 74).
- [HO08] J. Helsing and R. Ojala. “On the evaluation of layer potentials close to their sources”. In: *Journal of Computational Physics* 227.5 (2008), pp. 2899–2921 (cit. on p. 75).
- [KT16] L. af Klinteberg and A.-K. Tornberg. “A fast integral equation method for solid particles in viscous flow using quadrature by expansion”. In: *Journal of Computational Physics* 326 (2016), pp. 420–445 (cit. on p. 75).
- [KT14] L. af Klinteberg and A.-K. Tornberg. “Fast Ewald summation for Stokesian particle suspensions”. In: *International Journal for Numerical Methods in Fluids* 76.10 (2014), pp. 669–698 (cit. on p. 75).
- [LS12] M. Lenoir and N. Salles. “Evaluation of 3-D Singular and Nearly Singular Integrals in Galerkin BEM for Thin Layers”. In: *SIAM Journal on Scientific Computing* 34.6 (2012), A3057–A3078 (cit. on p. 76).
- [MRZ21] M. J. Morse, A. Rahimian, and D. Zorin. “A robust solver for elliptic PDEs in 3D complex geometries”. In: *Journal of Computational Physics* 442 (2021), p. 110511 (cit. on p. 75).
- [New86] J. N. Newman. “Distributions of sources and normal dipoles over a quadrilateral panel”. In: *Journal of Engineering Mathematics* 20.2 (1986), pp. 113–126 (cit. on pp. 79, 81).
- [Poz92] C. Pozrikidis. *Boundary integral and singularity methods for linearized viscous flow*. Cambridge university press, 1992 (cit. on pp. 53, 59).
- [RC92] D. Rosen and D. E. Cormack. “Analysis and evaluation of singular integrals by the invariant imbedding approach”. In: *International Journal for Numerical Methods in Engineering* 35.3 (1992), pp. 563–587 (cit. on p. 74).
- [SS11] S. A. Sauter and C. Schwab. *Boundary Element Methods*. Vol. 39. Springer Series in Computational Mathematics. Berlin, Heidelberg: Springer Berlin Heidelberg, 2011 (cit. on p. 74).
- [TB19] S. Tlupova and J. T. Beale. “Regularized single and double layer integrals in 3D Stokes flow”. In: *Journal of Computational Physics* 386 (2019), pp. 568–584 (cit. on pp. 75, 76).

- [TG08] A-K. Tornberg and L. Greengard. “A fast multipole method for the three-dimensional Stokes equations”. In: *Journal of Computational Physics* 227.3 (2008), pp. 1613–1619 (cit. on p. 66).
- [TPG92] D. L. Tullock, N. Phan Thien, and A. L. Graham. “Boundary element simulations of spheres settling in circular, square and triangular conduits”. In: *Rheologica Acta* 31.2 (1992), pp. 139–150 (cit. on p. 84).
- [Wac+15] A. Wachs, A. Hammouti, G. Vinay, and M. Rahmani. “Accuracy of Finite Volume/Staggered Grid Distributed Lagrange Multiplier/Fictitious Domain simulations of particulate flows”. In: *Computers & Fluids* 115 (2015), pp. 154–172 (cit. on p. 50).
- [WK19] M. Wala and A. Klöckner. “A fast algorithm for Quadrature by Expansion in three dimensions”. In: *Journal of Computational Physics* 388 (2019), pp. 655–689 (cit. on p. 75).
- [Wan+06] X. Wang, J. Kanapka, W. Ye, N.R. Aluru, and J. White. “Algorithms in FastStokes and Its Application to Micromachined Device Simulation”. In: *IEEE Transactions on Computer-Aided Design of Integrated Circuits and Systems* 25.2 (2006), pp. 248–257 (cit. on p. 66).
- [Yan+20] W. Yan, E. Corona, D. Malhotra, S. Veerapaneni, and M. Shelley. “A scalable computational platform for particulate Stokes suspensions”. In: *Journal of Computational Physics* 416 (2020) (cit. on p. 50).
- [YBZ06] L. Ying, G. Biros, and D. Zorin. “A high-order 3D boundary integral equation solver for elliptic PDEs in smooth domains”. In: *Journal of Computational Physics* 219.1 (2006), pp. 247–275 (cit. on p. 75).
- [ZV21] H. Zhu and S. Veerapaneni. “High-order close evaluation of Laplace layer potentials: A differential geometric approach”. In: *arXiv:2105.12683 [cs, math]* (May 2021) (cit. on p. 75).

Contacts: numerical schemes based on convex optimization problems

Collaborators: Frédéric Bernicot (Labo. Jean Leray, Nantes) - Sylvain Faure (LMO, Orsay) - Philippe Gondret (FAST, Orsay) - Hugo Martin (IPGP, Paris) - Bertrand Maury (LMO, Orsay) - Antoine Seguin (FAST, Orsay) - Benoît Semin (PMMH, ESPCI, Paris)

Related publications:

[14] *Dynamic Numerical Investigation of Random Packing for Spherical and Nonconvex Particles*. With S. Faure and B. Semin. In: *ESAIM: Proceedings 28 (2009)*. Ed. by M. Ismail, B. Maury, and J.-F. Gerbeau, pp. 13–32.

[15] *Existence results for non-smooth second order differential inclusions, convergence result for a numerical scheme and application to the modelling of inelastic collisions*. With F. Bernicot. In: *Confluentes Mathematici 2.4 (2010)*, pp. 445–471.

[16] *Clustering and flow around a sphere moving into a grain cloud*. With A. Seguin, S. Faure, and P. Gondret. In: *The European Physical Journal E 39.6 (2016)*, p. 63.

Expected applications of the results presented in this chapter:

- *Rheology of granular flows: Numerical simulation including friction and based on convex optimization solvers. Extension to non-spherical (but convex, regular) particles.*
 - *Rheology of suspensions: Taking friction into account in numerical simulation of suspensions for spherical and non-spherical particles.*
-

As mentioned in the introduction, the **consideration of contacts and more particularly of friction is essential to obtain behaviour close to experiments in numerical simulation of suspensions. Moreover, the simulation of dry granular materials is also of great interest**: as for suspensions, numerical simulation still has much to contribute to the understanding of their rheology. The models and numerical schemes developed in the dry granular framework are reusable in the framework of simulation of suspensions (through the coupling of the contact algorithms with a fluid-particle solver).

The first method to model the contacts between grains is the so-called **Discrete Element Method (DEM)**, (which is also found in the literature under the name of **Molecular Dynamics (MD)**). It dates back to 1979 with the work of Cundall and Strack [CS79]. The contact is taken into account through a repulsive force which becomes very large as the grains approach each other. The method consists of computing the explicit contact forces and solving the ordinary differential equations resulting from the fundamental principle of dynamics (see [Lud08] for a detailed description). It has been very successful and has the advantage of being easy to implement. One of its main drawbacks is its computational cost: due to the stiffness of the forces, it requires the use of small time steps when solving the differential equation. Various refined contact force models have been developed, which allow an accurate physical description of contact phenomena (see for example [Cor+21] for a list of about 40 possible contact models). These models involve a large number of parameters and the method is therefore subject to a delicate calibration step. A parallel implementation of the method has been achieved, for example, in the code Grains3D, where various shapes of particles can be considered [Wac+12; RW18; Rak+19]).

Another class of methods is the so-called **Non-Smooth Contact Dynamics (NSCD)** method, developed by Moreau and Jean in the 1990s. It is limited to the main features of the contact, such as the non-overlapping of the grains, without further refinement. We refer to the seminal papers [Mor88; JM92; Mor99; Jea99] for a detailed description. These models fall into the framework of **non-smooth convex analysis** (see the work of Jean-Jacques Moreau in the 1970s [Mor66; Mor70]). This provides a solid theoretical basis, allowing a fine study of their properties as well as of the corresponding numerical schemes. **The contact forces are implicit**, deduced from the Lagrange multipliers associated with the non-interpenetration constraints. This solves the difficulty due to the rigidity of the forces and makes it possible to obtain stable and efficient algorithms, supporting large time steps. This type of method has been implemented for example in the LMGC code [DJ06; DR14].

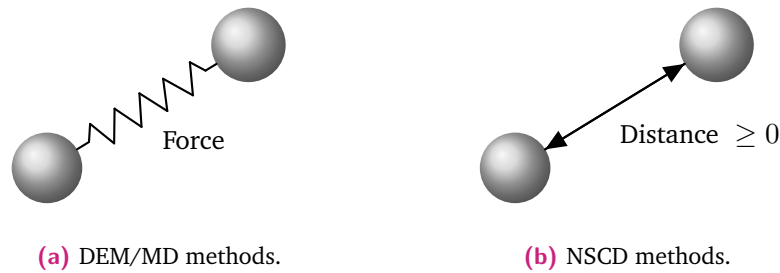


Fig. 4.1: Contact modelling.

B. Maury proposed in [Mau06] an NSCD-like algorithm for frictionless contacts. It is based on a constrained optimisation problem to be solved at each time step. During my PhD thesis, I extended this model into a so-called viscous contact model in order to model lubrication between the grains. I implemented the frictionless and viscous models, which led to the code SCoPI (Simulation of Collection of Particles in Interaction).

In what follows, I first describe the algorithm that was proposed in [Mau06] and which is the starting point of the work presented in this chapter. I then detail the convergence result that we obtained for this scheme with Frédéric Bernicot [15]. Then, I show how, with Sylvain Faure, we have improved the code SCoPI to make it an efficient tool, adapted to rheological studies of granular materials. The resulting code has led to collaborations with Benoît Semin, now at the PMMH laboratory of ESPCI [14], and Philippe Gondret and Antoine Seguin of the FAST laboratory in Orsay [16].

Finally, I present a recent on-going work, initiated in the framework of Hugo Martin's thesis on dry granular flows, supervised by Anne Mangeney (IPGP) and Yvon Maday (LJLL). With Bertrand Maury, we participated to the development of a stable algorithm for frictional contacts. The idea driving this work is to follow the frictionless case and to design an **algorithm based on a single resolution, at each time step, of a convex optimization problem.**

4.1 Non Smooth Contact Dynamics for frictionless contacts

▷ A toy problem

For the sake of simplicity, I present the models and algorithms in the case of a single spherical particle located above an inclined plane Π (see figure 4.2). The normal to to

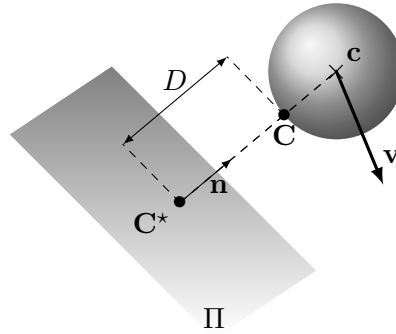


Fig. 4.2: Toy problem. Notation.

the plane, oriented upwards is denoted by \mathbf{n} . The rigid sphere has given fixed radius $r > 0$, mass $m > 0$ and moment of inertia J . The center of sphere is denoted by $\mathbf{c} \in \mathbb{R}^3$, and its instantaneous velocity by $\mathbf{v} \in \mathbb{R}^3$. Since the grain is spherical and the contact is frictionless, we shall not follow its orientation and angular velocity.

We denote by \mathbf{C} the point on the surface of the sphere which realizes the minimal distance and \mathbf{C}^* its projection on plane Π (with $\mathbf{C} = \mathbf{C}^*$ if the sphere is in contact with the plane).

The signed distance between the sphere and the plane is defined by :

$$D(\mathbf{c}) = |(\mathbf{c} - \mathbf{C}^*)| - r,$$

so that the non-overlapping condition writes $D \geq 0$.

Since there is no friction, the contact force \mathbf{f} exerted on the sphere at point \mathbf{C} is collinear to \mathbf{n} :

$$\mathbf{f} = f_n \mathbf{n} \quad \text{where} \quad f_n \in \mathbb{R}.$$

▷ **Normal contact modelling: a unilateral constraint**

The specificity of the Contact Dynamics models lies in the fact that they explicitly express that the two bodies cannot interpenetrate. This means that the distance D must remain non negative so that the set of admissible configurations is:

$$\mathcal{Q} = \left\{ \mathbf{c} \in \mathbb{R}^3, \quad D(\mathbf{c}) \geq 0 \right\}.$$

This implies that the normal force $f_n \mathbf{n}$ is a repulsive force at contact: $f_n \geq 0$. Moreover, the contact force must vanish as soon as the contact is broken. This can be expressed by the equality $D f_n = 0$ which implies that f_n cannot be active (i.e. it has to vanish) as long as the distance is not zero. These conditions are known as the *Signorini conditions*:

$$D(\mathbf{c}) \geq 0, \quad f_n \geq 0, \quad D(\mathbf{c}) f_n = 0.$$

We will see later that the force f_n can be seen as the Lagrange multiplier associated to the constraint $D \geq 0$. The last equality in Signorini conditions then translates the corresponding complementarity condition.

When two rigid bodies come into contact, expressing the Signorini condition is not sufficient to determine the motion. Indeed, if the reaction f_n must be positive, no information is given on its value. The model lacks an impact law, relating the normal impact velocity before contact to the velocity after contact.

Let us denote in the following $P_{\mathcal{C}}$ the orthogonal projection on a given set \mathcal{C} , and \mathbf{w}^+ (resp. \mathbf{w}^-) the right-sided (resp. left-sided) limit of a given function \mathbf{w} .

One can for example write the inelastic contact law as:

$$\mathbf{v}^+ = P_{\mathcal{C}_c} \mathbf{v}^- \quad \text{where} \quad \mathcal{C}_c = \left\{ \mathbf{v} \in \mathbb{R}^3, \quad \nabla D(\mathbf{c}) \cdot \mathbf{v} \geq 0 \text{ if } D(\mathbf{c}) = 0 \right\}. \quad (4.1)$$

The set \mathcal{C}_c is the so-called set of admissible velocities. It reflects the fact that, to avoid overlaps, the distance must increase as soon as it vanishes. Since $\nabla D(\mathbf{c}) = \mathbf{n}$, any admissible speed satisfies $\mathbf{n} \cdot \mathbf{v}^+ \geq 0$. The particle being spherical, we obtain that the relative normal velocity at point \mathbf{C} must be positive after contact: $\mathbf{n} \cdot \mathbf{v}_{\mathbf{C}}^+ \geq 0$. Moreover, due to the projection step, we finally have that it cancels after the contact, modelling as desired an inelastic contact.

Let us note, at this point of the discussion, that the velocity of the particle is likely to be non-smooth. In particular, the post-collisional velocity \mathbf{v}^+ can be different from the

pre-collisional velocity \mathbf{v}^- . This raises the question of the meaning to be given to the different equations stated. To deal with the discontinuous character of the velocity, the space to consider is the space of functions with bounded variations. This allows to define the velocities before and after contact time. In that case, the force f_n is an impulse at contact time and, since the distance is continuous, the Signorini conditions can be understood in the sense of distributions or even in the sense of measures.

So we can now state the equations of dynamics, driven by the fundamental principle of dynamics. We consider that no external torque is exerted on the grains. $\mathbf{f}^{ext} \in \mathbb{R}^3$ is the external force exerted on the particle and we define the mass matrix as $M = \text{diag}(m, m, m)$. The equations of motion writes, in the sense of distributions or measures:

$$\dot{\mathbf{c}} = \mathbf{v}, \quad (4.2)$$

$$M \frac{d\mathbf{v}}{dt} = \mathbf{f}^{ext} + f_n \mathbf{n}, \quad (4.3)$$

$$D(\mathbf{c}) \geq 0, \quad f_n \geq 0, \quad D(\mathbf{c}) f_n = 0, \quad (4.4)$$

$$\mathbf{v}^+ = P_{\mathcal{C}_c} \mathbf{v}^-. \quad (4.5)$$

4.2 A convex scheme for frictionless contacts

▷ A natural time stepping discretization, leading to a convex optimization problem

We denote the time step by Δt , by $\mathbf{c}^k \in \mathbb{R}^3$ the center of particle at time $k\Delta t$ and by $\mathbf{v}^k \in \mathbb{R}^3$ the velocity at step k . The scheme is based on a Euler discretization to compute the position at time $k+1$:

$$\mathbf{c}^{k+1} = \mathbf{c}^k + \Delta t \mathbf{v}^{k+1}.$$

To compute \mathbf{v}^{k+1} , the founding algorithms [JM92; Jea99] discretize the set of admissible velocities \mathcal{C}_c (4.1) using the corresponding discrete constraint

$$\nabla D(\mathbf{c}^k) \cdot \mathbf{v}^{k+1} \geq 0 \quad \text{if} \quad D(\mathbf{c}^k) \leq 0.$$

Doing so, the constraint is implicit in the velocity unknown. However, if $D(\mathbf{c}^k) > 0$, \mathbf{v}^{k+1} is not constrained and the time discretization can make $D(\mathbf{c}^{k+1}) = D(\mathbf{c}^k + \Delta t \mathbf{v}^{k+1})$ strictly negative so that the particle overlaps the plane. To avoid this situation, a Taylor

expansion of the constraint is used in [Mau06] where the author defines the discrete set of constraints as

$$K = \left\{ \mathbf{v} \in \mathbb{R}^3, D(\mathbf{c}^k) + \Delta t \nabla D(\mathbf{c}^k) \cdot \mathbf{v} \geq 0 \right\}. \quad (4.6)$$

In that case, the constraint is implicit again and one has

$$D(\mathbf{c}^{k+1}) = D(\mathbf{c}^k) + \Delta t \nabla D(\mathbf{c}^k) \cdot \mathbf{v} + O(\Delta t^2) \geq 0.$$

Thus, the discrete constraint can be seen as a first order implicit approximation of the continuous non-overlapping constraint, the error being of order $O(\Delta t^2)$. Moreover, due to the convexity of the distance function, this constraint returns feasible configurations (i.e. it avoids numerical interpenetration):

$$D(\mathbf{c}^{k+1}) \geq D(\mathbf{c}^k) + \Delta t \nabla D(\mathbf{c}^k) \cdot \mathbf{v}^{k+1} \geq 0.$$

From this, the natural Euler-based time discretization of (4.3,4.4) proposed in [Mau06] is

$$\begin{aligned} M \frac{\mathbf{v}^{k+1} - \mathbf{v}^k}{\Delta t} &= \mathbf{f}^{ext} + f_n \mathbf{n}^k, \\ f_n &\geq 0, \quad D(\mathbf{c}^k) + \Delta t \nabla D(\mathbf{c}^k) \cdot \mathbf{v}^{k+1} \geq 0, \\ (D(\mathbf{c}^k) + \Delta t \nabla D(\mathbf{c}^k) \cdot \mathbf{v}^{k+1}) f_n &= 0. \end{aligned} \quad (4.7)$$

One of the great advantages of this scheme, besides being **stable** and providing **feasible configurations**, is that it can be seen as the optimality condition of a convex minimization problem, submitted to an affine constraint.

Indeed, let us denote by $\|\mathbf{w}\|_M$ the M -norm $\|\mathbf{w}\|_M^2 := \mathbf{w} \cdot M \mathbf{w}$, and consider the following problem: find $\mathbf{v} \in \mathbb{R}^3$ solution to the minimization problem

$$\min_{\mathbf{v} \in K} J(\mathbf{v}), \quad (4.8)$$

$$J(\mathbf{v}) = \frac{1}{2} \left\| \mathbf{v} - \mathbf{V}^{k+1} \right\|_M, \quad \mathbf{V}^{k+1} = \mathbf{v}^k + \Delta t M^{-1} \mathbf{f}^{ext},$$

where K is the discrete set of admissible velocities defined in (4.6). \mathbf{V}^{k+1} is the discrete free flight velocity: it is equal to the velocity that would be computed using an explicit Euler scheme without contact. The particle velocity \mathbf{v}^{k+1} is the projection of \mathbf{V}^{k+1} on

the discrete set of admissible velocities K . This can be seen as a discretization of the continuous contact law (4.5). Let us now rewrite the discrete constraint set K as

$$K = \left\{ \mathbf{v} \in \mathbb{R}^3, g(\mathbf{v}) \leq 0 \right\}, \quad g(\mathbf{v}) = -D(\mathbf{c}^k) - \Delta t \nabla D(\mathbf{c}^k) \cdot \mathbf{v}. \quad (4.9)$$

For each time step, one then has to minimize the convex functional J under the affine inequality constraint $g \leq 0$. There exists a unique solution to this constrained minimization problem. Moreover, the constraint g is qualified (scalar affine constraint). Then, if \mathbf{v}^{k+1} is solution to (4.8), there exists a Lagrange multiplier $f_n \geq 0$ such that the following Kuhn Tucker optimality condition is verified:

$$\begin{aligned} \nabla J(\mathbf{v}^{k+1}) &= -f_n \nabla g(\mathbf{v}^{k+1}), \\ g(\mathbf{v}^{k+1}) &\leq 0, \quad f_n \geq 0, \quad g(\mathbf{v}^{k+1}) f_n = 0. \end{aligned} \quad (4.10)$$

Computing ∇J and ∇g , and using the fact that $\nabla D(\mathbf{c}^k) = \mathbf{n}^k$, one can see that these optimality conditions precisely correspond to the discrete scheme (4.7). So finally, the solution to the continuous problem can be approximated by **solving the convex constrained problem (4.8) at each time step**.

► Convergence result in the multi-particle case [15]

In the multi-particle case, let us consider N rigid spherical particles. The center (resp. the generalized velocity) of particle i is denoted by \mathbf{c}_i (resp. \mathbf{v}_i). The set of centers $\mathbf{c} = (\mathbf{c}_1, \dots, \mathbf{c}_N)$ as well as the set of generalized velocities $\mathbf{v} = (\mathbf{v}_1, \dots, \mathbf{v}_N)$ now belong to \mathbb{R}^{3N} . The contact law has to be written for each pair (i, j) of particles so that the set of admissible configurations and velocities writes:

$$\begin{aligned} \mathcal{Q} &= \bigcap_{i \neq j} \left\{ \mathbf{c} \in \mathbb{R}^{3N}, \quad D_{ij}(\mathbf{c}) \geq 0 \right\}, \\ \mathcal{C}_{\mathbf{c}} &= \bigcap_{i \neq j} \left\{ \mathbf{v} \in \mathbb{R}^{3N}, \quad \nabla D_{ij}(\mathbf{c}) \cdot \mathbf{v} \geq 0 \text{ if } D_{ij}(\mathbf{c}) = 0 \right\}, \end{aligned}$$

where D_{ij} is the distance between particles i and j .

Then, the multi-particle scheme proposed in [Mau06] is based on the projection of the free-flight velocity onto the discrete set of admissible velocities K :

$$K = \bigcap_{i \neq j} \left\{ \mathbf{v} \in \mathbb{R}^{3N}, \quad D_{ij}(\mathbf{c}^k) + \Delta t \nabla D_{ij}(\mathbf{c}^k) \cdot \mathbf{v} \geq 0 \right\}.$$

Each of the constraints leads to a Lagrange multiplier, corresponding to the contact force between the involved particles. The convergence to the continuous problem (up to a subsequence) is proved in [Mau06] in the case of a unique contact. It is also shown numerically that the scheme is stable, robust and has a good behaviour for large time steps. As for me, I have used it in the context of particles undergoing inelastic or gluey contacts [6]. That is why, with Frédéric Bernicot, we were interested in continuing its numerical analysis in the multi-constraint case, and proposing some extensions like the time-dependence of the constraints [15].

Let us describe the model we considered in [15]. We place ourselves in a general theoretical framework of which our contact model is a special case. The dimension is denoted by n and we consider P continuous constraints depending on time:

$$\text{(Admissible configurations)} \quad \mathcal{Q}(t) = \bigcap_{p=1}^P \{ \mathbf{c} \in \mathbb{R}^n, \quad g_p(t, \mathbf{c}) \geq 0 \}$$

$$\text{(Admissible velocities)} \quad \mathcal{C}_{t,\mathbf{c}} = \bigcap_{p=1}^P \{ \mathbf{u} \in \mathbb{R}^n, \quad \partial_t g_p(t, \mathbf{c}) + \nabla_{\mathbf{c}} g_p(t, \mathbf{c}) \cdot \mathbf{u} \geq 0 \}$$

$$\text{(Discrete admissible velocities)} \quad K = \bigcap_{p=1}^P \left\{ \mathbf{u} \in \mathbb{R}^n, \quad g_p(t^{k+1}, \mathbf{c}^k) + \Delta t \nabla_{\mathbf{c}} g_p(t^{k+1}, \mathbf{c}^k) \cdot \mathbf{u} \geq 0 \right\}$$

From a mathematical point of view, the continuous model enters in the framework of **second order differential inclusions**. The admissible configuration set \mathcal{Q} is the intersection of complements of smooth convex sets. The existence of a solution for such second-order problems is still open in a general framework. Furthermore, the hypotheses of existing results are not fulfilled in the case of frictionless contacts we are interested in. Some results were obtained for one constraint ($P = 1$) [Mon13; PS02] or for convex admissible sets [Pao05]. Unfortunately, it is easy to see that the admissible configuration set \mathcal{Q} is not convex in general. Indeed, consider for example two circular particles in dimension two that cannot overlap and the admissible set \mathcal{Q} containing the position of their centers. In this case, $n = 4$, $P = 1$ and g_p is the distance between the two particles. We can observe on figure 4.3 that the set \mathcal{Q} is not convex: the two configurations \mathbf{c} and $\bar{\mathbf{c}}$ belong to \mathcal{Q} but their mean does not. In the case of non-convex sets, some results were obtained for $P = 1$ in [DM07; DMP09; MP06; Sch01]. The non-convex multi-constraint case was studied in [Pao10], supposing the linear independence of the active gradients. Again, this result cannot be used when modelling granular media with too many particles.

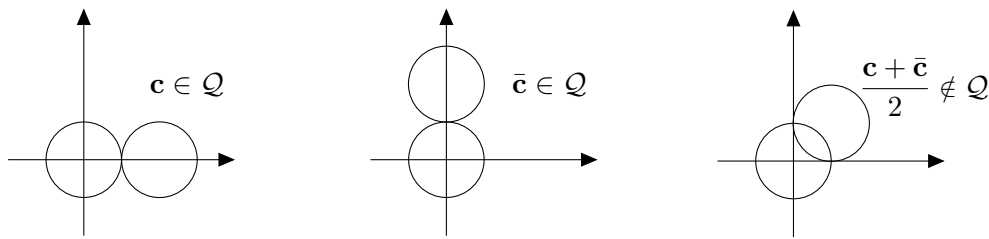


Fig. 4.3: Non convex admissible configuration set Q .

Indeed, in that case, the number of active non-interpenetration constraints can become greater than the dimension so that their gradients cannot be linearly independent.

We prove in [15] that the solution to the numerical scheme we propose converges (up to a subsequence) to a solution to the continuous problem, under weaker assumptions on the gradients than the ones made in [Pao10]. This shows at the same time the existence of a solution to the continuous model. Our assumptions are met in the case of the frictionless contact model so that a direct consequence of this result is the **convergence of the multi-particle numerical scheme** proposed in [Mau06] for frictionless contact. The proof we propose follows the same reasoning as the proof in [Mau06] for one contact with some new arguments in order to solve the difficulties raised by the multiple constraints and the time-dependence. These new arguments already appeared in [Ven11] in which the author models crowd motion using first order differential inclusions with constraint sets similar to ours.

▷ **C++ code SCoPI and mechanical studies [14,16]**

As already said, I implemented during my PhD thesis the previous algorithm to simulate granular flows undergoing frictionless contacts and an extension of this model taking into account lubrication. The corresponding code C++ was named SCoPI for "Simulation of Collection of Particles in Interaction". Since then, a part of my activity has consisted, with Sylvain Faure (LMO), in developing and optimizing SCoPI. Our goal was to be able to perform numerical rheological studies of granular materials using the code. Up to now, it allowed us to realize two mechanical studies in the frictionless case.

Dynamic numerical investigation of random packing for spherical and nonconvex particles [14]

This work, in collaboration with B. Semin and S. Faure, was initiated during the summer school Cemracs 2008 and continued afterwards. It gave rise to a proceeding [14]. The project was financially supported by Lafarge and the objective was to understand how the random compaction of a granular medium evolves according to the shape of the particles. More precisely, we modified the code to make it possible to consider particles composed of two interpenetrating spheres. We described the compactness as well as the mean value and the distribution of the number of contacts of the final configuration as a function of the interpenetration length of the spheres constituting particles (see figure 4.4). Two post-processing functions were implemented to obtain the parameters characterizing the packing: a Monte-Carlo method was used to compute the packing fraction of the system in a subdomain and a function was developed to provide the distribution and the mean numbers of contacts and neighbours for the particles contained in a subdomain.

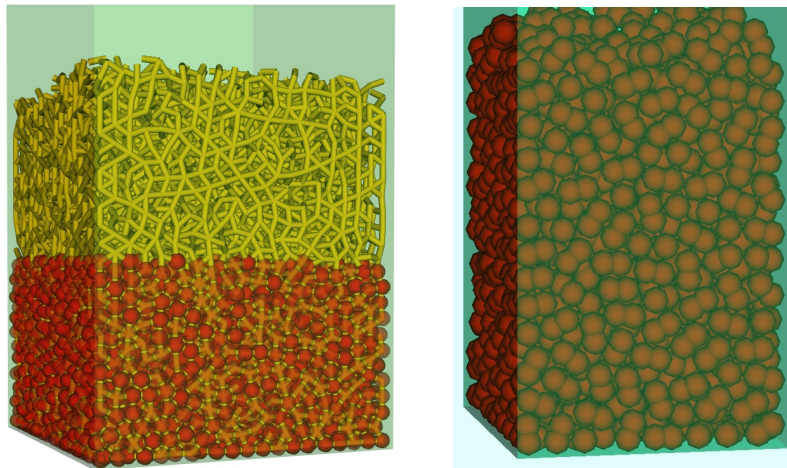


Fig. 4.4: Random packing. Left: 16 000 spherical particles, lower half of the grains in red and contacts in yellow tubes. Right: 10 000 non-convex particles.

Clustering and flow around a sphere moving into a grain cloud [16]

This work is the result of a collaboration that started at the beginning of the ANR Stabingram (2011). Philippe Gondret and Antoine Seguin (FAST, Orsay) had set up an experiment consisting in pulling a ball at constant speed in a granular medium enclosed in a box (2d experiment). The goal was to study the rheology in the cluster formed in front of the moving sphere. To do so, they measured the velocities as well as the contact

forces exerted of the grains. Unfortunately, their results were tainted by noise and difficult to interpret. We therefore decided to set up numerical simulations in order to answer some of their questions.

Some optimization of the code were needed to run these simulations involving several hundred thousand balls. Sylvain Faure implemented a shared memory parallelism (using the Intel TBB library) and revised the format of the output files in order to make them usable in view of the large amount of data generated. This allowed us to run some tests involving about 1 million of spheres in 3 dimensions. We also developed the post-processing capabilities in order to calculate at any point of the granular medium, quantities of physical interest such as pressure, strain tensor, stresses or local density.

We finally launched a simulation campaign, the granular medium being composed of up to 300 000 grains (see figure 4.5). The results were treated by Philippe Gondret and Antoine Seguin as experimental results. They studied the cluster size in front of the moving sphere and conducted a detailed study of the rheology of the system inside the cluster [16]. The results proved that a local rheology based on the inertial number I (i.e. an explicit link between the different local physical quantities and I) can be observed even in the case of non-parallel flows, which had not been observed before.

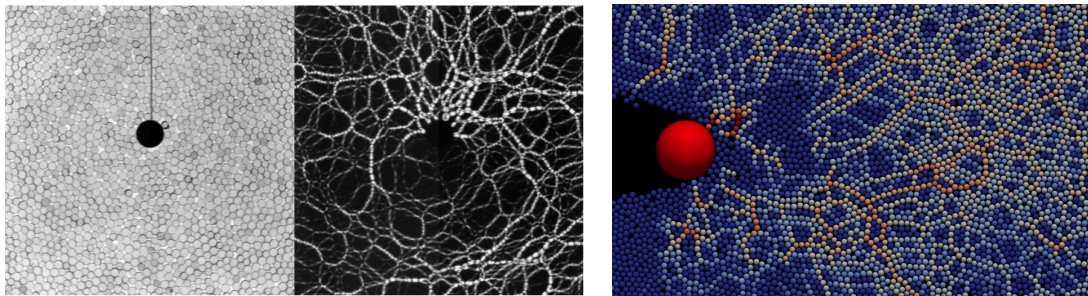


Fig. 4.5: Sphere moving in a grain cloud. Left: physical experiment conducted at FAST laboratory (grains on the left and pressure exerted on the grains on the right, the lighter the sphere, the more it is compressed). Right: Corresponding numerical simulation with SCoPI (300 000 grains), the red sphere moves to the right and the grains are colored according to the pressure exerted on them (from blue for minimum pressure to red for maximum pressure).

4.3 A convex scheme for frictional contacts.

The work presented in this section has been initiated in the framework of Hugo Martin's PhD thesis, supervised by Anne Mangeney (IPGP) and Yvon Maday (LJLL). The objective of Hugo Martin's work was to develop a numerical tool to study granular collapse on erodible beds and the relations between granular assemblies and elastic wave propagations. With Bertrand Maury (LMO), we participated in the development of an algorithm for the numerical simulation of granular media with frictional contact. One of the main difficulties in designing schemes for frictional contacts is that, unlike the frictionless case, the natural Euler-based scheme do not correspond to a convex optimization problem. This makes its resolution tricky. I present in the following an extension of the frictionless algorithm described in the previous sections, leading to a scheme for frictional contacts which is based on convex optimization. This is a work in progress, for which an article is being prepared.

▷ Modelling friction

Notation.

We extend the notation to describe the tangential velocity and contact force. First we now need to take into account the instantaneous rotation vector $\boldsymbol{\omega} \in \mathbb{R}^3$. We denote by

$$\mathbf{u} = (\mathbf{v}, \boldsymbol{\omega}) \in \mathbb{R}^6$$

the generalized velocity vector and we define the position vector $\mathbf{r} = \mathbf{C} - \mathbf{c}$. The linear operator A maps the generalized velocity field $\mathbf{u} \in \mathbb{R}^6$ to the velocity $\mathbf{v}_{\mathbf{C}} \in \mathbb{R}^3$ of point \mathbf{C} (see Figure 4.6):

$$A\mathbf{u} = \mathbf{v}_{\mathbf{C}} = \mathbf{v} + \boldsymbol{\omega} \wedge \mathbf{r} \in \mathbb{R}^3.$$

Note that, since \mathbf{C} is the point that minimizes the distance, the normal direction to the sphere at point \mathbf{C} is \mathbf{n} . We denote by $P\mathbf{w} = \mathbf{w} - (\mathbf{w} \cdot \mathbf{n})\mathbf{n}$ the projection of a vector $\mathbf{w} \in \mathbb{R}^3$ on the tangent plane to the sphere at point \mathbf{C} (which is parallel to Π). The tangential velocity at point \mathbf{C} is therefore $P\mathbf{v}_{\mathbf{C}} = PA\mathbf{u}$. As for the contact force \mathbf{f} exerted

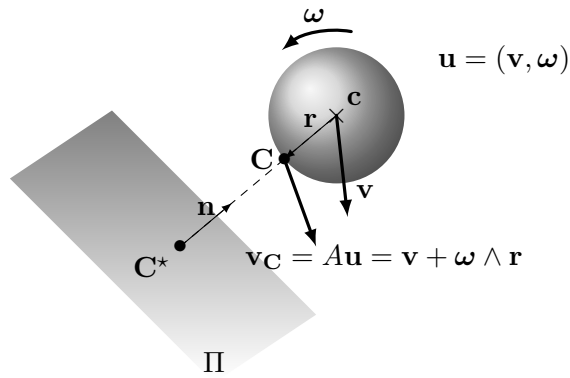


Fig. 4.6: Frictional contact. Notation.

on the sphere at point C , it is decomposed into a normal component and a tangential component as follows (see figure 4.7):

$$\mathbf{f} = f_n \mathbf{n} + \mathbf{f}_t \quad \text{where} \quad f_n \in \mathbb{R} \quad \text{and} \quad \mathbf{f}_t = P\mathbf{f} \in \mathbb{R}^3.$$

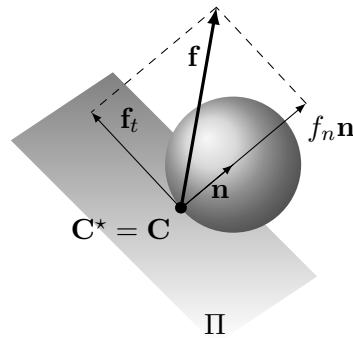


Fig. 4.7: Decomposition of the contact force $\mathbf{f} = f_n \mathbf{n} + \mathbf{f}_t$.

Contact laws.

The normal contact law is still driven by the non-overlapping constraint. The grains being spherical, the distance does not depend on the orientation of the particle: $D = D(c)$. We

denote its gradient along \mathbf{c} by $\nabla_{\mathbf{c}}D \in \mathbb{R}^3$. The constraint defining the set of admissible velocities is:

$$\mathbf{u}^+ = P_{\mathcal{C}_c} \mathbf{u}^- \quad \text{where} \quad \mathcal{C}_c = \left\{ \mathbf{u} = (\mathbf{v}, \boldsymbol{\omega}) \in \mathbb{R}^6, \quad \nabla_{\mathbf{c}}D(\mathbf{c}) \cdot \mathbf{v} \geq 0 \text{ if } D(\mathbf{c}) = 0 \right\}.$$

As for the tangential contact law, the oldest and best known law to describe frictional contact is *Coulomb's law*, which can be written as:

$$\text{If } P_{\mathbf{v}_C^+} \neq 0 \text{ (sliding motion), } \mathbf{f}_t = -\mu f_n \frac{P_{\mathbf{v}_C^+}}{|P_{\mathbf{v}_C^+}|},$$

$$\text{If } P_{\mathbf{v}_C^+} = 0 \text{ (no slip), } |\mathbf{f}_t| \leq \mu f_n,$$

where μ is the friction coefficient and depends on the physical properties of the surfaces. In particular, the contact force must belong to the so-called Coulomb cone:

$$\mathcal{C}_\mu^{\text{Coulomb}} = \left\{ \mathbf{f} \in \mathbb{R}^3 \text{ s.t. } |\mathbf{f}_t| \leq \mu f_n \right\}.$$

Dynamics.

We suppose that no external torque is exerted on the grains. If $\mathbf{f}^{\text{ext}} \in \mathbb{R}^3$ is the external force exerted on the particle, we define the generalized force vector as $\mathbf{F}^{\text{ext}} = (\mathbf{f}^{\text{ext}}, 0) \in \mathbb{R}^6$. The generalized mass matrix (masses and moments of inertia) is defined as $M = \text{diag}(m, m, m, J, J, J)$.

Let us finally remark that for any generalized velocity $\mathbf{u} \in \mathbb{R}^6$ and any vector $\mathbf{f} \in \mathbb{R}^3$, we have $A\mathbf{u} \cdot \mathbf{f} = \mathbf{u} \cdot A^T \mathbf{f}$ with

$$A^T \mathbf{f} = (\mathbf{f}, \mathbf{r} \wedge \mathbf{f}) \in \mathbb{R}^6, \tag{4.11}$$

so that A^T maps a vector $\mathbf{f} \in \mathbb{R}^3$ to the generalized force/moment vector corresponding to a force \mathbf{f} exerted on the sphere at point \mathbf{C} .

We can now state the corresponding equations of dynamics:

$$\dot{\mathbf{c}} = \mathbf{v}, \quad \mathbf{u} = (\mathbf{v}, \boldsymbol{\omega}), \quad (4.12)$$

$$M \frac{d\mathbf{u}}{dt} = \mathbf{F}^{ext} + A^T (f_n \mathbf{n} + \mathbf{f}_t), \quad (4.13)$$

$$D(\mathbf{c}) \geq 0, \quad f_n \geq 0, \quad D(\mathbf{c}) f_n = 0, \quad (4.14)$$

$$\mathbf{u}^+ = P_{C_c} \mathbf{u}^-, \quad (4.15)$$

$$\text{If } PA\mathbf{u}^+ \neq 0 \text{ (sliding motion), } \mathbf{f}_t = -\mu f_n \frac{PA\mathbf{u}^+}{|PA\mathbf{u}^+|}, \quad (4.16)$$

$$\text{If } PA\mathbf{u}^+ = 0 \text{ (no slip) , } |\mathbf{f}_t| \leq \mu f_n. \quad (4.17)$$

From the expression of A^T , we can decompose equation (4.12) in two equations driving the translational and the angular velocities respectively:

$$\begin{aligned} m \frac{d\mathbf{v}}{dt} &= \mathbf{f}^{ext} + (f_n \mathbf{n} + \mathbf{f}_t), \\ J \frac{d\boldsymbol{\omega}}{dt} &= \mathbf{r} \wedge (f_n \mathbf{n} + \mathbf{f}_t). \end{aligned}$$

One can recognize the fundamental principle of dynamics written for the particle, submitted to the external force \mathbf{f}^{ext} and to the contact force $f_n \mathbf{n} + \mathbf{f}_t$, exerted at point C. Equations (4.14-4.17) correspond to the normal and tangential contact laws. Again, these equations have to be understood in the sense of distributions or measures.

▷ A "natural" Euler-based scheme

A natural Euler-based scheme to approximate (4.12-4.17) is

$$M \frac{\mathbf{u}^{k+1} - \mathbf{u}^k}{\Delta t} = \mathbf{F}^{ext} + A^{k,T} (f_n \mathbf{n}^k + \mathbf{f}_t), \quad (4.18)$$

$$f_n \geq 0, \quad g(\mathbf{u}^{k+1}) \leq 0, \quad f_n g(\mathbf{u}^{k+1}) = 0,$$

$$\text{If } P^k A^k \mathbf{u}^{k+1} \neq 0 \text{ (sliding motion), } \mathbf{f}_t = -\mu f_n \frac{P^k A^k \mathbf{u}^{k+1}}{|P^k A^k \mathbf{u}^{k+1}|},$$

$$\text{If } P^k A^k \mathbf{u}^{k+1} = 0 \text{ (no slip) , } |\mathbf{f}_t| \leq \mu f_n.$$

where P^k and A^k are respectively the projection on the local tangent plane and the velocity of the contact point associated to configuration \mathbf{c}^k . A natural choice for the normal constraint discretization g is given by $g(\mathbf{u}^{k+1}) = \nabla D(\mathbf{c}^k) \cdot \mathbf{v}^{k+1}$ if $D(\mathbf{c}^k) \leq 0$ [ST96;

AP97]. Following [Mau06], it can also be substituted by the Taylor expansion (4.9) to generate feasible configurations.

Although these schemes are stable, in the case of multiple contacts they require solving, at each time step, a non-convex linear complementarity problem which proves to be expensive to solve. The most widely spread numerical strategies to deal with the friction cone constraint are based on projection/splitting methods, Gauss-Seidel like relaxations or generalized Newton methods (see [ABH18] for a review of these methods). Unfortunately, no convergence result for the corresponding iterative methods are available.

▷ Notion of subdifferential

To make the problem easier to solve, we follow the idea of the frictionless algorithm: we search for a time discretization leading to a convex constrained optimization problem to be solved at each time step. To do so, we want to find an optimization problem for which the optimality conditions are discretization of (4.12-4.17), the contact force being the corresponding Lagrange multiplier.

However, one can see that the tangential force \mathbf{f}_t cannot be expressed as the gradient of a constraint. For example, from equation (4.17), we only know that it belongs to the Coulomb cone in case of sliding motion. In order to obtain this kind of optimality constraint, we have to consider non-differentiable constraints (of conic type) and substitute the notion of sub-differential of a function for that of gradient.

Definition.

The notion of subdifferential allows to describe the local variations of a convex function, not necessarily derivable. We refer to [HL93, Chap. VI] for an extensive description of subdifferentials and their use in optimisation. Let us consider a convex function $\phi : \mathbb{R}^n \rightarrow \mathbb{R}$. The subdifferential of ϕ at point $\mathbf{x} \in \mathbb{R}^n$, denoted by $\partial\phi[\mathbf{x}]$, can be defined through minorization by affine functions:

$$\partial\phi[\mathbf{x}] = \{\mathbf{y} \in \mathbb{R}^n / \forall \hat{\mathbf{x}} \in \mathbb{R}^n, \phi(\hat{\mathbf{x}}) \geq \phi(\mathbf{x}) + \mathbf{y} \cdot (\hat{\mathbf{x}} - \mathbf{x})\}.$$

Let us illustrate this notion in one dimension (see Figure 4.8). In that case, the subdifferential contains the slopes of the lines issued from point $(\mathbf{x}, \phi(\mathbf{x}))$ and remaining under the graph. If ϕ is derivable at point x_0 , we have $\partial\phi[x_0] = \{\phi'(x_0)\}$ and if ϕ is left and right derivable at point x_1 , $\partial\phi[x_1]$ is a closed interval: $\partial\phi[x_1] = [\phi'(x_1^-), \phi'(x_1^+)]$.

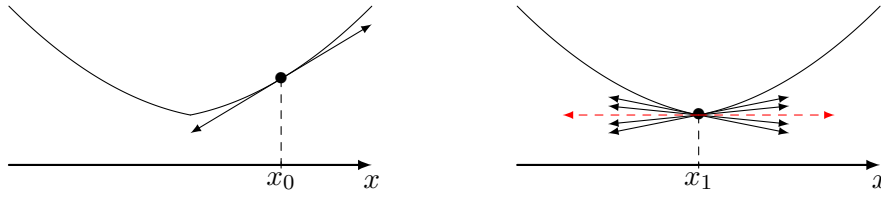


Fig. 4.8: Subdifferential. Left: the function is differentiable at point x_0 . Right: the function is not differentiable at point x_1 .

For example, if $\text{abs} : \mathbb{R} \rightarrow \mathbb{R}$ is the absolute value, $\text{abs}(x) = |x|$, then

$$\partial \text{abs}[x] \underset{x>0}{=} \{1\}, \quad \partial \text{abs}[x] \underset{x<0}{=} \{-1\}, \quad \text{and} \quad \partial \text{abs}[0] = [-1, 1].$$

Note that, whatever is the dimension, a function $\phi : \mathbb{R}^n \rightarrow \mathbb{R}$ is differentiable at \mathbf{x}_0 if and only if the set $\partial\phi[\mathbf{x}_0]$ contains only one point. In that case, this point is the gradient of ϕ at \mathbf{x}_0 . Then we have:

$$\phi \text{ differentiable at } \mathbf{x}_0 \implies \partial\phi[\mathbf{x}_0] = \{\nabla\phi(\mathbf{x}_0)\}.$$

Optimality conditions and Lagrange multipliers for non-differentiable functions.

The notion of subdifferential allows to generalize optimality conditions for non-differentiable functions. Indeed, as illustrated by the red dashed slope on figure 4.8, if ϕ is convex we have

$$\mathbf{x} \text{ is a minimum of } \phi \iff 0 \in \partial\phi[\mathbf{x}].$$

In case ϕ is differentiable, we find the usual optimality condition for convex functions: \mathbf{x} is a minimum of ϕ if and only if $\nabla\phi(\mathbf{x}) = 0$.

Another generalization of optimality condition, that will be useful in the following, is the generalization to a non-differentiable constraint of the Kuhn Tucker optimality condition stated in the equation (4.10). Let us consider the minimization problem

$$\min_{\mathbf{x} \in K} J(\mathbf{x}), \quad K = \{\mathbf{x} \in \mathbb{R}^n, g(\mathbf{x}) \leq 0\},$$

where $J : \mathbb{R}^n \rightarrow \mathbb{R}$ is a differentiable convex function and $g : \mathbb{R}^n \rightarrow \mathbb{R}$ is convex. Then, if the constraint at point \mathbf{x} is *qualified* (see below), \mathbf{x} is a minimum of J on K if and only

if there exists a Lagrange multiplier λ such that the following Kuhn Tucker optimality condition is verified [HL93, Thm. 2.1.4 p. 305]:

$$\begin{aligned} \nabla J(\mathbf{x}) &\in -\lambda \partial g[\mathbf{x}], \\ g(\mathbf{x}) &\leq 0, \quad \lambda \geq 0, \quad g(\mathbf{x})\lambda = 0. \end{aligned} \quad (4.19)$$

As for the differentiable case, the qualification of the constraint is needed to prove the existence of the Lagrange multipliers when \mathbf{x} is a minimum (it is not necessary for the reverse implication, which follows from the convexity assumptions). In our case, we can use the Slater qualification assumption saying that, if g is not affine, one has to check that there exists a point \mathbf{x}_0 in K for which the constraint is strictly satisfied:

$$\exists \mathbf{x}_0 \in K \text{ such that } g(\mathbf{x}_0) < 0 \quad (\text{Slater qualification condition}) \quad (4.20)$$

A useful example.

Let us consider an example that will prove useful in the following. We denote by P the projection onto a plane Π in dimension 3 and consider the following function

$$\begin{aligned} h : \mathbb{R}^3 &\rightarrow \mathbb{R} \\ \mathbf{v} &\rightarrow |P\mathbf{v}|. \end{aligned}$$

Let us prove that

$$|P\mathbf{v}| \neq 0 \implies \partial h[\mathbf{v}] = \left\{ \frac{P\mathbf{v}}{|P\mathbf{v}|} \right\}, \quad (4.21)$$

$$|P\mathbf{v}| = 0 \implies \partial h[\mathbf{v}] = \left\{ \mathbf{w} \in \mathbb{R}^3 \text{ s.t. } \mathbf{w} \in \Pi \text{ and } |\mathbf{w}| \leq 1 \right\}. \quad (4.22)$$

- In case $|P\mathbf{v}| \neq 0$, h is differentiable so that $\partial h[\mathbf{v}] = \{\nabla h(\mathbf{v})\}$. To compute the gradient of h , we simply write, using a Taylor expansion,

$$h(\mathbf{v} + \epsilon\mathbf{w}) = |P(\mathbf{v} + \epsilon\mathbf{w})| = |P\mathbf{v} + \epsilon P\mathbf{w}| = h(\mathbf{v}) + \epsilon \frac{P\mathbf{v}}{|P\mathbf{v}|} \cdot P\mathbf{w} + o(\epsilon^2).$$

It remains to remark that, since $P\mathbf{w} - \mathbf{w} \perp \Pi$ and $P\mathbf{v} \in \Pi$, we have $\frac{P\mathbf{v}}{|P\mathbf{v}|} \cdot P\mathbf{w} = \frac{P\mathbf{v}}{|P\mathbf{v}|} \cdot \mathbf{w}$ so that

$$h(\mathbf{v} + \epsilon\mathbf{w}) = h(\mathbf{v}) + \epsilon \frac{P\mathbf{v}}{|P\mathbf{v}|} \cdot \mathbf{w} + o(\epsilon^2).$$

which concludes the proof of (4.21).

- In case $|P\mathbf{v}| = 0$, h is no more differentiable at point \mathbf{v} . Let us first prove that

$$\partial h[\mathbf{v}] \subset \left\{ \mathbf{w} \in \mathbb{R}^3 \text{ s.t. } \mathbf{w} \in \Pi \text{ and } |\mathbf{w}| \leq 1 \right\}.$$

So let $\mathbf{w} \in \partial h[\mathbf{v}]$. First, we have $\mathbf{w} \in \Pi$. Indeed, if \mathbf{n} is the normal to Π , we consider $\hat{\mathbf{v}}_\lambda = \mathbf{v} + \lambda\mathbf{n}$. Since $\mathbf{n} \perp \Pi$, $h(\hat{\mathbf{v}}_\lambda) = |P(\mathbf{v} + \lambda\mathbf{n})| = |P(\mathbf{v})| = h(\mathbf{v})$. Then, from $\mathbf{w} \in \partial h[\mathbf{v}]$, we obtain

$$\forall \lambda \in \mathbb{R}, \quad h(\mathbf{v}) = h(\hat{\mathbf{v}}_\lambda) \geq h(\mathbf{v}) + \mathbf{w} \cdot (\hat{\mathbf{v}}_\lambda - \mathbf{v}) = h(\mathbf{v}) + \lambda\mathbf{w} \cdot \mathbf{n},$$

and this cannot be true for any $\lambda \in \mathbb{R}$ unless $\mathbf{w} \cdot \mathbf{n} = 0$ i.e. $\mathbf{w} \in \Pi$.

Let us now prove that $|\mathbf{w}| \leq 1$. To do so, we consider $\hat{\mathbf{v}} = \mathbf{v} + \mathbf{w}$. Using on the one hand that $P\mathbf{v} = 0$ and on the other hand that $P\mathbf{w} = \mathbf{w}$ (since $\mathbf{w} \in \Pi$), we obtain

$$|\mathbf{w}| = |P(\mathbf{v} + \mathbf{w})| = h(\hat{\mathbf{v}}) \geq h(\mathbf{v}) + \mathbf{w} \cdot (\hat{\mathbf{v}} - \mathbf{v}) = \mathbf{w} \cdot (\hat{\mathbf{v}} - \mathbf{v}) = |\mathbf{w}|^2,$$

so that $|\mathbf{w}| \leq 1$ as expected.

- In now remains to prove the reverse inclusion when $|P\mathbf{v}| = 0$. Suppose that $\mathbf{w} \in \Pi$ and $|\mathbf{w}| \leq 1$. In that case, for all $\hat{\mathbf{v}} \in \mathbb{R}^3$ we have

$$h(\mathbf{v}) + \mathbf{w} \cdot (\hat{\mathbf{v}} - \mathbf{v}) \underset{P\mathbf{v}=0}{=} \mathbf{w} \cdot (\hat{\mathbf{v}} - \mathbf{v}) \underset{\mathbf{w} \in \Pi}{=} \mathbf{w} \cdot (P\hat{\mathbf{v}} - P\mathbf{v}) \underset{P\mathbf{v}=0}{=} \mathbf{w} \cdot P\hat{\mathbf{v}} \underset{|\mathbf{w}| \leq 1}{\leq} |P\hat{\mathbf{v}}| = h(\hat{\mathbf{v}}),$$

which proves that $\mathbf{w} \in \partial h[\mathbf{v}]$.

To finish with the computations of subdifferentials, let us consider

$$h_A : \mathbb{R}^n \rightarrow \mathbb{R}, \quad h_A(\mathbf{u}) = h(A\mathbf{u}) = |PA\mathbf{u}|,$$

where $A : \mathbb{R}^n \rightarrow \mathbb{R}^3$ linear. The rule for pre-composition with a linear mapping [HL93, Thm. 4.2.1 p. 263] gives $\partial h_A(\mathbf{u}) = A^T \partial h(A\mathbf{u})$ so that

$$\begin{aligned} |PA\mathbf{u}| \neq 0 &\implies \partial h_A[\mathbf{u}] = \left\{ A^T \frac{PA\mathbf{u}}{|PA\mathbf{u}|} \right\}, \\ |PA\mathbf{u}| = 0 &\implies \partial h_A[\mathbf{u}] = \left\{ A^T \mathbf{w}, \mathbf{w} \in \mathbb{R}^3 \text{ s.t. } \mathbf{w} \in \Pi \text{ and } |\mathbf{w}| \leq 1 \right\}. \end{aligned} \tag{4.23}$$

▷ **Time stepping scheme based on convex optimization**

Now, in the spirit of [Ani06; TNA08], we can state the minimization problem we propose to solve at each time step. With evident notation, we search for the generalized velocity \mathbf{u}^{k+1} , solution to

$$\min_{\mathbf{u} \in K_\mu} J(\mathbf{u}) \quad (4.24)$$

$$J(\mathbf{u}) = \frac{1}{2} \left\| \mathbf{u} - \mathbf{U}^{k+1} \right\|_M, \quad \mathbf{U}^{k+1} = \mathbf{u}^k + \Delta t M^{-1} \mathbf{F}^{ext},$$

$$K_\mu = \left\{ \mathbf{u} = (\mathbf{v}, \boldsymbol{\omega}) \in \mathbb{R}^6, D(\mathbf{c}^k) + \Delta t \nabla_{\mathbf{c}} D(\mathbf{c}^k) \cdot \mathbf{v} \geq \mu \Delta t |P^k A^k \mathbf{u}| \right\}.$$

Let us first notice that this algorithm provides feasible configurations: we have

$$D(\mathbf{c}^{k+1}) \geq D(\mathbf{c}^k) + \Delta t \nabla_{\mathbf{c}} D(\mathbf{c}^k) \cdot \mathbf{v}^{k+1} \geq \mu \Delta t |P^k A^k \mathbf{u}^{k+1}|,$$

which is non-negative and may now be strictly positive. The constraint is over-imposed, especially when the tangential velocity is high.

The main advantage of this scheme, compared to the linear complementarity problem (4.18), is that the constraint for variable \mathbf{u} has been "convexified": the time sub-problem is a conic constrained optimisation problem. This allows the use of existing and convergent solvers to compute the velocity at each time step.

Using the framework of subdifferentials, we can check that the corresponding optimality conditions can be seen as a discretization of the continuous frictional model (4.12-4.17). To do so, we rewrite the discrete constraint set as

$$K_\mu = \left\{ \mathbf{u} = (\mathbf{v}, \boldsymbol{\omega}) \in \mathbb{R}^6, g(\mathbf{u}) \leq 0 \right\}, \quad g(\mathbf{u}) = -D(\mathbf{c}^k) - \Delta t \nabla_{\mathbf{c}} D(\mathbf{c}^k) \cdot \mathbf{v} + \mu \Delta t |P^k A^k \mathbf{u}|.$$

Then, under the condition that the constraint is qualified, there exists a Lagrange multiplier $f_n \in \mathbb{R}$ such that (see (4.19)):

$$\nabla J(\mathbf{u}) \in -f_n \partial g[\mathbf{u}], \quad g(\mathbf{u}) \leq 0, \quad f_n \geq 0, \quad g(\mathbf{u}) f_n = 0. \quad (4.25)$$

The aforementioned qualification of the constraint can be checked easily in the present situation. It amounts to show that Slater condition (4.20) is verified. To do so, we can consider for example the velocity vector $\mathbf{u}_0 = (\epsilon \mathbf{n}^k, 0)$ with $\epsilon > 0$ which satisfies $g(\mathbf{u}_0) < 0$ since the configuration at time k is feasible.

From (4.23), together with $\nabla_c D(\mathbf{c}^k) = \mathbf{n}^k$, we have

$$\begin{aligned} \text{If } P^k A^k \mathbf{u} \neq 0, \quad \partial g[\mathbf{u}] &= \left\{ \Delta t A^{k,T} \left(-\mathbf{n}^k + \mu \frac{P^k A^k \mathbf{u}}{|P^k A^k \mathbf{u}|} \right) \right\}, \\ \text{If } P^k A^k \mathbf{u} = 0, \quad \partial g[\mathbf{u}] &= \left\{ \Delta t A^{k,T} \left(-\mathbf{n}^k + \mu \mathbf{w} \right) / \mathbf{w} \in \Pi^k \text{ and } |\mathbf{w}| \leq 1 \right\}, \end{aligned}$$

where Π^k is the tangent plane at step k . From this, the optimality condition (4.25) can be written as

$$\begin{aligned} M \frac{\mathbf{u}^{k+1} - \mathbf{u}^k}{\Delta t} &= \mathbf{F}^{ext} + A^{k,T} (f_n \mathbf{n}^k - \mu f_n \mathbf{w}), \\ f_n \geq 0, \quad g(\mathbf{u}^{k+1}) &\leq 0, \quad f_n g(\mathbf{u}^{k+1}) = 0, \\ \text{If } P^k A^k \mathbf{u}^{k+1} \neq 0 \text{ (sliding motion),} \quad \mathbf{w} &= \frac{P^k A^k \mathbf{u}^{k+1}}{|P^k A^k \mathbf{u}^{k+1}|}, \\ \text{If } P^k A^k \mathbf{u}^{k+1} = 0 \text{ (no slip) ,} \quad \mathbf{w} &\in \Pi^k \text{ and } |\mathbf{w}| \leq 1. \end{aligned}$$

Setting the tangential force as $\mathbf{f}_t = -\mu f_n \mathbf{w}$, we finally obtain that \mathbf{u}^{k+1} is solution to the discrete problem

$$\begin{aligned} M \frac{\mathbf{u}^{k+1} - \mathbf{u}^k}{\Delta t} &= \mathbf{F}^{ext} + A^{k,T} (f_n \mathbf{n}^k + \mathbf{f}_t), \\ f_n \geq 0, \quad g(\mathbf{u}^{k+1}) &\leq 0, \quad f_n g(\mathbf{u}^{k+1}) = 0, \\ \text{If } P^k A^k \mathbf{u}^{k+1} \neq 0 \text{ (sliding motion),} \quad \mathbf{f}_t &= -\mu f_n \frac{P^k A^k \mathbf{u}^{k+1}}{|P^k A^k \mathbf{u}^{k+1}|}, \\ \text{If } P^k A^k \mathbf{u}^{k+1} = 0 \text{ (no slip) ,} \quad |\mathbf{f}_t| &\leq \mu f_n, \end{aligned}$$

which is a (formal) discretization of the continuous frictional problem (4.12-4.17).

► Multiparticle implementation, application to granular collapse on erodible beds

The arguments developed in the previous section for the toy model can be generalized to granular systems composed of spherical particles. Hugo Martin implemented the corresponding algorithm using Mosek optimization software [Mos] to solve the conic minimization problem at each time step.

As already said, the convex problem has been obtained to the price of a "convexification" of the normal constraint

$$D(\mathbf{c}^k) + \Delta t \nabla_{\mathbf{c}} D(\mathbf{c}^k) \cdot \mathbf{v}^{k+1} \geq \mu \Delta t |P^k A^k \mathbf{u}^{k+1}|,$$

that can over-estimate the non-overlapping constraint, especially in case of high tangential velocities. Since Hugo Martin was interested in granular collapse on erodible beds, a 2-dimensional simulation of column collapse has been achieved and compared to results obtained in [SH05]. In that article, the authors use the natural Euler-based scheme (4.18) for which the non-interpenetration constraint is $\nabla D(\mathbf{c}^k) \cdot \mathbf{v}^{k+1} \geq 0$ if $D(\mathbf{c}^k) = 0$. We observed that, in that case of interest, the results of the two codes match: the modification of the normal constraint does not influence the results. A study of the behaviour of the algorithm as a function of the time step and the Mosek stopping parameters was also carried out.

Hugo Martin then carried out several studies of granular collapse: comparisons with experiments with a special attention to the flowing/static interface evolution, study of the wave motion that appears at the beginning of the flow and exploration of the influence of the compaction in a 3D configuration. A snapshot of a simulation of granular collapse on an erodible bed is shown on figure 4.9.

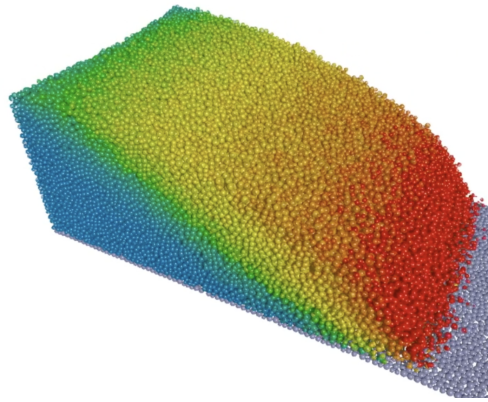


Fig. 4.9: Granular collapse on erodible beds. Snapshot of a 3d simulation with 112 000 spheres. The particles are colored according to their velocity (from blue for minimum velocity to red for maximum velocity).

To finish this chapter, let us say a word about a strategy that has been proposed in [Aca+11] to avoid the potential over-estimation of the non-overlapping constraint,

while ensuring the convergence of each time step iterations. In that article, the authors fix a parameter s and consider \mathbf{u}_s , solution to the minimisation problem with the following constraint:

$$\nabla_{\mathbf{c}} D(\mathbf{c}^k) \cdot \mathbf{v}^{k+1} \geq \mu |P^k A^k \mathbf{u}^{k+1}| - \mu \Delta t s \quad \text{if} \quad D(\mathbf{c}^k) = 0.$$

They propose to compute the solution to the frictional contact problem with the normal constraint

$$\nabla_{\mathbf{c}} D(\mathbf{c}^k) \cdot \mathbf{v}^{k+1} \geq 0 \quad \text{if} \quad D(\mathbf{c}^k) = 0.$$

as a fixed point of $F(s) = |P^k A^k \mathbf{u}_s^{k+1}|$. They prove that the fixed point iterations for F converge which ensures the convergence of their numerical algorithm at each time step. Doing so, they manage to obtain a solution verifying the natural discretization of the non-interpenetration constraint. This is done to the price of an unknown number of iteration of the fixed point algorithm at each time step, each of these requiring to solve a conic minimization problem similar to ours.

On-going work - Prospects

In this chapter we have presented algorithms for the simulation of granular materials. A single convex optimisation problem has to be solved at each iteration, under either affine or conical constraint, depending on whether or not the grains experience friction. The algorithms were validated by numerical tests for spherical particles and comparisons with experiments. They have proven to be effective in performing numerical rheological studies. Much remains to be done in several directions:

- From the **theoretical point of view**, we have shown, with Frédéric Bernicot, the convergence of the frictionless scheme. The first tests carried out with the scheme taking friction into account are very encouraging. Thus, comparisons with experiments or with other codes are positive. Moreover, the scheme allows rheological studies to be carried out for large numbers of particles and shows good stability behaviour. These results make us want to go further in its analysis. Results in this direction have been shown in [Ani06] for a similar algorithm based on a discretised Coulomb cone and leading to linear constraints. These results need to be extended to the conic framework. Another issue is to understand the link between the velocity

minimisation problem and energy dissipation models. The link between the two can be made by studying the dual problem to the minimisation problem.

- We are currently working on including **friction and non-spherical particles in the code SCoPI**. From a theoretical point of view, the algorithms described in this chapter extend to any particle shape, provided that we can find the points realising the distance. To do this, we write the equations characterising these points (such as the collinearity of the normals) and solve them using an iterative algorithm. We have chosen to focus on the family of **super-ellipsoids**. These are shapes for which there is a parametrisation of the surface, which provides a generic formula for the computation of normals for example. We only consider regular shapes of this family (twice derivable boundary). This provides sufficiently varied shapes for the applications we have in mind (see figure 4.10).

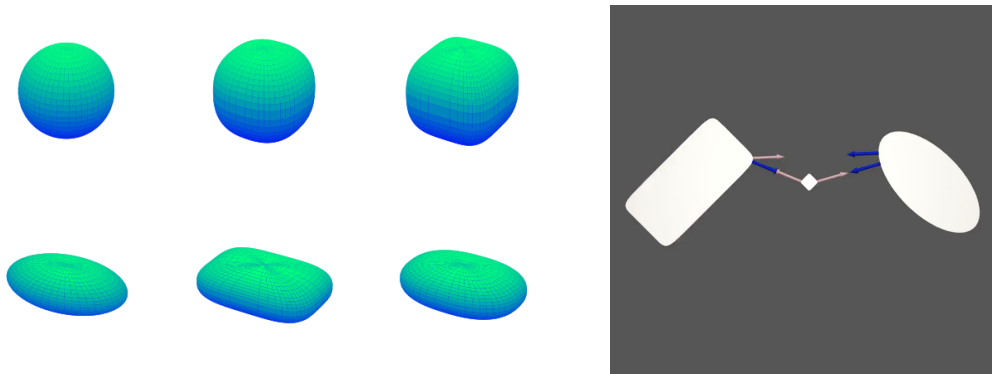


Fig. 4.10: Super-ellipsoids. Some 3d examples of available regular shapes (left) and a 2d configuration with normals at the points realising the distances (right).

- The extension of the code to non-spherical particles and to the consideration of friction opens the way to numerous **rheological studies of dry granular materials**. The main objective is to provide a code to make the link between the microscopic configurations and the macroscopic behaviour of granular media. A better understanding of the different microscopic physical quantities involved would allow to answer questions both from physicists and mathematicians, such as well-posedness of the macroscopic models. For example, an interesting study would be that of understanding the length scales of the chains of forces that are involved in non-local rheological models. The simulations we achieved of the moving sphere into a granular medium have shown that the code could estimate this parameter. Furthermore,

the behaviour of granular media composed of non-spherical particles is still poorly understood. The inclusion of non-spherical particles in the code should help to answer many open questions.

- Within the framework of the **ANR RheoSUNN** project that I am coordinating, we plan to **couple the new developments of SCoPI with the fluid solver CAFES** [FG12]. This is the goal of H el ene Bloch, a **post-doctoral fellow funded by RheoSUNN** from October 2021. It will allow to study the rheology of suspensions composed of non-monodisperse spheres or non-spherical grains. Furthermore, the algorithm we have developed for friction fits into the same framework as the gluey contact model I developed in my PhD thesis [6]. The mixing of the two models in SCoPI will provide a **contact algorithm that takes into account both friction and lubrication by an implicit and stable method**. Dealing with these two short-range phenomena was essential to meet the current challenges in suspension rheology.

References

- [ABH18] V. Acary, M. Brémond, and O. Huber. “On Solving Contact Problems with Coulomb Friction: Formulations and Numerical Comparisons”. In: *Advanced Topics in Nonsmooth Dynamics: Transactions of the European Network for Nonsmooth Dynamics*. Ed. by R. Leine, V. Acary, and O. Brüls. Springer International Publishing, 2018, pp. 375–457 (cit. on p. 108).
- [Aca+11] V. Acary, F. Cadoux, C. Lemaréchal, and J. Malick. “A formulation of the linear discrete Coulomb friction problem via convex optimization”. In: *ZAMM - Journal of Applied Mathematics and Mechanics* 91.2 (2011), pp. 155–175 (cit. on p. 114).
- [Ani06] M. Anitescu. “Optimization-based simulation of nonsmooth rigid multibody dynamics”. In: *Mathematical Programming* 105.1 (2006), pp. 113–143 (cit. on pp. 112, 115).
- [AP97] M. Anitescu and F. A. Potra. “Formulating Dynamic Multi-Rigid-Body Contact Problems with Friction as Solvable Linear Complementarity Problems”. In: *Nonlinear Dynamics* 14.3 (1997), pp. 231–247 (cit. on p. 108).
- [Cor+21] E. Corral, R. G. Moreno, M. J. G. García, and C. Castejón. “Nonlinear phenomena of contact in multibody systems dynamics: a review”. In: *Nonlinear Dynamics* (2021) (cit. on p. 93).
- [CS79] P. A. Cundall and O. D. L. Strack. “A discrete numerical model for granular assemblies”. In: *Géotechnique* 29.1 (1979). Publisher: ICE Publishing, pp. 47–65 (cit. on p. 93).
- [DJ06] F. Dubois and M. Jean. “The non smooth contact dynamic method: recent LMGC90 software developments and application”. In: *Analysis and Simulation of Contact Problems*. Ed. by Peter Wriggers and Udo Nackenhorst. Lecture Notes in Applied and Computational Mechanics. Berlin, Heidelberg: Springer, 2006, pp. 375–378 (cit. on p. 93).
- [DR14] F. Dubois and M. Renouf. *LMGC90*. 2014. URL: https://git-xen.lmgc.univ-montp2.fr/lmgc90/lmgc90_user/-/wikis/home (visited on Sept. 1, 2021) (cit. on p. 93).
- [DM07] R. Dzonou and M. D. P. Monteiro Marques. “A sweeping process approach to inelastic contact problems with general inertia operators”. In: *European Journal of Mechanics - A/Solids* 26.3 (2007), pp. 474–490 (cit. on p. 100).
- [DMP09] R. Dzonou, M. D. P. Monteiro Marques, and L. Paoli. “A convergence result for a vibro-impact problem with a general inertia operator”. In: *Nonlinear Dynamics* 58.1-2 (2009), pp. 361–384 (cit. on p. 100).
- [FG12] B. Fabrèges and L. Gouarin. *CAFES (Cartesian Finite Element Solver)*. 2012. URL: <https://github.com/gouarin/cafes> (visited on Sept. 1, 2021) (cit. on p. 117).

- [HL93] J-B. Hiriart-Urruty and C. Lemarechal. *Convex Analysis and Minimization Algorithms I: Fundamentals*. Grundlehren der mathematischen Wissenschaften, Convex Analysis and Minimization Algorithms. Berlin Heidelberg: Springer-Verlag, 1993 (cit. on pp. 108, 110, 111).
- [Jea99] M. Jean. “The non-smooth contact dynamics method”. In: *Computer Methods in Applied Mechanics and Engineering* 177.3 (1999), pp. 235–257 (cit. on pp. 93, 97).
- [JM92] M. Jean and J. J. Moreau. “Unilaterality and dry friction in the dynamics of rigid body collections”. In: *1st Contact Mechanics International Symposium*. Lausanne, Switzerland, 1992, pp. 31–48 (cit. on pp. 93, 97).
- [Lud08] S. Luding. “Introduction to discrete element methods”. In: *European Journal of Environmental and Civil Engineering* 12.7-8 (2008), pp. 785–826 (cit. on p. 93).
- [Mau06] B. Maury. “A time-stepping scheme for inelastic collisions”. In: *Numerische Mathematik* 102.4 (2006), pp. 649–679 (cit. on pp. 94, 98–101, 108).
- [Mon13] M. D. P. Monteiro Marques. *Differential Inclusions in Nonsmooth Mechanical Problems: Shocks and Dry Friction*. Birkhäuser, 2013 (cit. on p. 100).
- [MP06] M. D. P. Monteiro Marques and L. Paoli. “An Existence Result in Non-Smooth Dynamics”. In: *Nonsmooth Mechanics and Analysis*. Ed. by P. Alart, O. Maisonneuve, and R. T. Rockafellar. Advances in Mechanics and Mathematics. Boston, MA: Springer US, 2006, pp. 279–288 (cit. on p. 100).
- [Mor88] J. J. Moreau. “Unilateral Contact and Dry Friction in Finite Freedom Dynamics”. In: *Nonsmooth Mechanics and Applications*. Ed. by J. J. Moreau and P. D. Panagiotopoulos. International Centre for Mechanical Sciences. Vienna: Springer, 1988, pp. 1–82 (cit. on p. 93).
- [Mor70] J.-J. Moreau. “Convexité et frottement”. In: *Séminaire sur la convexité et ses applications*. Dpt Informatique, Université de Montréal, 1970 (cit. on p. 93).
- [Mor66] J.-J. Moreau. “Fonctionnelles convexes”. fr. In: *Séminaire Jean Leray*. Vol. 2. Collège de France, Paris, 1966, p. 110 (cit. on p. 93).
- [Mor99] J.J. Moreau. “Numerical aspects of the sweeping process”. In: *Computer Methods in Applied Mechanics and Engineering* 177.3-4 (1999), pp. 329–349 (cit. on p. 93).
- [Mos] Mosek. *Mosek website*. URL: <https://www.mosek.com/> (visited on Sept. 1, 2021) (cit. on p. 113).
- [Pao05] L. Paoli. “An existence result for non-smooth vibro-impact problems”. In: *Journal of Differential Equations* 211.2 (2005), pp. 247–281 (cit. on p. 100).
- [Pao10] L. Paoli. “Time-Stepping Approximation of Rigid-Body Dynamics with Perfect Unilateral Constraints. I and II”. In: *Archive for Rational Mechanics and Analysis* 198.2 (2010), pp. 457–503 (cit. on pp. 100, 101).

- [PS02] L. Paoli and M. Schatzman. “A Numerical Scheme for Impact Problems I and II: The One-Dimensional Case”. In: *SIAM Journal on Numerical Analysis* 40.2 (2002), pp. 702–733 (cit. on p. 100).
- [Rak+19] Andriarimina Daniel Rakotonirina, Jean-Yves Deleenne, Farhang Radjai, and Anthony Wachs. “Grains3D, a flexible DEM approach for particles of arbitrary convex shape—Part III: extension to non-convex particles modelled as glued convex particles”. In: *Computational Particle Mechanics* 6.1 (2019), pp. 55–84 (cit. on p. 93).
- [RW18] Andriarimina Daniel Rakotonirina and Anthony Wachs. “Grains3D, a flexible DEM approach for particles of arbitrary convex shape - Part II: Parallel implementation and scalable performance”. In: *Powder Technology* 324 (2018), pp. 18–35 (cit. on p. 93).
- [Sch01] M. Schatzman. “Penalty Method for Impact in Generalized Coordinates”. In: *Philosophical Transactions: Mathematical, Physical and Engineering Sciences* 359.1789 (2001). Publisher: The Royal Society, pp. 2429–2446 (cit. on p. 100).
- [SH05] L. Staron and E. J. Hinch. “Study of the collapse of granular columns using two-dimensional discrete-grain simulation”. In: *Journal of Fluid Mechanics* 545 (2005), pp. 1–27 (cit. on p. 114).
- [ST96] D. E. Stewart and J. C. Trinkle. “An Implicit Time-Stepping Scheme for Rigid Body Dynamics with Inelastic Collisions and Coulomb Friction”. In: *International Journal for Numerical Methods in Engineering* 39.15 (1996), pp. 2673–2691 (cit. on p. 107).
- [TNA08] A Tasora, D Negrut, and M Anitescu. “Large-scale parallel multi-body dynamics with frictional contact on the graphical processing unit”. In: *Proceedings of the Institution of Mechanical Engineers, Part K: Journal of Multi-body Dynamics* 222.4 (2008), pp. 315–326 (cit. on p. 112).
- [Ven11] J. Venel. “A numerical scheme for a class of sweeping processes”. In: *Numerische Mathematik* 118.2 (2011), pp. 367–400 (cit. on p. 101).
- [Wac+12] Anthony Wachs, Laurence Girolami, Guillaume Vinay, and Gilles Ferrer. “Grains3D, a flexible DEM approach for particles of arbitrary convex shape — Part I: Numerical model and validations”. In: *Powder Technology* 224 (2012), pp. 374–389 (cit. on p. 93).

Stokesian swimmers.

Collaborators: François Alouges (CMAP, Palaiseau) - Antonio Desimone (SISSA, Trieste) - Luca Heltai (SISSA, Trieste) - Benoît Merlet (Labo. Paul Painlevé, Lille)

Related publications:

[17] *Optimal Strokes for Low Reynolds Number Swimmers: An Example.* With F. Alouges and A. DeSimone. In: *Journal of Nonlinear Science* 18.3 (2008), pp. 277–302

[18] *Biological Fluid Dynamics: Swimming at low Reynolds numbers.* With F. Alouges and A. DeSimone. In: *Encyclopedia of complexity and systems science.* Ed. by Robert A Meyers. Springer, (2009)

[19] *Optimal strokes for axisymmetric microswimmers.* With F. Alouges and A. DeSimone. In: *The European Physical Journal E* 28.3 (2009), pp. 279–284

[20] *A stokesian submarine.* With Benoît Merlet. In: *ESAIM: Proceedings* 28 (2009). Ed. by M. Ismail, B. Maury, and J.-F. Gerbeau, pp. 150–161

[21] *Optimally swimming Stokesian robots.* With François Alouges, Antonio DeSimone, Luca Heltai, and Benoît Merlet. In: *Discrete & Continuous Dynamical Systems - B* 18.5 (2013), pp. 1189–1215

Expected applications of the results presented in this chapter:

- *Micro-swimmers: General control framework to study micro-robot swimmers. Extension to more general swimmers (e.g. deformable swimmers).*
-

Active suspensions, consisting of **swimmers in a Stokes fluid**, is a growing field of research. To better understand these suspensions, it is natural to try to investigate the behaviour of individual swimmers. Let us recall that, as stated in the introduction, swimming at low Reynolds number is a complex phenomenon that is still poorly understood. When studying such system, two questions arise: can a swimmer swim and if so, how can he do so with the least possible energy expenditure?

In the series of articles [17,18,20,21], we studied 3 self-propelled stokesian robots composed of assemblies of balls, moving respectively in dimension 1, 2 and 3. Swimming is rephrased in term of **controllability**: the displacement being given, can we find a cyclic shape change (the control) leading to this displacement? Once controllability is known, i.e., it is shown that it is possible to go from A to B, one can ask the question of how to go from A to B at minimal energetic cost. This is a question of **optimal control**. In [21], we end up proposing a general framework, covering the 3 swimmers, and we show that each of them can swim, i.e. control its position, as well as its orientation in 2d and 3d. The question of optimal swimming is also addressed and solved using numerical simulations. A similar framework also allowed us to study general axisymmetric micro-swimmers moving along a straight line in [19].

In the next section, I present the 3 stokesian robots we considered and describe the main ideas leading to the controllability result.

5.1 Stokesian robots.

The swimmers we focus on are composed of N non-intersecting balls centered at $(\mathbf{x}_i)_{1 \leq i \leq N}$ and the configurations are described by two sets of variables:

- the **shape variables**, denoted by $\xi \in \mathcal{S}$, where \mathcal{S} is an open connected subset of \mathbb{R}^M
- the **position variables**, denoted by $p \in \mathcal{P}$, which describes the global position and orientation in space of the swimmer.

The configuration of the swimmer is entirely determined by the data of couple (ξ, p) . The swimming problem comes back to find a periodic path in the shape domain $t \rightarrow \xi(t)$ (the control) in order to achieve a given displacement Δp .

The three swimmers we consider are:

- **The three sphere swimmer of Najafi and Golestanian (3S).** It is composed of three spheres aligned along the x -axis, as depicted in figure 5.1. The shape variables

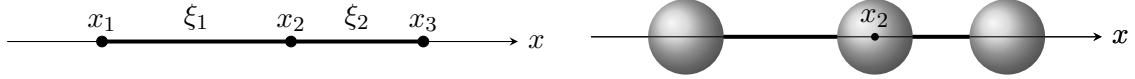


Fig. 5.1: The three sphere swimmer of Najafi and Golestanian (3S). Notation.

are $\xi = (\xi_1, \xi_2)$ the length of the arms and we choose to locate the position of the swimmer by that of its central sphere: $p = x_2$. The configuration \mathbf{x} of the swimmer can be expressed as a function of (ξ, p) :

$$x_1 = p - \xi_1, \quad x_2 = p, \quad x_3 = p + \xi_2.$$

- **The three sphere swimmer in a plane (3SP).** We consider a reference equilateral triangle (S_1, S_2, S_3) with center O in the horizontal plane such that $\text{dist}(O, S_i) = 1$. The swimmer is made of three spheres placed on the rays $[OS_i)$, as depicted in figure 5.2. The shape variables are the length of the arms: $\xi = (\xi_1, \xi_2, \xi_3)$ with $\text{dist}(O, \mathbf{x}_i) = \xi_i$. The position of the swimmer is described by a rigid displacement of the reference triangle. The coordinates of the center of the swimmer is $\mathbf{c} \in \mathbb{R}^3$ (but \mathbf{c} stays confined in the horizontal plane). Its orientation is given by the angle $\theta \in \mathbb{R}$ that one arm, say arm number 1, makes with a fixed direction, say (Ox) . The position variables are $p = (\mathbf{c}, \theta)$. Again, the configuration \mathbf{x} can be deduced from $(\xi, p) = (\xi, \mathbf{c}, \theta)$.
- **The four sphere swimmer (4S).** The last swimmer, depicted in figure 5.3, is the three-dimensional counterpart of the three sphere swimmer in the plane. It is now based on a reference tetrahedron. The position of the swimmer is described by: $p = (\mathbf{c}, \mathcal{R})$ where $\mathbf{c} \in \mathbb{R}^3$ is the center of the tetrahedron and $\mathcal{R} \in SO(3)$ its orientation. Its shape is given by the length of its four arms: $\xi = (\xi_1, \xi_2, \xi_3, \xi_4)$.

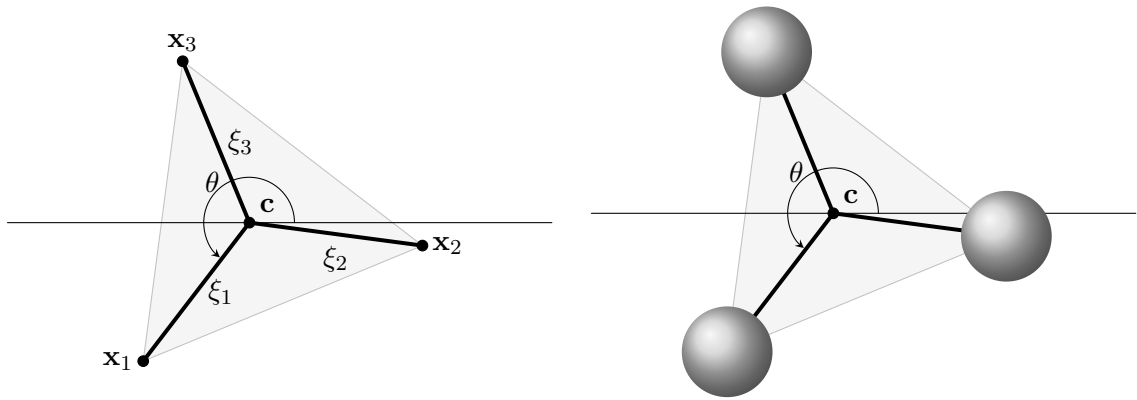


Fig. 5.2: The three sphere swimmer in a plane (3SP). Notation.

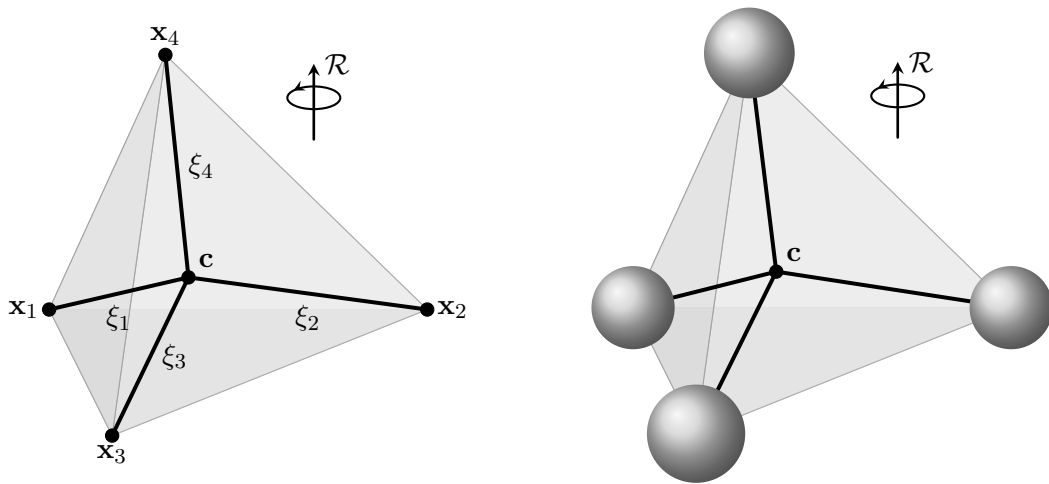


Fig. 5.3: The four sphere swimmer (4S). Notation.

▷ **The 3 sphere swimmer of Najafi and Golestanian (3S). [17-19]**

To make the general framework clearer, let us first present the computations for the three sphere swimmer of Najafi and Golestanian. It is the simplest of the three swimmers considered, has two controls $(\dot{\xi}_1, \dot{\xi}_2)$ and its position is given by $p = \mathbf{x}_2 \in \mathbb{R}$.

We denote by $\mathbf{U} = (u_1, u_2, u_3) = (\dot{x}_1, \dot{x}_2, \dot{x}_3)$ the balls' horizontal velocities and by (\mathbf{u}, p) the solution to the Stokes problem in the fluid domain Ω , with boundary condition $\mathbf{u} = u_i \mathbf{e}_x$ on ∂B_i . Due to the symmetry of the problem, the forces exerted by the fluid on the particles are along \mathbf{e}_x . We denote by $\mathbf{F} = (f_1, f_2, f_3) \in \mathbb{R}^3$ their horizontal components:

$$f_i = \left(\int_{\partial B_i} \sigma(\mathbf{u}, p) \mathbf{n} \right) \cdot \mathbf{e}_x \in \mathbb{R},$$

where $\sigma(\mathbf{u}, p) = \mu(\nabla \mathbf{u} + \nabla^T \mathbf{u}) - p \text{Id}$ is the corresponding stress tensor.

Dynamics. First, we write the dynamics of the swimmer: we express the rate of change of its position as a function of its shape. To do so, we use three fundamental properties of the micro-swimmer problem:

- *Linearity of Stokes equations.* From the linearity of Stokes equations, there exists a matrix R (the resistance matrix) such that

$$\mathbf{F} = R\mathbf{U}.$$

The resistance matrix R is symmetric, positive definite. Indeed, let us consider $\mathbf{V} = (v_1, v_2, v_3)$ and (\mathbf{v}, q) the corresponding solution to Stokes problem with boundary condition $\mathbf{v} = v_i \mathbf{e}_x$ on ∂B_i . We have

$$\mathbf{V}^T R\mathbf{U} = \mathbf{V}^T \mathbf{F} = \sum_i v_i f_i = \left(\sum_i v_i \int_{\partial B_i} \sigma(\mathbf{u}, p) \mathbf{n} \right) \cdot \mathbf{e}_x.$$

Now, we have

$$\begin{aligned} \left(\sum_i v_i \int_{\partial B_i} \sigma(\mathbf{u}, p) \mathbf{n} \right) \cdot \mathbf{e}_x &= \sum_i \int_{\partial B_i} v_i \mathbf{e}_x \cdot \sigma(\mathbf{u}, p) \mathbf{n} = \sum_i \int_{\partial B_i} \mathbf{v} \cdot \sigma(\mathbf{u}, p) \mathbf{n} \\ &= \int_{\partial \Omega} \mathbf{v} \cdot \sigma(\mathbf{u}, p) \mathbf{n} = 2\mu \int_{\Omega} D(\mathbf{u}) : D(\mathbf{v}), \end{aligned}$$

where the last equality results from an integration by part and $D(\mathbf{w}) = (\nabla \mathbf{w} + \nabla^T \mathbf{w})/2$ is the rate of strain tensor. So finally, the formula being symmetric with respect to (\mathbf{u}, \mathbf{v}) we obtain

$$\mathbf{V}^T R \mathbf{U} = \left(2\mu \int_{\Omega} D(\mathbf{u}) : D(\mathbf{v}) \right) = \mathbf{U}^T R \mathbf{V}$$

and matrix R is symmetric, definite positive.

- *Self propulsion.* The swimmer being self-propelled, the sum of the forces exerted by the fluid on the balls vanishes: $f_1 + f_2 + f_3 = 0$, which can be rewritten as

$$\mathbf{e}_1 \cdot \mathbf{F} = 0, \quad \text{where } \mathbf{e}_1 = (1, 1, 1).$$

- *Kinematics.* Finally, \mathbf{U} can be expressed as a linear function of \dot{p} and $\dot{\xi}$: $u_1 = \dot{p} - \dot{\xi}_1$, $u_2 = \dot{p}$, and $u_3 = \dot{p} + \dot{\xi}_2$, so that there is a matrix A such that

$$\mathbf{U} = \dot{p} \mathbf{e}_1 + A \dot{\xi}.$$

Finally, one obtains the following equation for \dot{p} :

$$0 = \mathbf{e}_1 \cdot \mathbf{F} = \mathbf{e}_1 \cdot R \mathbf{U} = \mathbf{e}_1 \cdot R (\dot{p} \mathbf{e}_1 + A \dot{\xi}) = (\mathbf{e}_1 \cdot R \mathbf{e}_1) \dot{p} + \mathbf{e}_1 \cdot R A \dot{\xi}.$$

The coefficient $\mathbf{e}_1 \cdot R \mathbf{e}_1$ is the drag force exerted on the swimmer corresponding to a rigid translation along Ox and does not vanish since the resistance matrix R is definite positive. This allows us to solve \dot{p} uniquely and linearly in terms of $\dot{\xi}$:

$$\dot{p} = V(\xi) \dot{\xi} \quad \text{with} \quad V(\xi) : \mathbb{R}^2 \mapsto \mathbb{R}. \quad (5.1)$$

We can decompose V as $V(\xi) \dot{\xi} = V_1(\xi) \dot{\xi}_1 + V_2(\xi) \dot{\xi}_2$ with $V_i(\xi) : \mathbb{R} \mapsto \mathbb{R}$ so that equation (5.1) can be rewritten as

$$\dot{p} = V_1(\xi) \dot{\xi}_1 + V_2(\xi) \dot{\xi}_2.$$

Note that the mapping $\xi \rightarrow V(\xi)$ is non linear. It is shape-dependent and encodes the hydrodynamics interactions between the swimmer and the surrounding fluid, due to shape changes at rate $\dot{\xi}$.

Swimming? So now, in view of equation (5.1) the question is to know whether the micro-robot can swim. That is, can we find periodic strokes on $[0, T]$ (i.e. periodic changes of shape $t \rightarrow \xi(t)$) such that the corresponding displacement $\Delta p = p(T) - p(0)$ is not zero and, better still, can we control this displacement? By controlling the displacement we mean, Δp being given, can we find a periodic control $t \rightarrow \xi(t)$ to achieve this displacement?

First, let us come back for a moment to the scallop theorem. In that case, the swimmer only has one control to swim in one dimension ($\xi \in \mathbb{R}$ and $V(\xi) : \mathbb{R} \mapsto \mathbb{R}$). Then, it is easy to see from (5.1) that a periodic stroke does not induce any displacement. Indeed, if $\Psi = \int V$ is a primitive of V , using the fact that $\xi(T) = \xi(0)$, we have

$$\Delta p = \int_0^T \dot{p}(t) dt = \int_0^T V(\xi(t)) \dot{\xi}(t) dt = \Psi(\xi(T)) - \Psi(\xi(0)) = 0.$$

So now, can the three sphere swimmer swim in one dimension, using its two controls? In view of (5.1), the rate of change of the position p is constrained to belong to a given tangent plane. In fact, the tangent plane depends on the shape ξ so that \dot{p} belongs to a distribution of tangent plane, varying with ξ . Is this dependence on ξ sufficient for p to reach any given position using a periodic change of shape? The answer to this question is not always positive. For example, as in the scallop case, if V is a gradient (if $\text{curl}V = 0$), the micro-robot cannot swim: there exists W such that $V = \nabla W$, then $p = W(\xi_1, \xi_2)$ and a periodic shape does not induce any displacement. In the general case, we have

$$\Delta p = \int_0^T V(\xi(t)) \dot{\xi}(t) dt = \int_{\omega} \text{curl}V,$$

where ω is the surface enclosed in the curve $t \rightarrow \xi(t)$ in the space of shapes and $\text{curl}V = \partial_{\xi_1} V_2 - \partial_{\xi_2} V_1$. Thus, the displacement induced by a periodic stroke is equal to the flux of $\text{curl}V$ through the surface ω . For example, if $\text{curl}V > 0$ everywhere, any periodic stroke will induce a displacement. The swimmer can also swim locally if its initial shape $\xi(0)$ is such that $\text{curl}V(\xi(0)) \neq 0$.

An affine control problem without drift. The good framework to answer the question of swimming is control theory. Let us denote by $X = (\xi, p) \in \mathbb{R}^3$ the pair composed of the shape and position variables. From the previous computations, we have

$$\dot{X} = \begin{pmatrix} \dot{\xi}_1 \\ \dot{\xi}_2 \\ \dot{p} \end{pmatrix} = \begin{pmatrix} 1 \\ 0 \\ V_1(\xi) \end{pmatrix} \dot{\xi}_1 + \begin{pmatrix} 0 \\ 1 \\ V_2(\xi) \end{pmatrix} \dot{\xi}_2.$$

We define

$$g_1(X) = \begin{pmatrix} 1 \\ 0 \\ V_1(\xi) \end{pmatrix}, \quad g_2(X) = \begin{pmatrix} 0 \\ 1 \\ V_2(\xi) \end{pmatrix},$$

so that X follows the following affine control problem without drift:

$$\dot{X} = \alpha_1(t)g_1(X) + \alpha_2(t)g_2(X), \tag{5.2}$$

where $\alpha_i(t) = \dot{\xi}_i(t)$, $i = 1, 2$ are the controls. Note that in our case, $g_i(X) = g_i(\xi, p) = g_i(\xi)$ only depend on ξ . The swimming problem in $[0, T]$ now reads:

- suppose the initial shape $\xi(0) = \xi_0$ and position $p(0) = p_0$ are given,
- suppose the final position $p(T) = p_T$ is given,
- does there exist controls $\alpha_1, \alpha_2 : [0, T] \mapsto \mathbb{R}$ such that

$$\begin{array}{l} \dot{X} = \alpha_1(t)g_1(X) + \alpha_2(t)g_2(X) \\ X(0) = (\xi_0, p_0) \end{array} \left| \implies X(T) = (\xi_0, p_T)? \right.$$

This is a well-known control problem. Suppose for example that X is solution to (5.2) and $X(0) = X_0$,

- if we choose $(\alpha_1, \alpha_2) \equiv (1, 0)$ on $[0, \epsilon]$ for a small value of ϵ , then

$$X(\epsilon) = X_0 + \epsilon g_1(X_0) + O(\epsilon^2).$$

- if we choose $(\alpha_1, \alpha_2) \equiv (0, 1)$ on $[0, \epsilon]$ for a small value of ϵ , then

$$X(\epsilon) = X_0 + \epsilon g_2(X_0) + O(\epsilon^2).$$

So we observe that the system can evolve, with well chosen controls, in directions that belong to the plane generated by $(g_1(X_0), g_2(X_0))$. The displacement proportional to the time ϵ . A plane being of dimension 2, this is of course not sufficient for X to be able to reach any point in a neighbourhood in \mathbb{R}^3 of X_0 . In fact, one can prove that the system can move in a third direction, independent of $(g_1(X_0), g_2(X_0))$. To do so, let us consider the following succession of controls:

$$\begin{aligned}(\alpha_1, \alpha_2) &\equiv (1, 0), & t \in [0, \epsilon] \\(\alpha_1, \alpha_2) &\equiv (0, 1), & t \in [\epsilon, 2\epsilon] \\(\alpha_1, \alpha_2) &\equiv (-1, 0), & t \in [2\epsilon, 3\epsilon] \\(\alpha_1, \alpha_2) &\equiv (0, -1), & t \in [3\epsilon, 4\epsilon]\end{aligned}$$

and let's proceed to Taylor's expansion again:

- First, $\dot{X} = g_1(X)$ for $t \in [0, \epsilon]$ so that

$$X(\epsilon) = X_0 + \epsilon g_1(X_0) + \frac{\epsilon^2}{2} \nabla g_1(X_0) g_1(X_0) + O(\epsilon^3).$$

- Then, $\dot{X} = g_2(X)$ for $t \in [\epsilon, 2\epsilon]$ so that

$$X(2\epsilon) = X(\epsilon) + \epsilon g_2(X(\epsilon)) + \frac{\epsilon^2}{2} \nabla g_2(X(\epsilon)) g_2(X(\epsilon)) + O(\epsilon^3).$$

and using the previous expansion for $X(\epsilon)$, together with further Taylor developments of g_1 and g_2 we obtain:

$$\begin{aligned}X(2\epsilon) &= X_0 + \epsilon [g_1(X_0) + g_2(X_0)] \\ &+ \frac{\epsilon^2}{2} [\nabla g_1(X_0) g_1(X_0) + \nabla g_2(X_0) g_2(X_0) + 2\nabla g_1(X_0) g_2(X_0)] + O(\epsilon^3).\end{aligned}$$

- We proceed that same way for $t \in [2\epsilon, 3\epsilon]$ where $\dot{X} = -g_1(X)$ to obtain

$$\begin{aligned}X(3\epsilon) &= X_0 + \epsilon g_2(X_0) \\ &+ \epsilon^2 [\nabla g_2(X_0) g_1(X_0) - \nabla g_1(X_0) g_2(X_0)] + \frac{\epsilon^2}{2} \nabla g_2(X_0) g_2(X_0) + O(\epsilon^3).\end{aligned}$$

- and finally, using $\dot{X} = -g_2(X)$ for $t \in [3\epsilon, 4\epsilon]$, we obtain

$$X(4\epsilon) = X_0 + \epsilon^2 [\nabla g_2(X_0)g_1(X_0) - \nabla g_1(X_0)g_2(X_0)] + O(\epsilon^3).$$

We thus obtain that the system can also evolve, with well chosen controls, in the direction of the so-called first order Lie-bracket of g_1 and g_2 : $[g_1, g_2](X_0) = \nabla g_2(X_0)g_1(X_0) - \nabla g_1(X_0)g_2(X_0)$. The displacement is now proportional to ϵ^2 .

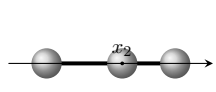
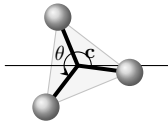
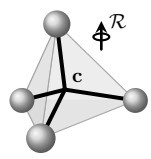
The question is to know whether this new direction $[g_1, g_2](X_0)$ will allow to move in the whole space \mathbb{R}^3 (i.e. to be controllable, to swim). As we will see in the following, the classical Chow's theorem says that the answer to this question is positive (at least locally), if the vectorial space generated by $(g_2(X_0), g_1(X_0), [g_1, g_2](X_0))$ has dimension 3. In that case, the three moving directions we identified allow X to reach any point in a neighbourhood of X_0 in \mathbb{R}^3 and the system is locally controllable.

► **Stokesian robots: a general framework. [20,21]**

We showed in [20,21] that the control framework I presented for the 3 sphere swimmer can be generalized to the two other swimmers we consider.

An affine control problem without drift.

Let us first recall here the M shape variables (controls) and the position variables for each swimmer:

	3S	3SP	4S
			
position	$p = x_2 \in \mathbb{R}$	$p = (\mathbf{c}, \theta) \in \mathbb{R}^2 \times \mathbb{R}$	$p = (\mathbf{c}, \mathcal{R}) \in \mathbb{R}^3 \times SO(3)$
shape	$\xi = (\xi_1, \xi_2) \in \mathbb{R}^2$	$\xi = (\xi_1, \xi_2, \xi_3) \in \mathbb{R}^3$	$\xi = (\xi_1, \xi_2, \xi_3, \xi_4) \in \mathbb{R}^4$

Using, as previously the linearity of Stokes equations together with self-propulsion, we showed in [21] that we can write, for any of these swimmers, \dot{p} linearly in terms of $\dot{\xi}$:

$$\dot{p} = V(\xi)\dot{\xi} = \sum_{i=1}^M V_i(\xi)\dot{\xi}_i \quad \text{with} \quad V(\xi) : \mathbb{R}^M \mapsto \mathbb{R}^P, \quad (5.3)$$

where P is the dimension of the position space. Setting again $X = (\xi, p) \in \mathbb{R}^d$, $d = M + P$ the problem reads again as an affine control problem without drift:

$$\dot{X} = \sum_{i=1}^M \alpha_i(t)g_i(X) \quad \text{with} \quad g_i : \mathbb{R}^d \mapsto \mathbb{R}^d. \quad (5.4)$$

Controllability.

Using the same Taylor expansions as for the 3S swimmer, one can see that the solution to system (5.4) can move:

- in the direction of $g_i(X_0)$, $1 \leq i \leq M$, with displacement proportional to time t (for $t \ll 1$),
- in the direction of the first order Lie-brackets $[g_i, g_j](X_0)$, $1 \leq i, j \leq M$, with displacement proportional to t^2 ?

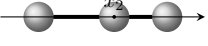
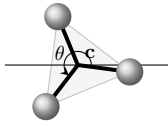
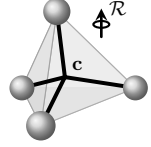
In fact, Lie-bracket directions of higher order can also be reached at the price of higher order expressions in t , leading to smaller displacements. A classical result by Rashevsky and Chow [Jur97; AS13] states that, if the Lie algebra generated by the iterated brackets is of full rank at X_0 :

$$\text{Lie}(g_i, i = 1 \dots M)(X_0) = \mathbb{R}^d,$$

every direction in \mathbb{R}^d can be reached and the system is locally controllable (the number of moving directions is sufficient to reach any point in a neighbourhood in \mathbb{R}^d of X_0).

To prove local controllability, it is then sufficient to find d independent directions among the iterated Lie-brackets.

Our three swimmers are designed in such a way that, the number of generated directions using the M controls together with their $M(M - 1)/2$ first-order Lie-brackets is in fact precisely equal to d :

	3S	3SP	4S
			
position variables	$p = x_2 \in \mathbb{R}$	$p = (\mathbf{c}, \theta) \in \mathbb{R}^2 \times \mathbb{R}$	$p = (\mathbf{c}, \mathcal{R}) \in \mathbb{R}^3 \times SO(3)$
dimension P	$P = 1$	$P = 3$	$P = 6$
shape variables (M controls)	$\xi = (\xi_1, \xi_2) \in \mathbb{R}^2$	$\xi = (\xi_1, \xi_2, \xi_3) \in \mathbb{R}^3$	$\xi = (\xi_1, \xi_2, \xi_3, \xi_4) \in \mathbb{R}^4$
	$M = 2$	$M = 3$	$M = 4$
nb. 1st order Lie-brackets	$M(M - 1)/2 = 1$	$M(M - 1)/2 = 3$	$M(M - 1)/2 = 6$
Size of $X = (\xi, p)$	$d = M + P = 3$	$d = M + P = 6$	$d = M + P = 10$

As a consequence, it is sufficient to prove that the $g_i(X_0)$, $1 \leq i \leq M$, together with their first Lie-brackets $[g_i, g_j](X_0)$, $1 \leq i, j \leq M$ are independent. Indeed, in that case we have:

$$\dim \text{Span} ((g_i(X_0))_{1 \leq i \leq M}, ([g_i, g_j](X_0))_{1 \leq i, j \leq M}) = M + \frac{M(M - 1)}{2} = d,$$

and the Lie-algebra is of full rank.

Using asymptotic expansions for large arms, we prove in [21], that for the three micro-swimmers we consider, the full rank condition is satisfied at one point X_0 , with first order Lie brackets only, proving local controllability at X_0 . We then go from local to global controllability using Hermann-Nagano theorem [Jur97]: the analyticity of the coefficients ensures that the dimension of the Lie-algebra is constant in the orbits of the system. From this result, together with the specific form of the system and the invariance of the problem with respect to the position, we prove that the Lie-algebra is of full rank everywhere, so that the system is globally controllable.

Optimal swimming.

After showing the controllability of the system, i.e. showing that the swimmer reach any target (position and orientation), it makes sense to ask how to achieve this target

with minimal energy cost. To do so, one can follow the notion of swimming efficiency suggested by Lighthill [Lig52] and adopt the following notion of optimality: energy minimizing strokes are the ones that minimize the kinematic energy dissipated while trying to reach a given net displacement.

We show in [21] that, mathematically speaking, the total energy dissipation due to a stroke $\xi : [0, T] \mapsto \mathcal{S}$ can be evaluated through an adequate quadratic energy functional:

$$\int_0^T \dot{\xi} \cdot \mathcal{G}(\xi) \dot{\xi} dt,$$

where the energy density \mathcal{G} is a function with value in the space of symmetric positive definite matrices with size $P \times P$.

The optimal swimming problem therefore comes back to minimize this energy for $(\xi, p) : [0, T] \mapsto \mathcal{S} \times \mathcal{P}$, under the following constraints:

- Initial configuration: $p(0)$ and $\xi(0)$ are given
- Dynamics: p is solution to (5.3)
- Stroke: $t \rightarrow \xi(t)$ is periodic
- Target: $p(T)$ is given

Note that some of these constraints can be relaxed. For example, it is possible to fix only the periodicity of the shape, but not its initial and final values, or to fix only some of the components of $p(T)$, leaving the others free to be optimized.

We present in [20,21] a numerical method to address this optimal control problem. The coefficients $V(\xi)$ in (5.3), encoding the dynamics, can be computed using a fluid solver. We used a FEM solver in [20] for axisymmetric swimmers and a BEM solver in [21] for the micro-robots we described in the previous sections.

Some optimal strokes for the three sphere swimmer of Najafi and Golestanian (3S) and another axisymmetric swimmer (Avron's Pushmepullyou swimmer) have been computed in [20]. In [21], we examine in detail several optimal strokes for the three balls swimmer in a plane (3SP) with a prescribed lateral displacement. Depending on whether the final orientation is also prescribed, and whether the initial shape is prescribed as well, or rather one treats it as a parameter to be optimized, we obtain dramatically different answers. Their variety illustrates the richness of behaviour of low Reynolds swimmers.

On-going work - Prospects

The series of articles [17-21], dating from 2008-2013, gave rise to new developments in which I was not involved. For example, N-link swimmers were studied in [Alo+13; Zop+17; Alo+19], elastic-swimmers in [PO12; MD15; CD16] or magneto-elastic swimmers in [Alo+17]. The influence of the presence of walls is studied in [AG13] and the structure of optimal strokes for the 3SP swimmer is investigated in [AD18; AD20].

I recently started working again in the domain of low Reynolds number swimmers, having in mind that my work on suspensions, contact or lubrication these last years could help in understanding these systems. I describe in the following some of the projects on control of micro-robots I am currently working on (as a co-supervisor of internships with François Alouges). I also describe a longer term project, about numerical simulation of active suspensions.

Control of micro-robots.

- During Philipp Weder internship (2020) we worked with François Alouges on the **description of the optimal strokes structure for the 4 sphere swimmer 4S**. This work was in continuation with [AD18; AD20], in which the optimal periodic strokes were found to be planar ellipses for the 3 sphere swimmer. We pursued the approach by considering the Four Sphere Swimmer 4S. In particular, using the symmetries of the artificial swimmer, we show how the formalism of bivectors can be used to express the optimal control problem in an elegant way for small strokes. Strikingly enough, there is a subtle distinction to make in the study of the optimal strokes, depending whether the prescribed displacement is a simple bivector or not. The results of this work are currently being written up for publication.
- Jessie Levillain M2 internship (2021) focuses on a **one-dimensional swimmer, consisting of a periodically activated rod attached to a series of elastic links (springs)**. This swimmer is an extension of the one described in [MD15], composed

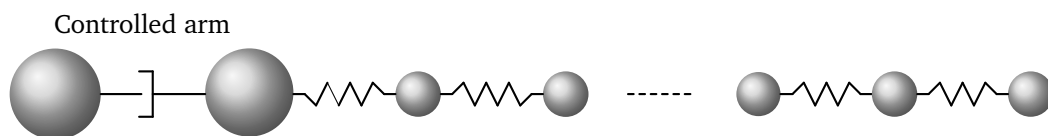


Fig. 5.4: One dimensional elastic swimmer with a unique control.

of a rod and a single elastic arm. In this case, the swimmer has a single control in dimension one. A qualitative and numerical study of the problem is achieved in [MD15]. If we place ourselves in the control framework of [17-21] that I described, the feedback with the elastic arm leads in that case to an affine control problem *with drift* and then the unique control makes it controllable. We want to generalize this result to the case of a series of elastic links and are interested in the description of a continuous limit model, when the number of springs tends to infinity. The objective is to propose a one dimensional framework for a swimmer made of a periodically activated head (the control) and a deformable body.

- The natural continuation of Jessie Levillain's internship (who will start a PhD thesis I will co-supervise with François Alouges) is to consider swimmers in two and three dimensions, made of **a magnetic head (controlled by a magnetic field) and an elastic passive body**. As in the one dimensional model, the deformations of the elastic body produced by the periodic displacement of the head should allow this swimmer to move with a single control (the magnetic field). In that case, unlike in the one dimensional case, no simple model is available. The use of direct simulations is then essential to compute the coefficients of the control system encoding the hydrodynamics interactions. The BEM tool we developed these last years, based on a discretization of the swimmer's surface, seems to be particularly adapted to this effect.

Towards direct simulations of active suspensions.

In most of the previous works, simplified models were used, neglecting non-local hydrodynamics interactions (e.g. resistive force theory for swimmers made of an assembly of rigid links). However, it has been shown in [GHD18] that the errors made in the prediction of swimming speed and efficiency was important when neglecting hydrodynamics interactions.

I believe that the use of direct solvers for the study of swimmers should allow new advances in the understanding of these systems, from micro-robots made of rigid spheres or links, to deformable swimmers. For example, the rheological signature of a two dimensional swimmer which controls its form has been studied in [Riz+19] using BEM computations. Recently, in [Guo+21b; Guo+21a], the authors also use BEM methods to optimize the boundary conditions (velocity or ciliary motion) for swimmers with arbitrary axisymmetric shape.

The internal forces exerted by a swimmer to change its shape generates large lubrication forces. As a consequence, it is essential to take into account the effect of these forces, not only on the swimmer, but also on other swimmers when simulating active suspensions. Direct fluid solvers, together with the decomposition method proposed in chapter 2 seem particularly adapted to solve this problem.

In the coming years, I would like to **take advantage of my work on suspensions, both related to BEM and close interactions, to study micro-robots, deformable swimmers and to study the behaviour of collections of swimmers (active suspensions).**

As mentioned in the introduction, the presence of active particles fundamentally changes the rheology of suspensions in a Newtonian fluid. Numerical simulations based on simplified models have been proposed to study the effective viscosity of suspensions of microswimmers in [IP07] or [Jib+17]. A two dimensional direct simulation of active bacterial suspension is reported in [DMM11], based on a finite element solver. There is no doubt that the development of direct simulation tools for three dimensional swimmer suspensions, taking into account contact and lubrication, would be of great help in improving the understanding of the macroscopic behaviour of active suspensions.

References

- [AS13] A. A. Agrachev and Y. Sachkov. *Control theory from the geometric viewpoint*. Vol. 87. Springer Science & Business Media, 2013 (cit. on p. 131).
- [Alo+19] F. Alouges, A. DeSimone, L. Giraldi, Y. Or, and O. Wiesel. “Energy-optimal strokes for multi-link microswimmers: Purcell loops and Taylor waves reconciled”. In: *New Journal of Physics* 21.4 (2019), p. 043050 (cit. on p. 134).
- [Alo+17] F. Alouges, A. DeSimone, L. Giraldi, and M. Zoppello. “Purcell magneto-elastic swimmer controlled by an external magnetic field”. In: *IFAC-PapersOnLine* 50.1 (July 2017), pp. 4120–4125 (cit. on p. 134).
- [Alo+13] F. Alouges, A. DeSimone, L. Giraldi, and M. Zoppello. “Self-propulsion of slender micro-swimmers by curvature control: N-link swimmers”. In: *International Journal of Non-Linear Mechanics* 56 (2013), pp. 132–141 (cit. on p. 134).
- [AD18] F. Alouges and G. Di Fratta. “Parking 3-sphere swimmer I. Energy minimizing strokes”. In: *Discrete & Continuous Dynamical Systems - B* 23.4 (2018), p. 1797 (cit. on p. 134).
- [AD20] F. Alouges and G. Di Fratta. “Parking 3-sphere swimmer: II. The long-arm asymptotic regime”. In: *The European Physical Journal E* 43.2 (2020), p. 6 (cit. on p. 134).
- [AG13] F. Alouges and L. Giraldi. “Enhanced Controllability of Low Reynolds Number Swimmers in the Presence of a Wall”. In: *Acta Applicandae Mathematicae* 128.1 (2013), pp. 153–179 (cit. on p. 134).
- [CD16] G. Cicconofri and A. DeSimone. “Motion planning and motility maps for flagellar microswimmers”. In: *The European Physical Journal E* 39.7 (2016), p. 72 (cit. on p. 134).
- [DMM11] A. Decoene, S. Martin, and B. Maury. “Microscopic Modelling of Active Bacterial Suspensions”. In: *Mathematical Modelling of Natural Phenomena* 6.5 (2011), pp. 98–129 (cit. on p. 136).
- [GHD18] N. Giuliani, L. Heltai, and A. DeSimone. “Predicting and Optimizing Microswimmer Performance from the Hydrodynamics of Its Components: The Relevance of Interactions”. In: *Soft Robotics* 5.4 (2018), pp. 410–424 (cit. on p. 135).
- [Guo+21a] H. Guo, H. Zhu, R. Liu, M. Bonnet, and S. Veerapaneni. “Optimal Ciliary Locomotion of Axisymmetric Microswimmers”. In: *arXiv:2103.15642 [cond-mat, physics:physics]* (2021) (cit. on p. 135).
- [Guo+21b] H. Guo, H. Zhu, R. Liu, M. Bonnet, and S. Veerapaneni. “Optimal slip velocities of micro-swimmers with arbitrary axisymmetric shapes”. In: *Journal of Fluid Mechanics* 910 (2021) (cit. on p. 135).

- [IP07] T. Ishikawa and T. J. Pedley. “The rheology of a semi-dilute suspension of swimming model micro-organisms”. In: *Journal of Fluid Mechanics* 588 (2007), pp. 399–435 (cit. on p. 136).
- [Jib+17] L. Jibuti, W. Zimmermann, S. Rafai, and P. Peyla. “Effective viscosity of a suspension of flagellar-beating microswimmers: Three-dimensional modeling”. In: *Physical Review E* 96.5 (2017). Publisher: American Physical Society, p. 052610 (cit. on p. 136).
- [Jur97] V. Jurdjevic. *Geometric control theory*. Cambridge university press, 1997 (cit. on pp. 131, 132).
- [Lig52] M. J. Lighthill. “On the squirming motion of nearly spherical deformable bodies through liquids at very small reynolds numbers”. In: *Communications on Pure and Applied Mathematics* 5.2 (1952), pp. 109–118 (cit. on p. 133).
- [MD15] A. Montino and A. DeSimone. “Three-sphere low-Reynolds-number swimmer with a passive elastic arm”. In: *The European Physical Journal E* 38.5 (2015), p. 42 (cit. on pp. 134, 135).
- [PO12] E. Passov and Y. Or. “Dynamics of Purcell’s three-link microswimmer with a passive elastic tail”. In: *The European Physical Journal E* 35.8 (2012), p. 78 (cit. on p. 134).
- [Riz+19] M. S. Rizvi, A. Nait-Ouhra, A. Farutin, et al. “Rheological signature of microswimmer phase-locking under flow”. In: *Physical Review Fluids* 4.10 (2019), p. 103302 (cit. on p. 135).
- [Zop+17] Marta Zoppello, Antonio DeSimone, François Alouges, Laetitia Giraldi, and Pierre Martinon. “Optimal Control of Slender Microswimmers”. In: *Multiscale Models in Mechano and Tumor Biology*. Ed. by A. Gerisch, R. Penta, and J. Lang. Vol. 122. Springer International Publishing, 2017, pp. 161–182 (cit. on p. 134).

Conclusion

Although present in everyday life, systems of interacting solids (such as suspensions, granular media, micro-swimmers, active suspensions, etc.) are still far from having provided all the answers to the questions raised about their behaviour. They are indeed particularly complex systems, each entity influencing all the others, through a very non-linear behaviour. One of the main difficulties lies in the close link between their microscopic and macroscopic behaviour. It is now well established that understanding the evolution of these systems from a microscopic point of view is necessary in order to identify macroscopic physical quantities of interest as well as well-posed macroscopic laws. For this, numerical simulation has an important role to play.

However, the complexity of these systems makes them difficult to study and simulate numerically: fluid/structure problems in three dimensions, demanding simulations for 3d dense systems, stiff short range interactions due to lubrication, non continuous behaviours due to contacts... These difficulties make this domain of research very stimulating and challenging for mathematicians!

The mathematical modelling of the physical phenomena involved is indeed essential for the understanding of these systems, but also for the development of codes that can answer the questions that arise. In this manuscript, we have presented some of these questions, which stem from current research in the domain of rheology, and for which mathematical developments have allowed progress, each community enriching the other.

To answer these problems, I have had the opportunity to work with various mathematical tools: asymptotic expansions of solutions to Stokes problems in order to take into account lubrication, finite elements and boundary finite elements to solve fluid/structure problems, fast methods and singular integrals for boundary elements methods, non-smooth convex analysis and conic optimisation problems to model contacts, control theory to study micro-swimmers... Again, this is only possible thanks to numerous exchanges between different fields of mathematics.

I end this manuscript by recapitulating the various projects to which the methods I presented opens the way:

Rheology of suspensions.

- New rheological studies for non-spherical particles, including lubrication (chapter 2 together with the viscous contact model [6]) and friction (chapter 4)

We plan to couple the fluid solver CAFES to the contact code SCoPI (post-doctoral fellowship funded by ANR RheoSUNN, starting in October 2021, in collaboration with Sylvain Faure and Loïc Gouarin). The friction algorithm, together with the viscous contact model already implemented in SCoPI, provides a contact algorithm that takes into account both friction and lubrication and leads to an implicit and stable method. In order to account for lubrication in the whole flow, we are currently working on an extension of the decomposition method described in chapter 2 to fictitious domain solvers (work in progress with Fabien Verget and Flore Nabet). With Georges Gautier, from the FAST laboratory, we wish to recruit and co-supervise a PhD student at the end of the ANR project, in order to carry out new rheological studies with the code resulting from the project.

- Further developments of the Stokes BEM solver (chapter 3) in order to simulate suspensions.

We need to choose an integral formulation and deal with the near-singular integrals arising for the double layer kernel when particles get close one to another (on going work with François Alouges and Antoine Sellier). To be able to deal with dense suspensions, it might be necessary to develop a multilevel implementation of the SCSD fast solver. Finally, I also have in mind to extend the decomposition method (chapter 2) to handle lubrication phenomena in BEM solvers.

- Use of direct solvers based on meshes fitting the fluid domain.

To date, most rheological studies performed with direct solvers are based on fictitious domain methods or boundary element methods. It would be interesting to test the behaviour of direct solvers based on meshes fitting the fluid domain. Compared to fictitious domain methods, these solvers, like the BEM solvers, respect the geometry of the particles. They must therefore be able to take into account precisely the close interactions. One of the difficulties in using this type of method is the need to remesh the fluid domain at each time step. As many advances have been made in remeshing techniques, it would now be interesting to see if these methods are now suitable for the numerical study of suspensions.

Rheology of granular flows.

- Theoretical study of the algorithm proposed in chapter 4.

We need to go further in the analysis of the properties of the scheme and of its link with dissipated power models (on going work with Bertrand Maury).

- Numerical study of granular media.

Lot of questions arise on the behaviour of granular materials. I would like to develop further the collaborations that have been set up with colleagues from FAST and IPGP around the code SCoPI. For example, we plan to extend the algorithm for friction developed in chapter 4 to the case of non-spherical particles, which would open the way to many new applications (collaboration with Sylvain Faure and Loïc Gouarin).

- From microscopic simulations to well posed rheological models.

I am convinced that the code we developed can help to better understand the different microscopic physical quantities involved and allow to answer questions both from physicists and mathematicians, such as well-posedness of the macroscopic models. I am particularly interested in the non-local rheological models and the study of the length scales of the chains of forces. Microscopic numerical simulations could also allow the identification of parameters of interest, linked to the structure of the medium for example, making it possible to propose new local rheological laws, that would lead to well-posed continuous problems.

Micro-swimmers and active suspensions.

- Further study of swimming micro-robots.

We are currently studying the structure of optimal strokes for the 4S micro-robot described in chapter 5 (Philipp Weder internship, co-supervised with François Alouges). We also plan to use the general control framework we have developed (chapter 5) to study more general robots such as magneto-elastic robots. We are currently working on a N-spring swimmer attached to a periodically activated rod in dimension one and plan to study swimmers with a magnetic head and an elastic passive body in two or three dimensions (Jessie Levillain M2 internship and PhD Thesis, beginning in October 2021, co-supervised with François Alouges). The corresponding numerical simulations will be achieved using the Stokes BEM solver we have developed (chapter 3).

- Direct simulation of active suspensions.

The rheology of active suspensions is fundamentally different from that of passive suspensions and is a very active domain of research. As detailed at the end of chapter 5, the simulation of such systems would benefit greatly from the tools I described in this manuscript. The use of direct solvers such as BEM solvers (chapter 3) as well as a careful care to close interactions such as lubrication (chapter 2) or friction (chapter 4) would be of great help to better understand these systems. This direction of research, which could take advantage of many tools that I had the opportunity to develop, would be a natural follow-up to this work.

Collective behaviour in colonies of bacteria.

- Using the code SCoPI to simulate colonies of bacteria.

A very recent and exciting project is being set up, following contacts with Vincent Calvez (ICJ Lyon) and Tãm Mignot (laboratoire de chimie bactérienne, Marseille). They are co-supervising a PhD thesis, one of the objectives of which is to understand the collective movements of bacteria. The study is based on very precise experimental observations at the individual level. Having developed a macroscopic model, they now wish to work at the microscopic level. The aim is to understand the importance of contacts between cells, which seems to play a primordial role. In order to observe the desired patterns, it is necessary to be able to take into account about 200 000 bacteria, moving in two dimensions and, in the first instance, of ellipsoidal shape. The recent inclusion of non-spherical particles in the code SCoPI should allow us to perform such simulations. Note that it is more a question here of considering a model of crowd movement than a model of suspension or granular media. However, the schemes for crowd motion are very similar to those used for granular media. Indeed, if the former are of order one in time and the latter of order two, the consideration of contacts is done in the same way.